

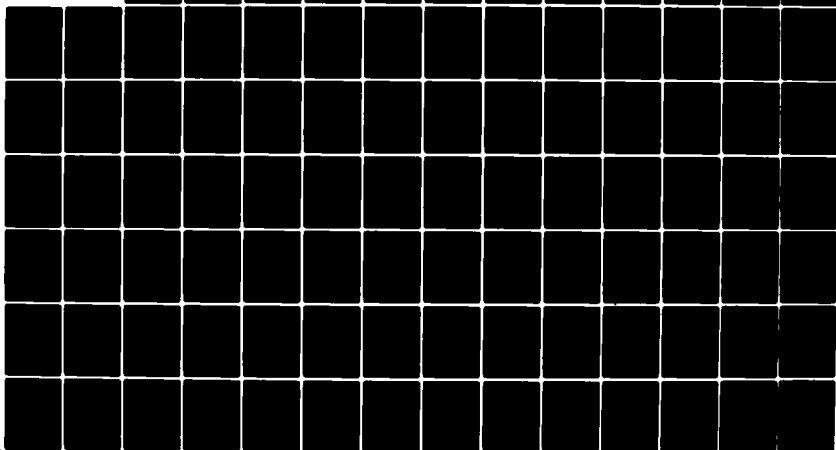
AD-A081 435

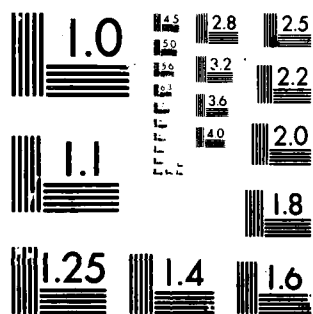
DAVID W TAYLOR NAVAL SHIP RESEARCH AND DEVELOPMENT CE--ETC F/G 13/10
ADVANCED CONCEPT DEVELOPMENT OF AN INTEGRATED SUPERSHIP SYSTEM.--ETC(U)
AUG 74 S T LIANG, J C ADAMCHEK, J S TEJSEN
NSRDC-3788-VOL-2

UNCLASSIFIED

NL

1 of 2
AD
AD-80-001





MICROCOPY RESOLUTION TEST CHART
NATIONAL BUREAU OF STANDARDS-1963-A

ADA081435

DOC FILE COPY

NAVAL SHIP RESEARCH AND DEVELOPMENT CENTER

Bethesda, Md. 20084

LEVEL II

ADVANCED CONCEPT DEVELOPMENT OF AN INTEGRATED SUPERSHIP SYSTEM: VOLUME II - TECHNICAL FEASIBILITY STUDIES

Edited by
Stephen T.W. Liang

Contributors:

John C. Adamchek
J. Strom Tejsen
Kenneth T. Page
Grant A. Rossignol

DTIC
ECTE
FEB 28 1980
C

APPROVED FOR public release;
distribution unlimited 2 SEP 1976

✓
SYSTEMS DEVELOPMENT DEPARTMENT
RESEARCH AND DEVELOPMENT REPORT

August 1974

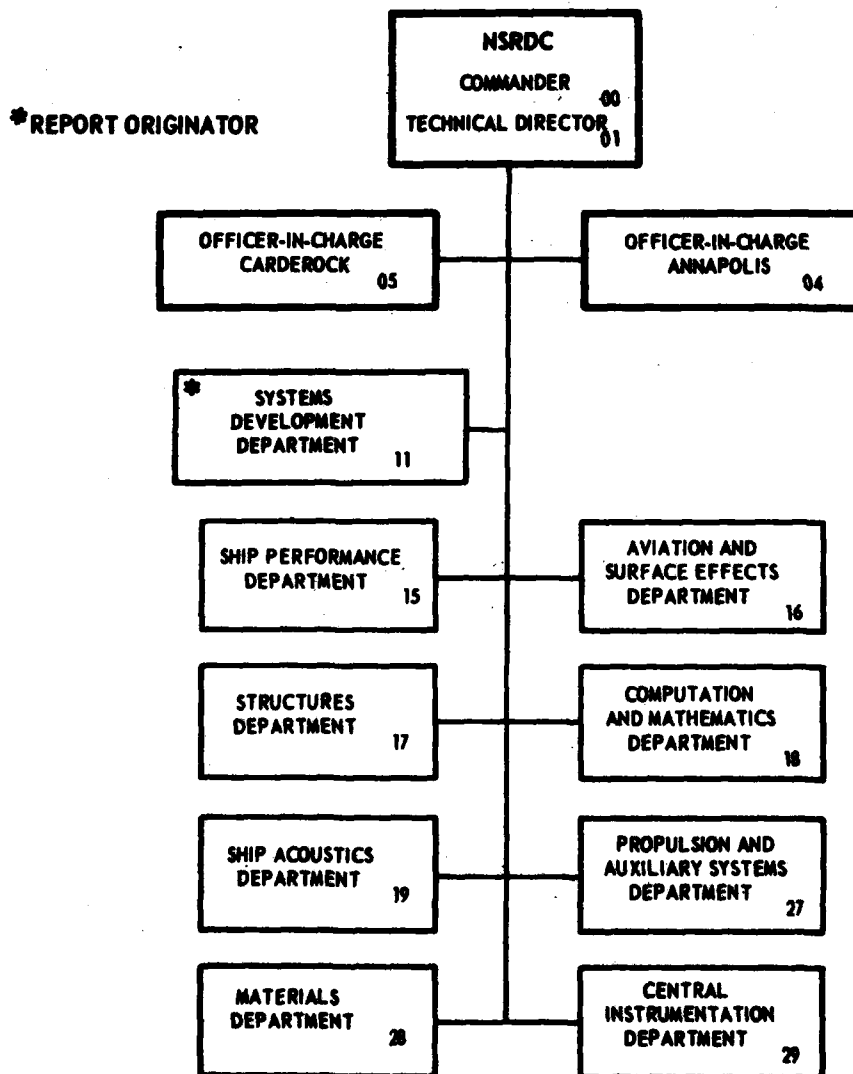
Report 3788 -
Vol. II

80 2 27 031

The Naval Ship Research and Development Center is a U. S. Navy center for laboratory effort directed at achieving improved sea and air vehicles. It was formed in March 1967 by merging the David Taylor Model Basin at Carderock, Maryland with the Marine Engineering Laboratory at Annapolis, Maryland.

Naval Ship Research and Development Center
Bethesda, Md. 20084

MAJOR NSRDC ORGANIZATIONAL COMPONENTS



UNCLASSIFIED

SECURITY CLASSIFICATION OF THIS PAGE (When Data Entered)

REPORT DOCUMENTATION PAGE		READ INSTRUCTIONS BEFORE COMPLETING FORM
1. REPORT NUMBER 3788 - Volume II ✓	2. GOVT ACCESSION NO.	3. RECIPIENT'S CATALOG NUMBER
4. TITLE (and Subtitle) ADVANCED CONCEPT DEVELOPMENT OF AN INTEGRATED SUPERSHIP SYSTEM, VOLUME II, TECHNICAL FEASIBILITY STUDIES 918639L		5. TYPE OF REPORT & PERIOD COVERED
7. AUTHOR(s) Edited by Stephen T.W./Liang Contributors: John C./Adamchek/J. Strom/Tejsen Kenneth T./Page/Grant A./Rossignol		6. PERFORMING ORG. REPORT NUMBER
9. PERFORMING ORGANIZATION NAME AND ADDRESS Naval Ship Research and Development Center Bethesda, Maryland 20084		8. CONTRACT OR GRANT NUMBER(s) 12142
11. CONTROLLING OFFICE NAME AND ADDRESS Naval Ship Research and Development Center Bethesda, Maryland 20084		10. PROGRAM ELEMENT, PROJECT, TASK AREA & WORK UNIT NUMBERS In-house IED Program of NSRDC under ZF61412001 - Work Unit 1-1170-033
14. MONITORING AGENCY NAME & ADDRESS (if different from Controlling Office) 1-577-11		12. REPORT DATE Aug 74
		13. NUMBER OF PAGES 144
		15. SECURITY CLASS. (of this report) UNCLASSIFIED
		15a. DECLASSIFICATION/DOWNGRADING SCHEDULE
16. DISTRIBUTION STATEMENT (of this Report) Distribution limited to U.S. Government agencies only, Test and Evaluation Information, 1974. Other requests for this document must be referred to Naval Ship Research and Development Center, Code 11.		
17. DISTRIBUTION STATEMENT (of the abstract entered in Block 20, if different from Report) 16 F61412, F35411 17 ZF61412001, SF35411001		
18. SUPPLEMENTARY NOTES Model experiments were partially funded by the Advanced Ship Development Program of the Naval Ship Systems Command under SF35411001. Preparation of this report funded by Work Unit 1-1170-033. ① Research and development rept.		
19. KEY WORDS (Continue on reverse side if necessary and identify by block number) Integrated Supership System, Mobile Ocean Base, Seaborne Base, Logistic System, Catamaran, Hinged Ship, Superpropeller 14 NSRDC — 3788-VOL-2		
20. ABSTRACT (Continue on reverse side if necessary and identify by block number) The concept of an integrated supership system was developed to support a substantial fleet of naval ships and to accommodate heavy air traffic in situations where the United States is denied access to or has withdrawn from operating bases in foreign countries. Critical areas were identified and recommendations for further development made on the basis of an exploratory study during which the vital elements were investigated in depth. (Continued on reverse side)		

DD FORM 1473
1 JAN 73EDITION OF 1 NOV 65 IS OBSOLETE
S/N 0102-014-6601

UNCLASSIFIED 387682

SECURITY CLASSIFICATION OF THIS PAGE (When Data Entered)

UNCLASSIFIED

SECURITY CLASSIFICATION OF THIS PAGE(When Data Entered)

(Block 20 Continued)

The basic system is envisioned as consisting of three catamaran ship modules each with a transit speed of 18 knots and totaling about 1,800,000 tons. The supership is considered to offer more flexibility, more mobility, and less vulnerability than a stationary floating platform.

The complete report is divided into three volumes: the first (System Overview, NSRDC Report 3788) includes pertinent information and general aspects; the second and present volume on technical feasibility studies includes the engineering aspects of hydrodynamics, structure, propulsion, and machinery; and the third (Vulnerability and Defense Analysis, NSRDC Report S-4024) contains the survivability studies and its contents are classified SECRET.

A series of model tests of the integrated supership system was conducted to determine and verify the motions and loads in waves. Two motion picture films were compiled from a number of selected tests for future reference.

Analytical and model test results confirm that the integrated supership system concept is operationally workable and technically feasible; however, much research and development work must be done in critical areas before a viable technological base can be established.

Accession For	
NTIS GRA&I	<input checked="checked" type="checkbox"/>
DDC TAB	<input type="checkbox"/>
Unannounced	<input type="checkbox"/>
Justification	
By _____	
Distribution/_____	
Avail Codes	
Dist	Special
A	

UNCLASSIFIED

SECURITY CLASSIFICATION OF THIS PAGE(When Data Entered)

TABLE OF CONTENTS

	Page
ABSTRACT	1
ADMINISTRATIVE INFORMATION	1
INTRODUCTION	1
SYSTEM CONCEPT	2
CHAPTER 1: CRITICAL STRUCTURAL ASPECTS	3
NOMENCLATURE	3
INTRODUCTION	4
STATISTICS OF LONG WAVES	4
WIND WAVES	5
SWELL	5
TSUNAMIS	6
FREAK WAVES	7
WAVE LOADS ON THE ISUS	7
WAVE LOADS FOR RIGID OR SEMIRIGID CONNECTIONS	7
WAVE LOADS FOR HINGED-TYPE CONNECTIONS	12
DESIGN LOADING CONDITIONS	13
SUPERSHIP JOINING MECHANISM DESIGN	14
CONCLUSIONS	17
CHAPTER 2: PROPULSION DESIGN AND ARRANGEMENT	19
NOMENCLATURE	19
INTRODUCTION	20
PROPULSION WITH LOW-SPEED ENGINE ARRANGEMENT	20
CHARACTERISTICS OF PROPELLER OPTIMIZED FOR SHAFT SPEED OF 80 RPM	20
PERFORMANCE OF PROPULSION SYSTEM IN OFF-DESIGN CONDITION	22
PROPULSION ARRANGEMENT WITH RESTRICTED PROPELLER DIAMETER	23
CHARACTERISTICS OF PROPELLER OPTIMIZED FOR GIVEN DIAMETER	23
PERFORMANCE OF 30-FOOT PROPELLERS IN OFF-DESIGN CONDITIONS	24

	Page
COMPARISON OF RESULTS FROM PROPULSION STUDY	24
CAVITATION AND VIBRATION CONSIDERATIONS	24
CAVITATION	24
VIBRATION	25
PROPELLER HUB AND TAILSHAFT DESIGN	26
CONCLUSIONS	27
CHAPTER 3: PROPULSION MACHINERY	29
PROPULSION SYSTEM OVERVIEW	29
DIESEL SYSTEM	29
GAS TURBINE SYSTEM	29
NUCLEAR-POWERED SYSTEM	30
OIL-FIRED STEAM SYSTEM	30
COMPARISON OF CANDIDATE POWER PLANTS	31
PROPULSION OF ISUS WITH ONE SHAFT PER DEMIHULL	31
CHARACTERISTICS OF OIL-FIRED STEAM SYSTEM	31
GEARING	33
SHAFTING	34
CONCLUSION	34
CHAPTER 4: STOPPING AND CONTROL	37
INTRODUCTION	37
STOPPING DISTANCE AND TIME	37
CONTROL DURING BRAKING	39
DIRECTIONAL CONTROL DURING STATIONKEEPING	39
CONCLUSIONS	42
CHAPTER 5: MODEL STUDY OF INTEGRATED SUPERSHIP	43
NOMENCLATURE	44
INTRODUCTION	45
MODEL PARTICULARS	45
PROCEDURE	45
INSTRUMENTATION AND TEST SETUP	45
MEASURED VARIABLES AND DATA REDUCTION TECHNIQUES	46
TEST PROGRAM	47
RESULTS	47
CONCLUSIONS	49

	Page
APPENDIX A – FORMULAS AND EQUATIONS	127
APPENDIX B – LOGS OF MOTION PICTURES	137
ACKNOWLEDGMENTS	50
REFERENCES	132

LIST OF FIGURES

1 – Air-to-Sea Interface, Integrated Supership System	51
2 – Supership Modules	52
3 – Estimated Power for the Supership and Its Catamaran Ship Modules	52
4 – Vertical Bending Moment Nondimensional Transfer Function for Rigid ISUS	53
5 – Significant Vertical Bending Moment versus Significant Wave Height for Rigid ISUS	54
6 – Hull Moment of Inertia Distribution for Rigid ISUS	55
7 – Sagging Load Distribution on the ISUS	56
8 – Hogging Load Distribution on the ISUS	57
9 – Influence of Joint Stiffness on Vertical Bending Moment	58
10 – Significant Relative Pitch Angle as a Function of Significant Wave Height for Hinged ISUS	59
11 – Significant Vertical Shear Force as a Function of Significant Wave Height for Hinged ISUS	60
12 – Significant Horizontal Shear Force as a Function of Significant Wave Height for Hinged ISUS	61
13 – Significant Torsional Moment as a Function of Significant Wave Height for Hinged ISUS	62
14 – Significant Horizontal Bending Moment as a Function of Significant Wave Height for Hinged ISUS	63
15 – Hinged Joining Mechanism Concept	64

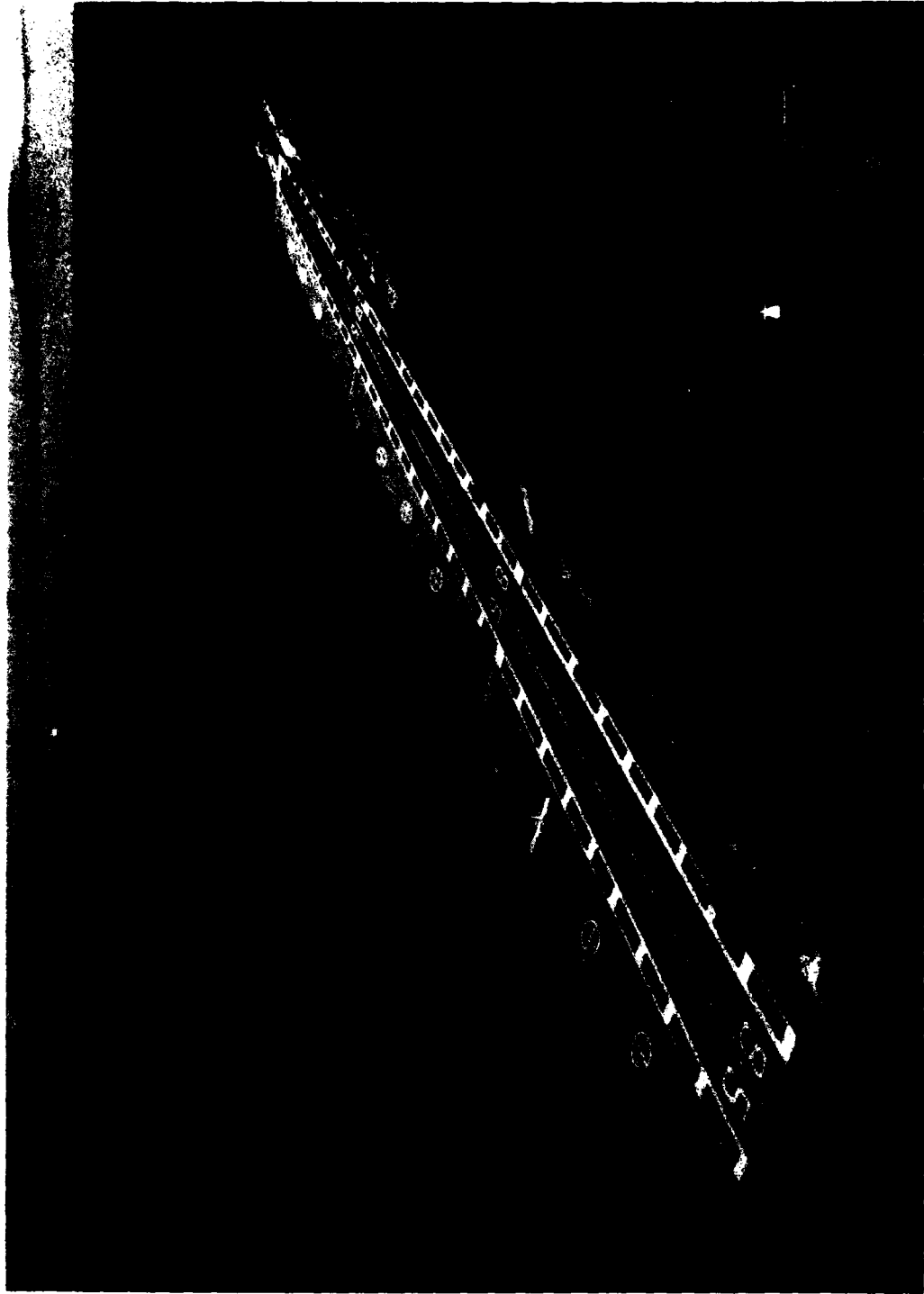
	Page
16 – Characteristics of Propellers Optimized for Shaft Speed of 80 RPM as a Function of Delivered Shaft Power for Various Ship Speeds	65
17 – Weight of Optimum Fixed-Bladed and Built-up Propellers of Different Materials	66
18 – Open Water Characteristics for Propellers Designed to Absorb 100,000 SHP at 80 RPM	68
19 – Performance Curve of Steam Turbine	69
20 – Off-Design Performance of Twin-Screw Propulsion Arrangement with Propellers Designed as Optimum for 12 and 18 Knots	70
21 – Characteristics of Propellers Optimized at a Specific Speed for Given Diameter as a Function of Delivered Shaft Power	71
22 – Weights of Optimum Fixed-Bladed and Controllable-Pitch Ni-Al-Bronze Propellers Designed for Specific Ship Speeds	73
23 – Open Water Characteristics for Propellers Designed to Absorb 100,000 SHP on 30-Foot Diameter	75
24 – Off-Design Performance of Twin-Screw Propulsion Arrangements with 30-Foot-Diameter Propellers Optimized for 12 and 18 Knots	76
25 – Propulsion Study Results for Performance of 37-Foot, 80-RPM Built-up Propeller and 30-Foot, 102-RPM CP Propeller	77
26 – Diesel Engine Procurement Cost	78
27 – Steam Plant Installation Cost	79
28 – Typical Fuel Consumption for a 70,000-HP Steam Turbine	80
29 – Fuel Consumption as a Function of Speed for ISUS with Oil-Fired Steam Plant	81
30 – Triple-Reduction, Parallel-Torque Path Gear	83
31 – Double-Reduction Gears	83
32 – Propulsion Machinery Arrangement for ISUS	84
33 – Stopping Distance and Time for the 1600-Foot Module as a Function of Astern Power Times Propeller Diameter of Each Shaft	85
34 – Stopping Distance and Time for 5000-Foot ISUS as a Function of Astern Power Times Propeller Diameter of Each Shaft	86
35 – Side Thruster Arrangement for ISUS	87
36 – Integrated Supership Model	88

	Page
37 – Shock Cord Hookup of Model to Carriage	89
38 – Transducer Locations on ISUS Model	90
39 – Details of Block Gage Assembly	91
40 – Motions of ISUS Model	92
41 – Positive Directions of ISUS Model Forces and Moments	93
42 – Experimental Long-Crested Irregular Wave Spectra in State 7 Sea	94
43 – Pitch Amplitude/Wave Slope of the Individual Modules versus Total ISUS Length/Wave Length	95
44 – Heave Amplitude/Wave Amplitude of the Individual Modules versus Total ISUS Length/Wave Length	98
45 – Relative Pitch Amplitude between Wave Slope of Two Modules versus Total ISUS Length/Wave Length	101
46 – ISUS Roll/Wave Slope versus Total ISUS Length/Wave Length	103
47 – Nondimensional Transfer Function of Vertical Shear Force between the Modules versus Total ISUS Length/Wave Length	104
48 – Nondimensional Transfer Function of Horizontal Shear Force between the Modules versus Total ISUS Length/Wave Length	106
49 – Nondimensional Transfer Function of the Longitudinal Force between the Modules versus Total ISUS Length/Wave Length	108
50 – Nondimensional Transfer Function of the Longitudinal Axial Moment between the Modules versus Total ISUS Length/Wave Length	110
51 – Nondimensional Transfer Function of the Vertical Axial Moment between the Modules versus Total ISUS Length/Wave Length	112
52 – Pierson-Moskowitz Wave Spectra for Various Sea States	114

LIST OF TABLES

1 – Principal Characteristics of Integrated Supership System	51
2 – Characteristics of 100,000-SHP Propellers Optimized at 80 RPM	115
3 – Characteristics of 30-Foot-Diameter Propellers for 100,000 SHP	116

	Page
4 – Power Plant for 1600-Foot Catamaran Ship Module	117
5 – Power Plant for 1800-Foot Catamaran Ship Module	117
6 – Steam Plant Component Weights	118
7 – Fuel Weights of Merchant Ships	119
8 – Fuel Weights for Supership and Components	119
9 – Steam Plant Component Block Volumes	120
10 – Propeller Shaft Stress Characteristics	121
11 – Comparison of Stopping Time and Distance for 5000-Foot ISUS, 1600-Foot Module, and 250,000-Ton Tanker	122
12 – Characteristics of Model and Full-Scale Supership	123
13 – Measured and Predicted Significant Double Amplitudes of Motions	124
14 – Measured and Predicted Significant Double Amplitudes of Forces and Moments	125



Artist's Concept of Integrated Supership System

ABSTRACT

The concept of an integrated supership system was developed to support a substantial fleet of naval ships and to accommodate heavy air traffic in situations where the United States is denied access to or has withdrawn from operating bases in foreign countries. Critical areas were identified and recommendations for further development made on the basis of an exploratory study during which the vital elements were investigated in depth.

The basic system is envisioned as consisting of three catamaran ship modules each with a transit speed of 18 knots and totaling about 1,800,000 tons. The supership is considered to offer more flexibility, more mobility, and less vulnerability than a stationary floating platform.

The complete report is divided into three volumes: the first (System Overview, NSRDC Report 3788) includes pertinent information and general aspects; the second and present volume on technical feasibility studies includes the engineering aspects of hydrodynamics, structure, propulsion, and machinery; and the third (Vulnerability and Defense Analysis, NSRDC Report S-4024) contains the survivability studies and its contents are classified SECRET.

A series of model tests of the integrated supership system was conducted to determine and verify the motions and loads in waves. Two motion picture films were compiled from a number of selected tests for future reference.

Analytical and model test results confirm that the integrated supership system concept is operationally workable and technically feasible; however, much research and development work must be done in critical areas before a viable technological base can be established.

ADMINISTRATIVE INFORMATION

This report describes the work accomplished during FY71 and FY72. Funding was provided principally by the in-house Independent Exploratory Development Program of the Naval Ship Research and Development Center (NSRDC) under Task Area ZF61412001. Model experiments were partially funded by the Advanced Ship Development Program of the Naval Ship Systems Command (NAVSHIPS) under Task Area SF35411001. Preparation of this volume was done under Work Unit 1-1170-033.

INTRODUCTION

Volume II covers the technical details which support the feasibility study of the integrated supership system (ISUS) concept undertaken in FY71-72. The system overview

(Volume I) has been presented in NSRDC Report 3788, March 1974. The vulnerability and defense analysis, NSRDC Report S-4024, November 1972, is the classified portion of the complete (ISUS) study report.

SYSTEM CONCEPT

The ISUS shown in the frontispiece and in Figure 1, is a very large multipurpose mobile military basing system designed to respond to an anticipated denial or lack of a land operating base. Its principal mission is concerned with rapid deployment and logistic support of expeditionary forces. This system is formulated as a logistic base with facilities to accommodate heavy air traffic (i.e., the C-5A) and to support a substantial fleet of naval ships. In peace time, this system could be used as an offshore airport, logistic station, or overseas operational base.

The ISUS is envisioned as consisting of three catamaran ship modules, with displacement totaling 1,800,000 tons. The ship characteristics are shown in Table 1. The forward and aft modules each displace about 500,000 tons and the center module about 800,000 tons. This very large size is in line with recent progress in the shipbuilding industry.

Each ship module (Figure 2) is self-propelled at speeds up to 18 knots and has an endurance of over 20,000 nm. After the supership is integrated, it will be propelled by the aft ship module at a speed of 10 to 12 knots with about 200,000 shp as shown in Figure 3. This is about 80 percent of the power of a large attack aircraft carrier.

When not connected to form an integrated system, the ship modules can be operated as separate mobile logistic bases. Their large deck space can accommodate helicopters, V/STOL aircraft, and other vehicles. Many complex activities can be managed by utilizing automation and computer networks. Air and sea traffic control, receipt and redistribution of materials and supplies, and inventory of containerized freight systems are some of the functions which could be automated.

The significance of the system lies in its superior mobility and flexibility of operation compared to a stationary floating platform.¹ It can be operated in both integrated and/or modular modes. This, in turn, should reduce operational cost and vulnerability.

Exploratory studies have identified the most critical areas as (1) hydrodynamic loadings and motions, (2) design of joints between individual modules, (3) propulsion, and (4) ship stopping and control. Detailed studies of these areas are covered in the following chapters.

¹Lin, A.C.M., "A Feasibility Study of a Stable Mobile Ocean Platform as a Naval Base," NSRDC Report 3743 (Feb 1973). A complete listing of references is given on page 132.

CHAPTER 1: CRITICAL STRUCTURAL ASPECTS

by

John C. Adamchak
Structures Department

NOMENCLATURE

$A(\omega)$	Wave amplitude
B	Beam of individual catamaran hulls
B_c	Overall beam of catamaran
C_{mv}	Nondimensional transfer function for the vertical bending moment
C_{mh}	Nondimensional transfer function for the horizontal bending moment
D	Depth of hulls
g	Gravitational constant
H	Draft of hulls
h_w	Wave height, double amplitude
I	Moment of inertia of hull cross section, vertical plane about neutral axis
$I_{\overline{x}}$	Moment of inertia of hull cross section at midship station of middle catamaran, vertical plane about neutral axis
L	Overall length of integrated supershhip
M_h	Horizontal (lateral) bending moment (about vertical axes)
M_v	Vertical bending moment
$M_{v\overline{x}}$	Vertical bending moment at midship station of middle catamaran for rigid hulls—rigid joint configuration
T	Wave period
v	Wind speed
θ_{AAC}	Relative pitch angle between aft and mid catamarans
θ_{AFC}	Relative pitch angle between forward and mid catamarans
λ	Wave length
ρ	Mass density of seawater
ω	Deep water wave circular frequency
ω_L	Deep water wave circular frequency of a wave of length L

INTRODUCTION

This chapter addresses the critical structural considerations which affect the feasibility of designing and constructing the study model of the ISUS and its modules. Although the individual catamaran ship modules are certainly "large" even by present day standards, the fact is that monohull vessels of approximately comparable size and tonnage are presently being designed and built. Therefore, the construction of such a ship appears to be technically feasible. Much exploratory work has still to be done, however, with respect to the joints that connect the individual modules. This chapter concentrates primarily on the structural feasibility of this concept in two critical areas: the primary loads on the ISUS and the design of the joining mechanisms.

STATISTICS OF LONG WAVES

As a prelude to consideration of sea loads on the ISUS, it is pertinent to devote some discussion to the subject of long ocean waves. Since this terminology is not precisely defined, the term "long ocean wave" will be used herein to describe waves with approximate lengths of 1000 to 20,000 ft. With respect to other characteristics often used to describe waves, and deep ocean waves, in particular, this length corresponds to a range of wave periods T from 14 to 62.5 sec and a range of circular frequencies ω from 0.45 to 0.10 rad/sec.

Both the static and dynamic responses of a ship to waves are intimately connected with the relative wave frequency and, in fact, the now familiar response amplitude operator (RAO) is precisely a measure of that relationship. As will be more clearly demonstrated later, the loading responses of primary interest for the 5000-ft ISUS occur for waves with the characteristics just described. In addition, the inadequacy of the traditional standard wave (height $L/20$, $1.1\sqrt{L}$, or 34 ft) bending moment calculation for a ship of such great length makes it necessary to develop an understanding of the action of the sea loads on the supershhip.

Unfortunately, information is not readily available on deep ocean waves of these great lengths. In the past, this subject was mainly of academic interest because such waves are so long compared to the lengths of surface ships of conventional size that there is very little noticeable ship response. In fact, vessels that encounter such long waves in the open sea may not even be aware of their presence. In addition to the fact that there has been little need for quantitative data on these very low frequency waves, the difficulties involved in detecting and measuring their characteristics have also been responsible for the scarcity of data.

Nevertheless, some pertinent information of a generally descriptive nature is available on long ocean waves. The primary areas of interest concern the frequencies of occurrence of such waves and the relationships between wave lengths and wave heights.

As an aid in the discussion, long waves in the deep ocean can be roughly grouped into four categories: (1) wind waves, (2) swell, (3) tsunamis, and (4) freak waves.

WIND WAVES

Most attention in the literature has been given to wind waves generated by friction as wind blows over the free surface of the water. It has become common to describe sea states generated in this manner by the so-called one-dimensional sea spectrum, for which a number of formulations presently exist. Unlike wave length and velocity, wave height does not bear any direct functional relationship to the wave period, and so these sea spectra are used to describe the relationship between wave amplitudes (energy) and wave frequency for given sea states.

For a given sea state, most of the wave energy is normally concentrated in a relatively narrow frequency band. This means that one wave frequency will be dominant in the spectrum and that waves of this frequency will tend to be highest. Waves at the peak frequency travel only slightly faster than the speed of the generating wind, that is, wave energy appears almost entirely as waves traveling at the speed of the wind or slower. As a result, there will be many waves of high frequency for a given sea state and very few of them will have frequencies less than that of the peak.

An examination of the sea spectra for various sea states clearly indicates that in the range of frequencies of interest, a significant amount of energy is present in long waves only for the higher sea states (severe storm conditions). This suggests that at any given location, long wind waves of moderate height occur somewhat rarely and those whose heights approach the asymptotic maximum deep-water wave height (which is on the order of 100 ft) are very rare indeed. It seems clear that in view of the potential investment involved in the construction and operation of a supership, much more definitive statistics on long wind waves are required in order to determine realistic sea conditions for design purposes.

SWELL

Long wind waves that leave their storm-generating area are known as swell. These waves may travel long distances before they lose their identity. Because wave length and

speed are directly related, waves of differing frequencies tend to separate as they travel. Consequently a swell condition essentially represents a single-frequency sea state. As they travel outward from the generating area, such waves lose height slowly, mainly by spreading their energy over a widening area of ocean, but they maintain their length, traveling as a wave train at one-half the velocity of the individual waves making up the train.

Swell heights are obviously related to the heights of the waves while in the generating area. They tend to be halved after traveling approximately 1000 miles from the generating area; thereafter, the rate of attenuation is reduced steadily with increasing distance. Inasmuch as long waves with a significant height of 100 ft occur only rarely in the generating areas, it seems apparent that swell of comparable height is also quite rare. Once again, however, there is a definite need for more precise statistical information.

TSUNAMIS

Waves caused by vertical displacements along earthquake faults on the sea bottom, by submarine landslides, and by volcanic eruptions beneath the sea are called tsunamis. Also commonly called tidal waves, they seem to occur principally following earthquakes of magnitude greater than 6.5 on the Richter scale, yet not all such earthquakes produce tsunamis. Tsunamis quickly lose height because of circular spreading and also because the wave length increases with distance from the origin. Wave periods vary from about 1/2 to 60 min although relatively little energy goes into waves of periods shorter than 5 min. Tsunami waves travel at very high velocity in the deep ocean (600 ft/sec) and are barely noticeable at sea from shipboard, except in the immediate vicinity of their origin. Since they are generally of such great length and small amplitude, the effect of the gradual rise and fall of the ship is imperceptible. Tsunamis have been of interest mainly because of their potential for destruction when they enter shallower waters.

Tsunamis can also be generated by nuclear devices of high yield. Waves generated in this manner are shorter and steeper than the normal tsunamis, with periods ranging from 30 sec to a few minutes only, but near the origin of the wave, their heights can attain more than several hundred feet.

Tsunamis are of interest with regard to the supership concept mainly in the vicinity of their origin. Outside this region, wave lengths grow too long and wave heights too small to produce significant ship response. Tsunamis are particularly frequent in areas of high seismic activity, such as the coasts of the Pacific Ocean and the Mediterranean areas, but they are rare on the Atlantic coasts. As a result, the prediction of the occurrence of tsunamis is intimately connected with the problem of earthquake prediction.

FREAK WAVES

The category of freak waves includes all those waves of abnormally large size for which it is difficult or impossible to account. Their existence is a fact but because their nature is unexplained, they are impossible to predict. Throughout the years many ships seem literally to have vanished from the face of the earth without a sign. Some ascribe such disappearances to freak waves.

The long ocean waves of primary interest in determining the sea loads acting on the 5000-ft integrated supertanker are thus described. However, more definitive statistical data are needed if realistic design loads are to be determined. Some of these data may already exist, awaiting only careful analysis, but most likely additional hydrographic measurements at sea will be required.

WAVE LOADS ON THE ISUS

Wave loads on the ISUS are discussed in three parts. Consideration is first given to the general case of a supertanker with rigid or semirigid joint connections. A more specific case is then treated, namely an integrated supertanker with hinge-type joints that allow for freedom of rotation in the vertical plane. Finally, the subject of supertanker wave loads is considered from the structural point of view, with emphasis on methods for determining design loading conditions.

WAVE LOADS FOR RIGID OR SEMIRIGID CONNECTIONS

Virtually no data are presently available on wave loads applicable to the ISUS with rigid or semirigid connections. Wave load information for catamarans is meager compared to that for monohulls. In addition, the unusual proportions of the ISUS and the length-depth (L/D), length-draft (L/H), and length-beam (L/B) ratios place the supertanker so far outside the range of available data that extrapolation is of questionable validity.

Some preliminary estimates of wave loads were made based on a mathematical model of the ISUS as a completely rigid, 5000-ft-long catamaran with a block coefficient of 0.60. The results of these estimates were proven far from practical. They are shown later in comparison with the results of other studies.

Vertical Wave Loads

In an effort to provide better estimates of the vertical wave loads acting on the ISUS, a more refined mathematical model was developed for use in static balance calculations. It exhibits a more realistic buoyancy distribution and is also capable of taking into account the influence of hull and joining mechanism flexibility. This model consists of three symmetrical (about their own midship section) wall-sided catamarans; their characteristics are presented in Table 1. The weight is assumed to be uniformly distributed for each catamaran ship module.

Static balance calculations were performed with this model for three configurations: (1) rigid hulls with rigid connections, (2) flexible hulls with rigid connections, and (3) rigid hulls with flexible connections. The results of these calculations are discussed in the following paragraphs.

Figure 4 presents the nondimensional transfer function C_{mv} for the vertical bending moment of the rigid hulls-rigid connections model. In this case the quantity C_{mv} is defined in terms of the beam of the individual hulls as follows:

$$C_{mv} = \frac{M_v}{\rho g h_w (2B) L^2}$$

where the double amplitude moment M_v is for the catamaran as a whole. The dashed portion of the curve on this figure indicates that plotted values of C_{mv} are suspect for frequencies above $\omega/\omega_L \approx 1.5$; additional wave balances would be necessary to determine peak moment values more exactly.

Figure 5 is a plot of significant vertical bending moment (double amplitude) versus significant wave height at the midship station of the middle catamaran ship module for the rigid hulls-rigid connections configuration. The line curve on this figure represents the values obtained with the mathematical model described earlier, using the transfer function presented in Figure 4 and the Pierson-Moskowitz (amplitude) wave spectrum formulation. Spectral density ordinates for wave amplitude are given in this formulation by

$$[A(\omega)]^2 = (16.768/\omega^5) \exp \left[\frac{-79.281 \times 10^4}{\omega^4 v^4} \right] \text{ ft}^2\text{-sec}$$

Also plotted on this figure (banded area) are the values calculated by considering the ISUS as a single catamaran. As expected, these values lie above those generated by the somewhat more refined model.

The midship station of the middle catamaran ship module represents the approximate location of the maximum vertical bending moment, but the locations of the ship connections represent the areas of major interest. Although vertical bending moment was not specifically calculated, indications are that significant values of about 80 percent of the midship station values represent reasonable approximations at the ship joining locations.

Primarily as a means of preventing excessive hull flexibility, conventional ships for oceangoing service are designed so that the length-depth ratio is less than 14. In the case of the ISUS with an assumed depth of 200 ft, the L/D ratio is 25, or approximately twice the conventional maximum. By allowing the ship to conform somewhat to the shape of the water surface, hull flexibility has a mitigating effect on the magnitude of the primary hull loading distribution. Since shallow vessels (those with high L/D) such as the ISUS require a smaller moment of inertia to provide the necessary hull section modulus value, it is to be expected that they will benefit greatly from the mitigating effect of a relatively limber hull. In an attempt to determine the magnitude of this effect for the supership, a hull moment of inertia distribution as shown in Figure 6 was assumed and several static balance calculations were performed. The ship joints were considered rigid for these calculations.

Figures 7 and 8 present the results of these calculations for sagging and hogging loading conditions on a wave 5000 ft long and 70 ft high (this wave height is an arbitrary value). In both cases the magnitudes of the bending moments of the flexible hulls showed a reduction of roughly 20 percent compared to that of rigid hulls, but those achieved for the shear forces were somewhat less. Although these reductions, both in forces and moments, do improve the loading situation, they are not significant enough to alter the design problem of the joining mechanism. To be realistic, a reduction in joint loads of at least one or two orders of magnitude would be required. To consider the hull flexibility alone in loading calculation does not appear to offer that potential.

Stiffness of the joining mechanisms themselves is one characteristic which can significantly influence the loads at the joints and, in turn, can affect the rest of the hulls. It is difficult to estimate the stiffness of a joining mechanism design because it is uncertain whether an absolutely rigid joining mechanism can be built. A semirigid or flexible joining mechanism can be modeled as a rotational spring and the joint stiffness expressed in terms of a rotational spring constant. The curves in Figure 9 were generated by using such a model. They illustrate the influence of joint stiffness on vertical bending for the sagging and hogging conditions. Since the alleviating effects of hull flexibility on loads decreases with decreasing joint stiffness, the individual hulls were considered rigid in these cases. The curves in this figure demonstrate that the behavior of the vertical bending moments as a function of joint stiffness is divided into three distinct ranges: (1) an upper plateau where

the behavior is essentially that of an ISUS with completely rigid joints, (2) a middle range of rapid transition, and (3) a lower plateau where the behavior is similar to that of a ship with completely flexible (hinged) joints. The distribution of bending moment and shear force for such a supship with hinged joints were presented in Figures 7 and 8. The substantial reduction of load levels is quite apparent.

It is important to note that the magnitudes of the joint loads given in these figures do not necessarily represent the maximum values experienced on a wave of the given dimensions. As used here, sagging and hogging refer to wave crest at bow (and stern) and at amidships, respectively. Maximum joint loads will generally occur with the wave crest located at some intermediate point between these two extremes. Nevertheless it can be expected that the type of behavior observed in Figure 9 is identical to that of the maximum joint loads as a function of joint stiffness.

Horizontal Wave Loads

Horizontal wave shearing forces and bending moments for conventional monohull ships are known to approach or exceed the vertical wave forces in corresponding waves. Such horizontal or lateral wave forces are very sensitive to ship heading angle and effective wave length. No serious consideration is given to these loads in the design stages primarily because the relative values of L/D and L/B for conventional hulls more or less ensure that a design whose strength is adequate for vertical loads will also be adequate for horizontal loads.

Such would also be the case for the ISUS except for the presence of the two ship joints. The value of L/B_c for the supship is not particularly excessive by present day standards; consequently it appears to offer no serious problem in providing adequate horizontal strength *within* the length of each hull. The joining mechanisms, however, represent the weak points in this respect. It will be a major problem to provide adequate horizontal strength at the joints without making them excessively large and/or complex.

Data on horizontal wave loads are relatively scarce, particularly for catamarans. In addition, the analytical problem is more complex than for vertical loads and not nearly as susceptible to so-called "quick and dirty" solutions. Consequently, no attempt was made in this study to develop any type of analytical model for horizontal loads.

Vossers et al.² presented data on monohull model tests performed to measure wave horizontal bending moments and covering a range of conventional ship proportions. When

²Vossers, G. et al., "Vertical and Lateral Bending Moment Measurements on Series 60 Models," International Shipbuilding Progress, Vol. 8, No. 83 (Jul 1961).

these data are roughly modified for catamarans, a dimensionless transfer function C_{mh} for the horizontal bending moment is defined as follows:

$$C_{mh} = \frac{M_h}{\rho g h_w (2B) L^2}$$

Plots² of this coefficient as a function of various hull parameters clearly indicate that C_{mh} is sensitive to length-draft (L/H) ratio and length-beam (L/B) ratio as well as to wave heading and wave length. Lateral bending decreases with increasing length-draft ratio, whereas for small wave lengths bending increases with increasing length-beam ratio. It is virtually impossible to extrapolate for a value of C_{mh} with any degree of confidence because of the competing nature of these two effects and the fact that the proportions of the ISUS place it far off the scale of the data plots. Analytical work or model testing is clearly called for here.

The picture is further complicated by the need to consider nonrigid joints since it seems clear that joints of this type may significantly influence the horizontal loading level. The only known measurements of horizontal bending moments on models with nonrigid connections appear to be those by Eda for tug and barge models connected with hinge-type joints.³ As would be expected, his report concluded that the horizontal bending moment in quartering seas can be the most important component in the resultant force on the connections. Unfortunately, the extreme dissimilarity between hull forms of barges and the ISUS make other than qualitative use of the results of this study all but impossible.

Miscellaneous Wave Loads

Use of the term "miscellaneous" is not intended to suggest that the wave load phenomena described below are necessarily of secondary importance. However, because of their generally complex analytical nature and the lack of adequate quantitative information, discussion will necessarily be brief and mainly descriptive.

Wave loads which fall into this category include hull torsion, transverse bending, slamming loads, and whipping loads. The available data on these loads are generally of questionable value for the two reasons already cited: the unusual proportions of the ISUS

³Eda, H., "Studies of Barge Trains in a Coastal Seaway," Davidson Laboratory Technical Note 806 (Jun 1969).

and the effects of nonrigid hull connections. Of the loads in this category, hull torsion is a particularly critical loading condition for the ship joining mechanisms. Also of considerable significance, although not particularly so at the hull joints, is transverse bending since the beam B_c of the supership is of the same order of magnitude as the wave lengths in which most of the wave energy is concentrated for normal sea states. In addition, this loading must be borne chiefly by the cross structure which has considerably less depth than the hulls.

The gross loads acting on the bridging or cross-structural component of the supership represent an important category of wave loads in themselves. Such loads include axial forces, torques, vertical shears, and moments. Methods have been developed⁴ for obtaining reasonable estimates of these loads, but they do not have the capability of including the effects of nonrigid ship connections or the transfer of loading from one hull to adjacent ones.

WAVE LOADS FOR HINGED-TYPE CONNECTIONS

It is apparent that a special case of the ISUS is of particular interest, namely, one with hinge-type connections that allow for freedom of rotation in the vertical plane only. This interest led to a series of model tests on three catamaran models connected by hinged joints. The tests are described in detail in a later section of this report. Selected motions and loads measured at the joint connections of these models included relative joint angles, horizontal and vertical shear forces, and horizontal bending and torsional moments.

Because existing models were employed for the tests, their proportions did not exactly match those of the ISUS study model given in Table 1. Nevertheless, the differences are not so large that reasonable estimates of the relevant motions and loads cannot be obtained when model data are scaled up to the dimensions of Table 1.

The model test results include plots of the nondimensional transfer functions of the selected motions and loads for beam, head, and port bow regular waves at zero ship speed. Details are presented later in the chapter entitled "Model Study of Integrated Supership." Certain transfer functions were selected for use with the Pierson-Moskowitz wave spectrum formulation to produce plots of predicted significant double amplitudes of response versus significant wave height for the ISUS study model. These plots are shown in Figures 10-14.

⁴Dinsbacher, A.L., "A Method for Estimating Loads on Catamaran Cross-Structure," Marine Technology, Vol. 7, No. 4 (Oct 1970).

The selection of the transfer functions was made on the basis of expected maximum response. The particular significance of these relationships is discussed later in connection with joining mechanism design.

DESIGN LOADING CONDITIONS

Since the traditional "standard wave" concept for ship structural design is completely inadequate for ships as large as the ISUS, the structural designer is forced to look elsewhere for approaches with which to determine design loads.

To a greater or lesser extent, most attempts at "rational" structural design have resorted to the use of some type of statistical method for determining load.⁵ In general, all these approaches require a capability to determine the ship response under certain given environmental conditions and some type of statistical description of these environmental conditions.

If the necessary information is at hand, such approaches can probably provide reasonable estimates for design loads. Unfortunately such is not the case for the ISUS. The need for improved statistics on long ocean waves at prospective base sites has already been mentioned. Such information might be obtained from an analysis of available data and/or from additional measurements. Improved wave spectrum formulations are required which more reasonably model the energy content of realistic seas at the lower frequencies, the range of interest for the ISUS. In addition to this lack of an adequate statistical description of the environment, no data are presently available for predicting the more critical aspects of the response of the ISUS to a given environment, except for the special case of the hinged connection.

The need clearly exists for both experimental and analytical work in the area of wave load response. Since the characteristics of the ship joining mechanisms have not been finalized, it would be particularly desirable to develop the capability for predicting ISUS wave response for some general, perhaps elastic, joint characteristics. At present there is virtually no information in this area.

⁵Thomas, G.O., "An Extended Static Balance Approach to Longitudinal Strength," Trans. SNAME, Vol. 76 (1968).

SUPERSHIP JOINING MECHANISM DESIGN

The concept of detachable ships is critical to the concept represented by the ISUS. The requirement for a relatively rapid attach-detach capability imposes rather severe constraints on the joining mechanisms. The feasibility of the entire concept rests on the ability to design and build ship joining mechanisms that are capable of sustaining all the loads imposed on them and, at the same time, possess characteristics that allow for the successful completion of the ISUS mission.

Based on the system requirements and the available relevant data, a hinged joint system (Figure 15) was selected which would allow freedom of rotation in the vertical plane between adjacent hulls but would resist other relative translations and rotations. It is felt that such a design represents the most reasonable concept consistent with the current state of knowledge. This system involves the use of a minimum of two connections at each joint, employing large hollow pins about which the adjacent hulls would be free to pivot. The size of the pins would be governed primarily by fabrication considerations, the desirability of providing smooth load transmission into the hull structure, and the necessity of maintaining reasonable levels of bearing pressure.

One of the primary reasons for adopting this relatively simple concept was the requirement for a rapid attach-detach capability. The mechanical simplicity of this concept offers a definite bonus with regard to the speed of the engaging and disengaging process. In addition, the lack of data relevant to the joining problem of the ISUS raises the question of the appropriateness of selecting a complex joining system at the concept stage of technical development.

The simplicity of the concept is not the only reason for its choice, however. The following additional arguments also support this choice:

- (1) Being a shallow ship (high L/D), the ISUS has relatively little depth available to resist the large vertical bending moments which would accompany rigid or semirigid joints. If the full depth of the modules were involved in the joining mechanism, parts of the mechanism would be below the waterline; this would certainly not be a very desirable feature from the viewpoint of maintenance and ease of attaching and detaching the modules.
- (2) Unless it can be demonstrated that the levels of the motions resulting from hinge-type connections are unacceptable, there is no particular reason to adopt rigid or semirigid joints which would involve large vertical bending moments. The extreme length of the ISUS suggests that motion and load responses, being highly frequency dependent, will be acceptably low for all but the most severe sea conditions. Accordingly, flexible deck sections can be used in the vicinity of the joints to avoid discontinuities from one hull section to the next.

(3) Rigid or semirigid joining mechanisms would transmit vertical loads and moments throughout the supership (particularly into the center catamaran module), thus requiring stronger and heavier primary structure. Most structural sea loads would be higher for an ISUS with rigid or semirigid joints than with hinged joints because of the relative inability of the rigid types to conform to the shape of the water surface. This is particularly true for the center catamaran module.

(4) The concept of articulated ships using hinged joints has been examined previously and appears to be feasible.⁶

Results of the model tests (Figures 11–15) undertaken to investigate the hinged-joint concept demonstrated that for the sea states of interest, the expected motions and loads of the ISUS would be low enough to make the concept feasible. This conclusion is based on the assumption that to fulfill the supership mission the three modules must remain joined together only while operating in conditions up to and including a State 6 sea (corresponding to a maximum significant wave height of approximately 20 ft). The conclusion reached on the basis of this assumption, however, should not be interpreted to imply that the hinged-joint concept is not feasible for rougher seas; any conditions requiring the consideration of seas higher than State 6 would necessitate further investigation. In any case it seems clear that much more precise definition of sea-state operations than presently available will be required to demonstrate the true feasibility of this or any other joint concept for the ISUS.

One of the primary justifications for adopting the hinged-joint concept was the hypothesis that the expected values of the relative angles between the adjacent hull sections would not become so large in operational sea states as to preclude aircraft landings. Although the maximum "acceptable" angle is not defined (and most likely depends on aircraft type), the curves in Figure 10 suggest that the relative orientations of the hulls up to and including a State 6 sea would pose no great problem for aircraft landings. These curves indicate significant relative angles (double amplitudes) on the order of 1 deg for both forward and after joints in a State 6 sea. The presence of such small angles would hardly be noticeable. It is reasonable to conclude from this that the model tests do indeed support the basic hypothesis that the use of hinged joints will not lead to excessive angular displacements.

Figures 11 and 12 indicate that expected load levels for the various forces and moments fall within limits that can be resisted by carefully designed components of the hinged joining mechanisms without overstressing. The only possible exception may be the

⁶Boylston, J.W. and W.A. Wood, "The Design of a Hinged Tanker," *Marine Technology*, Vol. 4, No. 3 (Jul 1967).

horizontal bending moment component for which expected values are shown in Figure 14. The extreme length of the ISUS and the requirement of zero relative angle in the horizontal plane between adjacent ship modules lead to large horizontal bending moment components in oblique seas. It seems questionable at this stage whether the use of jaws alone, as illustrated in Figure 15, will be sufficient to resist these large horizontal bending moment components. It is more likely that additional systems will be necessary, e.g., cables under tension, hydrodynamic thrusters, dampers, etc., to provide resisting moments to prevent separation of the ship modules. It may even be necessary or desirable to so design the joint system that small angular excursions will be allowed above certain load levels. Such a system might be required to prevent possible failure of the joining mechanisms and of primary ship structure.

The model test measurements indicated large magnitudes of the horizontal bending moment components. It must be noted, however, that like other loads, these moments are time dependent. Although their peak values applied statically might be sufficient to cause hull separation, the dynamics of the ISUS may well be such that no hull separation would occur in an actual seaway. This suggests the need for additional model experiments to specifically consider the elastic-dynamic behavior of the hinged joint concept.

All things considered, it appears that loads due to horizontal bending represent the greatest unknown problem associated with the design of hinged joining mechanisms. This is not to imply that it is simple to design the joints to handle the other loads but rather that the results of the model tests clearly indicate the critical nature of the horizontal bending moment components. It is further noted that such moments will be about equally large for any joint system, rigid or nonrigid, which restricts relative angular movement in the horizontal plane at the joint locations.

As a final point on joint loads and design, Figures 10–14 and data from Boylston⁶ illustrate the importance of ship heading in a seaway. It is evident that in most cases, oblique seas produce the most severe motion and load responses for the ISUS. This is not too surprising; wave energy for normal sea states is concentrated in waves whose lengths are considerably shorter than that of the ISUS. An oblique heading into such waves will cause an increase in their effective lengths and tend to produce responses more equivalent to head sea responses in much longer waves, those considerably closer to the peak response frequency. Ordinarily, a self-propelled ship has control over its heading in a seaway. In the case of the ISUS, however, certain operations may eliminate this freedom of choice, for example, when the supertanker is operating as a landing strip for aircraft. Consequently, the influence of ship heading will have to be very carefully considered in determining the design loading system for the joining mechanisms and throughout the whole design process.

CONCLUSIONS

This chapter has concentrated on two areas of principal interest to the ISUS; namely, the primary loads and the design of the mechanism for joining the modules. Many technical and design problems have been brought out; only the more significant results and conclusions are summarized here:

1. Available statistical information on long ocean waves is inadequate for estimating design values of motions and loads (such as frequencies of occurrence, wave height/length relationships, geometries, etc.). Measurements of wave data of this type at prospective base locations will probably be required. Improved wave spectrum formulations are also needed in order to more reasonably model the energy content of realistic seas at the lower wave frequencies.
2. Horizontal (about vertical axis) bending moments in oblique seas are very large for joint systems which allow no relative angular displacements in the horizontal plane between adjacent ship modules. For the hinged joint concept, where vertical moments are absent, at the joints, the horizontal bending moments represent the single most critical loading condition for the joining mechanisms.
3. Oblique seas generally produced the greatest motion and load responses of the ISUS study model with hinged joints.
4. Model experiments indicated that the hinged-joint concept is feasible for the ISUS within the bounds of the assumptions stated. As hypothesized, expected levels of motions and loads of the supership in a seaway are acceptable, with the possible exception of the horizontal bending moment components. Manageable levels of these moment components appear achievable if the hinged joints are carefully designed. Additional analytical and experimental work will be necessary to explore possibilities for reducing these large bending moments.
5. The true feasibility of the hinged joint or other joining system cannot be convincingly demonstrated until the specific mission requirements of the ISUS concept are more precisely defined. Future research should include mission refinement and other associated questions which have a marked influence on feasibility.

CHAPTER 2: PROPULSION DESIGN AND ARRANGEMENT

by

J. Strom-Tejsen
Ship Performance Department

NOMENCLATURE

A_E/A_0	Ratio of expanded blade area to disk area
C_{Th}	Thrust loading coefficient
D	Propeller diameter
h	Submergence of propeller shaft
J	Propeller advance coefficient
K_Q	Torque coefficient
K_T	Thrust coefficient
N	Shaft or propeller speed/rpm
n	Shaft or propeller speed/rps
n_s	Number of shaft of each catamaran ship module
$P_{0.7}$	Propeller pitch at seven-tenths radius
P/D	Propeller pitch-diameter ratio
F_s	Power of shaft or propeller
Q	Torque of shaft or propeller
T	Thrust of shaft or propeller
t	Thrust deduction fraction
V	Ship speed
V_A	Propeller speed of advance
W_p	Propeller weight
w	Wake fraction
Z	Number of propeller blades per propeller
η_H	Hull efficiency
η_0	Propeller efficiency
$\sigma_{x,0.7}$	Cavitation number at seven-tenths of propeller radius

INTRODUCTION

To ensure that individual catamaran ship modules can proceed independently at a speed of approximately 18 to 20 knots, each module will require a power installation of from 200,000 to 250,000 hp. When they are integrated to form the ISUS, propelled by the aft module alone, this power level would result in a speed of approximately 12 to 13 knots.

Transmission of the aforementioned power is technically feasible with a quadruple-screw arrangement. To obtain the simplest arrangement--and eventually the most efficient also--it is attractive to consider a twin-screw arrangement whereby the installation on each catamaran demihull corresponds to a single-screw arrangement absorbing up to 120,000 hp. This chapter discusses the feasibility of such a twin-screw propulsion arrangement and considers the problems involved in transmitting great powers by a single propeller.

The study has been divided in two parts. In the first, the propeller is optimized for a fixed engine rpm, assuming use of a steam turbine with triple gear reduction, corresponding to a shaft speed of 80 rpm. The optimum design results in so heavy a propeller that it can be manufactured only as a built-up propeller.

In the second part, the optimum propeller design is determined as a function of propeller diameter. Both a fixed-bladed propeller and a controllable pitch (CP) propeller are considered.

The problems associated with cavitation and propeller-induced vibratory forces will be discussed along with the mechanical problem of fitting a large propeller to a propeller shaft.

PROPULSION WITH LOW-SPEED ENGINE ARRANGEMENT

To obtain high propulsion efficiency and reduce problems associated with cavitation and vibration, it is advantageous to use a low-speed engine arrangement. At present the slowest practical shaft speed is approximately 80 rpm. The resulting propulsion system is a steam turbine with triple reduction gears. This is the rpm value which has been used in the first part of the propulsion study for the ISUS.

CHARACTERISTICS OF PROPELLER OPTIMIZED FOR SHAFT SPEED OF 80 RPM

The characteristics of a propeller operating at 80 rpm were determined as a function of engine power and ship speed; both were taken as variables at this point. The propeller characteristics (see Table 2) were determined for a five-bladed propeller at three different

values of ship speed corresponding to 12, 18, and 24 knots, a wake fraction of 0.20, and engine power from 20,000 to 120,000 hp. The optimizations were performed in the usual way by designing the propellers to absorb the available power at given speed and rpm. Calculations were carried out on an analytical representation of the Wageningen B-screw series, with propeller blade areas determined from the Burrill cavitation criteria.^{7,8} A shaft submergence of 60.0 ft was assumed, and a 5-percent cavitation margin was used in the study, as is usual for merchant ships.

Results of the optimization (Figure 16) give propeller diameter D , expanded blade-area ratio A_E/A_0 , pitch ratio at 0.7 radius $P_{0.7}/D$, and propeller efficiency η_0 for the three speed values as a function of shaft horsepower.

Propeller weights were determined for two different materials. Results of the weight calculations for manganese bronze and nickel-aluminum-bronze shown in Figure 17 are for fixed-bladed and for built-up propellers. The weight of the hub of the built-up propeller is also shown. Weight figures for the built-up propeller will correspond closely to those of CP propellers.

Figure 17 also indicates the limitations of propeller foundries. At present, the maximum finished propeller weight that can be poured by either United States or foreign manufacturers is approximately 160,000 lb. It is anticipated this limit can be increased to 225,000 lb, if needed.

The curves show that weight limitations put an upper bound on the shaft horsepower that can be delivered by a fixed-bladed propeller.* According to Figure 17, the limit for a manganese-bronze, 18-knot propeller is approximately 45,000 hp at present; this can be raised to 60,000 hp, given several years lead time. Both these power levels are much less than those anticipated for the ISUS; thus the weight limit eliminates the use of a single-casting propeller optimized at 80 rpm. A built-up propeller, on the other hand, is limited only by the weight of the hub and, from a casting point of view, can be manufactured to absorb much greater power.

The upper limit for the CP propeller would be imposed by size rather than weight. One with a diameter of 30 to 32 ft appears to be the maximum that can be manufactured in the foreseeable future.

With a built-up propeller, it should be feasible to deliver 100,000 hp or more on a single shaft. However, the total weight of the propeller will create problems in transporting,

⁷Van Lammeren, W.P.A. et al., "The Wageningen B-Screw Series," Trans. SNAME, Vol. 77 (1969).

⁸Todd, F.H., "Resistance and Propulsion," Chapter 7 of "Principles of Naval Architecture," The Society of Naval Architects and Marine Engineers, New York (1967).

*The term "fixed-bladed" is intended to describe a propeller cast and manufactured in one piece.

assembling, mounting, and balancing at a shipyard. Static stern-bearing loads will be critical, and propeller overhang should be reduced as much as possible.

PERFORMANCE OF PROPULSION SYSTEM IN OFF-DESIGN CONDITION

Assuming that the installed power on each shaft of the ISUS would be 100,000 hp, it is a straightforward matter to use Figures 16 and 17 to determine the characteristics of various propellers designed to absorb this power. Table 2 shows two such propeller designs for a 12- and an 18-knot ship; the corresponding open water propeller curves are given in Figure 18. The 12-knot propeller would correspond approximately to a design developed for the 5000-ft ISUS and the 18-knot propeller to one for the 1600-ft module.

To judge the merits of each design, it is of interest to consider performance when operating in off-design conditions. For instance, how well will the design of the 12-knot supership propeller perform when propelling the 1600-ft module, and vice versa?

Off-design performances of the two propeller designs were determined from the propeller open water curves (Figure 18) and from the steam turbine performance curve shown in Figure 19. The turbine curve, which has been derived on the basis of the performance of a 12,000-shp DeLaval steam turbine, provides the upper limit for the engine torque-rpm relationship when operation is at less than the 80-rpm rated shaft speed. In agreement with common maritime practice, 100-percent propeller rpm has been established as the upper limit for the engine rpm.*

Results of the off-design calculations for the two propeller designs are shown in Figure 20 as the maximum effective thrust versus ship speed which can be developed by the propellers in a twin-screw arrangement. Effective thrust is obtained as twice the propeller thrust reduced by the thrust deduction fraction. Figure 20 also indicates the resistance of the 1600-ft catamaran module and the 5000-ft supership. Note that the 18-knot propeller design is far superior for propelling the catamaran ship module and results in a speed of 19 knots compared to 17.3 knots by the 12-knot propeller design. The difference in obtainable speeds for the ISUS with the two designs is much smaller. The 18-knot propeller design seems better, although a tradeoff between the two designs could be considered.

*The maximum permitted⁹ is 15 percent higher than rated speed.

⁹American Bureau of Shipping, "Rules for Building and Classing Steel Vessels," New York (1970).

The achievable performance with a CP propeller for both of the operating conditions would come close to that of a propeller operating at the design condition. As mentioned previously, however, CP propellers can be built up to 32-foot diameter, a size somewhat smaller than needed for the ISUS.

PROPULSION ARRANGEMENT WITH RESTRICTED PROPELLER DIAMETER

The previous part of the propulsion study was carried out for a shaft speed of 80 rpm. At the power level considered for the ISUS, this results in weights and sizes that exceed casting capacity for both single-casting and CP propellers.

By restricting the propeller diameter and increasing shaft speed, it is possible to develop propeller designs which can be manufactured. The effect of limiting the propeller diameter is now discussed.

CHARACTERISTICS OF PROPELLERS OPTIMIZED FOR GIVEN DIAMETER

Optimum propeller characteristics were determined for five-bladed propellers with maximum diameters from 28 to 40 ft. The designs were carried out for engine powers from 40,000 to 120,000 hp and ship speeds of 12 and 18 knots, and a wake fraction $w = 0.20$.

The propeller optimizations were carried out by using a cavitation margin of 5 percent at a 60-ft shaft submergence as in the first part of the study.

Results of the optimizations are shown in Figures 21 and 22. Figure 21 presents propeller shaft speed N , pitch ratio at 0.7 radius $P_{0.7}/D$, expanded blade-area ratio A_E/A_0 , and propeller efficiency η_0 for five different values of shaft power as a function of propeller diameter. Weights of nickel-aluminum-bronze propellers for both fixed-bladed and built-up or CP propellers are shown in Figure 22.

For a 100,000-hp design, the maximum projected casting capacity estimated for propeller manufacturers limits the fixed-bladed propeller diameter to approximately 30 ft for both 12- and 18-knot cases. This diameter has also been considered the maximum acceptable as a CP propeller design.

PERFORMANCE OF 30-FOOT PROPELLERS IN OFF-DESIGN CONDITIONS

For 30 ft as the maximum diameter in a 100,000-shp design, optimum propeller characteristics can be read from Figures 21 and 22; Table 3 gives dimensions for both a 12- and an 18-knot ship. Again, the 12-knot propeller would be typical as a design for the 5000-ft ISUS and the 18-knot propeller for the 1600-ft catamaran module. It is seen from the figures and Table 3 that the optimum shaft-speed values for both propellers are from 102 to 105 rpm, which is common for steam turbines with usual gearing.

Performance in design and off-design conditions for propulsion arrangements using either of these 30-ft propellers has been determined from the propeller open water curves (Figure 23) and the engine characteristics (Figure 19). The results are given in Figure 24 which, like Figure 20, shows the maximum effective thrust that can be developed by the turbines and propellers in a 200,000-hp twin-shaft arrangement. For the 1600-ft module, the 18-knot propeller design would result in an 18.4-knot speed compared to 17.0 knots with the 12-knot design. For the 5000-ft ISUS, the difference between the speeds obtainable with the two designs is small. A CP propeller design would perform near the optimum for both conditions; the approximate performance curve for this propeller type is also shown in Figure 24.

COMPARISON OF RESULTS FROM PROPULSION STUDY

A comparison of the results from the two parts of the propulsion study is presented in Figure 25. On the basis of the low-speed engine study (Figure 20), the performance obtained with the 18-knot propeller design is more advantageous than with the 30-ft CP propeller (Figure 24). The difference in performance due to propeller size and shaft speed is evident. Although the CP propeller does not perform as well, it might still be preferable because of improved stopping and control characteristics that will be discussed later.

CAVITATION AND VIBRATION CONSIDERATIONS

CAVITATION

The propeller designs discussed previously were derived by using simple cavitation criteria. The blade-area ratios determined from these criteria indicate that cavitation would not be a serious problem. The extent to which the propellers can actually operate free of

cavitation depends, however, on the wake pattern behind the ships. Wake variations in the propeller disk will result in angle of attack changes of the various propeller sections; these might cause intermittent cavitation at certain angular positions of the rotating propeller. Brehme¹⁰ indicates that large wake variations cause considerable problems for large tankers. The low-speed, 80-rpm-propeller design might show an advantage over the 30-ft-diameter design in that the cavitation number at 0.7 radius ($\sigma_{x,0.7}$) would be slightly larger; see Tables 2 and 3. The cavitation margin against angle of attack variation consequently can be made larger.¹¹ Only a detailed propeller design and knowledge of the wake pattern in which the propeller will operate, however, can reveal the extent to which intermittent cavitation could become a problem. Such detailed studies are outside the scope of the present work.

Several considerations indicate that cavitation problems would be less for the ISUS than for a large tanker.

1. The ISUS can be designed with fine afterbody lines and large propeller clearances which will result in a homogeneous and uniform wake pattern.
2. Propellers can be submerged more deeply than feasible for large tankers. (As mentioned previously, a shaft submergence of 60 ft was used in the propulsion study.)
3. The propulsion system would not operate continuously at full power, and some cavitation in this condition might be acceptable.

New design techniques are being developed to utilize large skew values for the propellers; further preliminary indications suggest that these can lessen cavitation problems.

VIBRATION

The periodic forces emanating from a propeller operating behind an afterbody will result in vibratory surface and bearing forces. The actual magnitude of these propeller-excited forces depends on the wake pattern and its harmonic content, the clearance between propeller, propeller aperture and rudder, and propeller characteristics such as number of blades, skew, etc. The forces can be determined or estimated with some accuracy when details of the hull and aperture design and wake pattern are known. No attempt has been made, however, to include detailed calculations in the present work.

¹⁰Brehme, H., "Propellers for Single-Screw Ships with Large Engine Powers," (in German) Jahrbuch der Schiffbautechnischen Gesellschaft, Vol. 62 (1968).

¹¹Brockett, T., "Minimum Pressure Envelopes for Modified NACA-66 Sections with NACA = 0.8 Camber and BUSHIPS Type I and Type II Sections," David Taylor Model Basin Report 1780 (Feb 1966).

Considering the large powers to be delivered by the propellers, propeller-excited vibration could eventually be a serious problem, but the supership has certain mitigating features: (1) large propeller clearances can be provided; rudders might eventually be eliminated if control can be provided by CP propellers and (2) the fine afterbody lines should give a wake pattern that is homogeneous and uniform.

Propellers with large skewback are presently being developed. Their application appears to offer a very promising means of reducing both surface and bearing forces. (The extent to which full advantage of skewback can be used on either a CP or a built-up propeller is difficult to anticipate at present.)

PROPELLER HUB AND TAILSHAFT DESIGN

Up to the present it has been common practice to mechanically force a propeller onto the shaft taper and to use a mechanical extractor device to withdraw it. When the propeller has been driven onto the shaft, it is held by the friction between the boss and the shaft, and a key is fitted to secure it.

This method may be unreliable for large, heavy propellers which transmit large torque and torque fluctuations. It is unlikely that the grip achieved by this conventional method would be adequate to transmit the torque considered for the supership with an adequate margin of safety. If the friction between hub and shaft proves inadequate and the propeller slips on the shaft, making it necessary to transmit the force with the key, considerable damage to key, shaft taper, and propeller hub might occur.

To overcome this difficulty on the ISUS, it may be necessary to utilize a hydraulic method of cold shrinking the propeller onto a keyless shaft taper. Various forms of such techniques have been used, for instance, by Avondale in the United States, by the Pacific Orient Lines on the QE-2, and by Theodor Zeise.¹² Thus the method can be considered state-of-the-art.

Without undue effort, the hydraulic method can be used to so force the propeller up the shaft taper that an adequate and accurately predetermined grip is achieved.

¹²Meyne, K., "Hydraulic Method of Fitting Marine Propellers," International Shipbuilding Progress, Vol. 17, No. 193 (Sep 1970).

CONCLUSIONS

The problems associated with transmitting large powers with a single propeller have been considered as part of a study of the propulsion arrangement for the ISUS. With the assumption that shaft speed was to be fixed at 80 rpm, it was found that because of casting weight and size limitations, the maximum shaft power that can be delivered by a fixed-bladed or CP propeller is far short of the 100,000 hp required. At present the maximum finished propeller weighs approximately 160,000 lb. This limits the power of a manganese-bronze propeller to 45,000 hp. Given several years of lead time, it is anticipated that this capacity can be increased to 60,000 hp. On the other hand, a built-up propeller is limited only by the weight of the hub and can presently be manufactured to absorb 100,000 hp or more. The weight of the built-up propeller is so large, however, that bearing loads and propeller handling might present serious problems.

It is possible to deliver greater horsepower on a fixed-bladed propeller by increasing shaft speed and reducing diameter. The weight of a 30-ft propeller can absorb 100,000 hp at 102 rpm and be within the capacity anticipated for foundries in a few years. Understandably, the 30-ft propeller is less efficient than the 37-ft built-up propeller designed to operate at 80 rpm.

Comparison of propeller performance in the off-design condition indicates that it would be more advantageous to design propellers for the higher speed of the catamaran ship module (approximately 18 knots) than for the lower speed (12 knots) of the supership. The advantage of a CP propeller is that it gives nearly optimum performance for both applications.

Vibration and cavitation problems may be of concern in a 100,000-hp propeller design. The fine afterbody lines and large propeller clearances envisioned for the design of the ISUS will result in a homogeneous and uniform wake pattern. The fineness of the catamaran hulls and flexibility in designing the stern configuration should help to minimize vibration and cavitation problems. However, it is recommended that these characteristics be considered in greater depth in future studies of very large ships. Such a study, however, would necessitate certain information concerning wake patterns and the lines of the afterbody.

Transmission of high torque and heavy propeller weight may necessitate using hydraulic cold-shrinking on a keyless shaft taper. Such techniques have been employed and can be considered state-of-the-art.

The present work has been concerned with the twin-shaft propulsion arrangement (one shaft per demihull) and with some of the problems associated with the transmission of large power on a single shaft. Other propulsion arrangements that incorporate contrarotating

or overlapping propellers might result in higher efficiency and improved cavitation and vibration performance. It is suggested these arrangements be considered as possible alternatives in future studies of the supership concept.

CHAPTER 3: PROPULSION MACHINERY

by

K.T. Page

Propulsion and Auxiliary Systems Department

PROPULSION SYSTEM OVERVIEW

The four logical candidates for the propulsion system in a ship the size of the ISUS are oil-fired steam, nuclear steam, diesel, and gas turbine systems. The assumed utilization of the supership precludes the need for a combination of these systems in the manner required by many Navy ships. For instance, since no catapults would be required, auxiliary steam would be unnecessary for the gas turbine or diesel installation. Similarly, a nuclear steam system would not require an oil-fired system to accommodate the ship while in port since it would not be expected to be operable there.

Each propulsion system was considered separately to determine the most attractive arrangement for the ISUS. Weight, volume, procurement cost, and fuel consumption were compared for two power ratings based on maximum ship speeds of 18 and 15 knots. The maximum shaft power required at these two speeds is approximately 210,000 and 145,000 hp, respectively. Both powers are based on the performance characteristics of the built-up propeller.

DIESEL SYSTEM

The diesel data are based on a commercial unit, the 48,000-hp Sulzer RND 105. This engine weighs 1720 long tons and its dimensions are 1155 x 201 x 460 in.¹³ Diesel engine cost is based on the curve of Figure 26. Fuel consumption was taken as 0.4 lb/hp-hr.

A diesel installation for the ISUS would require two 50,000-hp engines in each hull. Although low-speed diesels are intended for use without reduction gearing, a large and costly combining gear would be required for a twin-engine, single-shaft installation.

GAS TURBINE SYSTEM

The gas turbine installation was based on the General Electric LM-2500 engine, a second-generation marine gas turbine in the size range of the largest marine gas turbines

¹³Wadman, B.W., "Diesel and Gas Turbine Catalog," Diesel and Gas Turbine Progress, Vol. 34 (1969).

presently available. Each engine weighs 8500 lb and its dimensions are 267 x 84 x 84 in.¹⁴ Eight LM-2500 engines would be required to meet the power level of the ISUS. The LM-2500 produces a normal power rating of 22,200 hp at a temperature of 100 F. The specific fuel consumption at normal power is 0.41 lb/hp-hr. It should be noted that the gas turbine requires more expensive fuel than do diesel or steam systems.

The use of multiple gas turbines would require a more complex power transmission system which includes the combination of reduction gear and reversing device or a CP propeller. Cost information for this gearing was not available or estimated.

NUCLEAR-POWERED SYSTEM

A nuclear-powered steam turbine system offers advantages for range and endurance. Since these were not the primary concerns of the ISUS, such an option was not considered in any detail. However, the nuclear-powered steam turbine must be included as an option in future studies when life-cycle cost tradeoffs are developed in more depth.

OIL-FIRED STEAM SYSTEM

The oil-fired steam plant is based on a commercial rather than a naval installation for maximum economy. General Electric has a steam turbine design, the MST-19, in the 100,000-hp range that is well suited to the twin-screw catamaran supership.¹⁵

The MST-19 power plant has not been used in a ship, and data are based on extrapolation of the existing General Electric MST-14 plant. This is a reheat steam power plant with several power ratings. A plant of 22,788 shp was used for data estimates. The total machinery weight is 980 long tons. The specific fuel consumption for this plant is 0.4 lb/hp-hr. Cost data were based on the extrapolated curve in Figure 27.

¹⁴"Sawyer's Gas Turbine Catalog," Gas Turbine Publications, Vol. 7 (1969).

¹⁵"Marine Steam Power Plant State of the Art Seminar," Babcock & Wilcox and General Electric (1970).

COMPARISON OF CANDIDATE POWER PLANTS

Tables 4 and 5 compare characteristics of the candidate power plants. Values for the 1600-ft module are shown in Table 4 and those for the 1800-ft module in Table 5. The figures in these tables are extrapolated from existing hardware or, in some cases, are based on specific weights, volumes, and costs.

A review of Tables 4 and 5 indicates that the gas turbine is superior to the oil-fired steam system on the basis of weight and volume. However, these are not significant factors in the case of the ISUS since both weight and volume of the propulsion machinery are insignificant portions (less than 1 percent) of the total weight and volume of the ship.

Specific fuel consumption is approximately the same for the three nonnuclear systems (gas turbines require more costly fuel).

The various systems must be put on an equal basis in order to compare initial costs. Table 4 indicates that a complete oil-fired steam system could be installed for approximately \$10 million. A comparable gas turbine system would cost nearly that much for the engines alone. Combining gearing would be extremely expensive and would drive the cost far above \$10 million. Costs of the diesel are similar; combining gearing and installation increase the basic engine cost. Installation is costly for very large diesels due to their size and weight, and the \$5 million engine cost would be tripled by the costs of installation and the combining gear system.

PROPULSION OF ISUS WITH ONE SHAFT PER DEMIHULL

The oil-fired steam plant was chosen as an example to illustrate propulsion of the ISUS with one shaft per demihull. It should not be construed to be the most suitable plant for the design. If a two shaft per demihull arrangement is considered, in future studies, direct-drive diesel propulsion would probably be competitive with conventional steam plants and would merit investigation.

CHARACTERISTICS OF OIL-FIRED STEAM SYSTEM

The General Electric-designed engine designated MST-19 has been carried out to the level of 120,000 hp per shaft. Such large steam turbines have not been built by General Electric as yet, but the company claims that they are within the state-of-the-art and can be built without great development cost.

Since the MST-19 has not been built, data for the ISUS were based on a General Electric MST-14, 22,800-shp steam plant in a 100,000-dwt tanker. The information on this engine was extrapolated to the power level required. The resulting data are not intended to represent the MST-19 engine but rather an arbitrary engine of the size required for the ISUS. The MST-19 design provides evidence that such an engine is feasible.

The total machinery weight of the MST-14 is 980 long tons. The installed machinery cost (1972 dollars) is \$3,118,000. The all-purpose fuel consumption rate is 0.4 lb/shp-hr.¹⁶ These characteristics were used as typical of a steam turbine prime mover.

Weight

Table 6 shows a weight breakdown of the components of a steam turbine propulsion system for the supership. These weights are based on the installation of the MST-14 unit in a 100,000-dwt ship. The machinery weight fractions are respectively 0.0058 and 0.0084 for the 15- and 18-knot horsepower ratings. The fuel weight for the ISUS is not a critical parameter, but it will serve the purpose in the stage of concept design. Data on merchant ships have been used to provide a suitable fuel fraction. Table 7 gives the total displacement, deadweight, and fuel weight for three merchant ships.¹⁷

In all three cases, the fuel capacity is 7.7 percent of the total ship displacement. If this same percentage is applied to the ISUS, the fuel weights and corresponding ranges appear to be more than adequate. Table 8 shows fuel weight and range for a fuel fraction of 7.7 percent of the displacement. The range was calculated by the simplified equation

$$R = \frac{V (W_f)}{P \times \text{SFC}}$$

where V = ship velocity

W_f = fuel weight

P = engine power

SFC = specific fuel consumption

The equation accounts only for a voyage at constant velocity with constant engine power requirement. These conditions are not realistic, of course, but the range figure indicates the general magnitude of the numbers involved.

¹⁶"Economic Comparison of Low Speed and Medium Speed Diesel and General Electric MST-13, MST-14 Non-Reheat and MST-14 Reheat Steam Power Plants for European Built and Operated Tankers," George G. Sharp Company, New York, N.Y. (Sep 1969).

¹⁷Arnot, D., "Design and Construction of Steel Merchant Ships," SNAME, New York (1955).

The values in Table 8 indicate that the range of the ship is not a problem and that the fuel weight fraction may be made lower than for a conventional merchant ship.

Volume

Table 9 is a breakdown of the dimensions of the steam propulsion system. These dimensions are for the box volumes of the machinery. All of these components are based on the MST-14 unit used for the weight breakdown.

Performance

Figure 28 shows a typical fuel consumption curve (specific fuel consumption (SFC) versus percent power), for a 70,000-hp steam turbine. The values were adjusted to the horsepower and fuel consumption of the ISUS power plant with the characteristic shape of the curve maintained. Figure 29 gives plots of specific fuel consumption and absolute fuel consumption both as a function of speed.

The characteristics described are those of a steam turbine of the size considered. They do not represent any specific engine but are intended to provide a general indication of what could be expected from an engine large enough for the ISUS.

GEARING

The results of the study indicate that in order to maintain an acceptable level of propulsion efficiency, the propeller speed should be kept as low as possible without upsetting the balance of the other critical parameters. The traditional Navy-type, locked-train, double-reduction gear may not be available within the projected time frame for power levels as high as those required in the ISUS. For this reason, the triple reduction concept was explored.

Figure 30 shows a triple-reduction, parallel-torque path gear driven by a cross-compound turbine.¹⁵ Rating of this unit is 100,000 hp at 80 propeller rpm. Tooth loadings are within current levels of marine applications. The eight pinions that drive the main gear are needed to control tooth loadings because of the very high torque.

A preliminary discussion with industry indicated that necessary steps have been already taken to ensure that completely reliable gearing will be available when power requirements for propulsion reach this level.

In the event that a four-shaft system (two shafts for each demihull at 60,000 hp each) should be selected, the locked-train, double-reduction gear would provide a better arrangement as illustrated in Figure 31. It offers greater simplicity and has fewer moving parts than a triple-reduction gear.

SHAFTING

A built-up propeller for the ISUS would weigh approximately 360,000 lb (Table 2). The shaft overhang (distance from hull to propeller hub) is generally about one-fifth of the propeller diameter for a commercial ship. The overhang for the supership would be 7.4 ft. The shaft must be capable of transmitting about 83,000,000 lb-in. of torque at 80 rpm or 105,000 hp. Using a 1.2 design factor per Navy requirements, the design torque load becomes $1.2 \times 83,000,000$ or 99,500,000 lb-in.

The shafting required would be quite large if built from standard Navy shafting steel (designated as AN steel). The Navy requires that outboard shafting on a ship be designed to a safety factor of 2.0. Additionally, the maximum allowable bending stress for the Navy material is 6000 psi. The rationale for this standard is that the fatigue strength of the material is reduced as it corrodes, and a 6000-psi limit provides an adequate shaft life for Navy ships. Because of the bending stress limitation, the diameter of the shaft for the ISUS would be 57 in. Table 10 presents propeller shaft stress characteristics for Navy AN steel.

The diameter of this shaft could be reduced considerably by choosing a stronger, more corrosion-resistant material. A careful material study would have to be made to ensure the practicality of the material selected for construction of such a large part. Any material that involved a great deal of alloying would be limited by the size of the ingot that could be made. This could affect selection of many of the stronger materials that are available.

One possible solution to the shaft sizing problem is to go to a twin-shaft arrangement for each hull. This would reduce the size of the shafts but would also increase the complexity of the propulsion machinery.

CONCLUSION

An oil-fired steam system is the most logical choice for a propulsion system to meet the requirements of the ISUS with a single shaft per demihull. If cost were not an important factor, other candidates would be competitive. The catamaran configuration of the

ship dictates the location of a complete propulsion unit (turbine, boiler, condenser, reduction gearing) in each demihull. The arrangement could be the same in both the mid-module and the fore and aft ship modules but with a slightly higher powered unit in the midmodule.

The machinery would consist of four major components: turbine, boiler, condenser, and reduction gearing. The turbine, boiler, and condenser units must be installed as approximately 100,000 hp per shaft arrangements. This entire arrangement could be laid out as shown in Figure 32.

It would be a great advantage if the main propulsion system in the after ship module could utilize fuel stored in the other two sections. This fuel should also be available to the propulsion units in the mid and forward ship modules when they are needed. This would entail a fuel system far more complex than that in a conventional ship. Such problems as the fuel and control systems on the ISUS can be readily solved, but it must be realized that these systems would be more costly than their counterparts on smaller, simpler ships.

CHAPTER 4: STOPPING AND CONTROL

by

J. Strom-Tejsen
Ship Performance Department

and

K.T. Page
Propulsion and Auxiliary Systems Department

INTRODUCTION

Stopping and control during braking would be important for the ISUS both when operating as a 1600-ft, 500,000-ton catamaran ship module and when operating as a 5000-ft, 1,800,000-ton integrated supership. It is known that braking large tankers presents extraordinary problems partly because of long stopping distances and times required and partly because of lack of control of the tanker during the stopping period. Consequently it is of interest to consider the extent to which the ISUS might present problems similar to those of large tankers.

STOPPING DISTANCE AND TIME

Preliminary estimates have been computed to establish guidelines for the stopping distance and time of the ISUS. The following expressions¹⁸ were utilized:

$$S = 216 \cdot \Delta^{1/3} \cdot \log_e \left[1 + 0.00957 \left(\frac{V_0^3 \Delta}{P_s D} \right)^{2/3} \right] + 1/2 V_0 \cdot t_r$$

$$t = 4.27 \frac{\Delta^{1/3}}{V_0} \left[0.00957 \left(\frac{V_0^3 \Delta}{P_s D} \right)^{2/3} \right]^{1/2} \cdot \arctan \left[0.00957 \left(\frac{V_0^3 \Delta}{P_s D} \right)^{2/3} \right]^{1/2} + 1/2 t_r$$

where S = stopping distance

t = stopping time

Δ = displacement for each catamaran demihull

¹⁸Clarke, D. and F. Wellman, "The Stopping of Large Tankers and the Feasibility of Using Auxiliary Braking Devices," Trans. Roy. Inst. Nav. Arch., Paper 4 (Apr 1970).

- V_0 = ship speed before stopping maneuver
- P_s = shaft power installed in each demihull
- D = propeller diameter
- t_r = time to reverse machinery

These expressions were derived by assuming that the ship will remain on a straight course, that a constant resistance coefficient $C_R = 0.65$ can be assumed for the speed range, and that propeller characteristics for a propeller running astern at zero advance $K_T/K_Q^{2/3}$ can be approximated by 2.25. These assumptions are all valid in the case of the ISUS. The equations for stopping distance and time were derived for conventional single-hull ships, but they are equally valid for a catamaran design wherein each demihull is treated as a single-hull ship. When the equations are used for the ISUS, only one-half of the total displacement and shaft horsepower should be entered to take the catamaran design into account.

Results of the calculations are shown in Figure 33 for the 1600-ft module and in Figure 34 for the 5000-ft ISUS. Stopping distances and times are given as functions of shaft horsepower installed on each shaft times propeller diameter $P_s \cdot D$, and the values are shown for different values of the initial speed covering the range from 6 to 18 knots. Curves are given for three different values of t_r (0, 1, and 2 min). The time required for a steam turbine to stop and reverse the shaft would fall between 1 and 2 min.

When entering the diagram, the horsepower P_s which should be used is the astern power which the steam turbine machinery can deliver. Following the usual practice with steam turbine vessels, the astern machinery would be designed to produce 80-percent ahead torque at 50-percent ahead rpm, and the available astern power would therefore be about 40 percent of the full-ahead power.

Considering the 18-knot, 1600-ft catamaran ship module as an example and assuming 40,000-hp astern power on each shaft with $t_r = 1$ min, Figure 33 indicates stopping times and distances of 13.5 min and 11,300 ft for the 30-ft propeller design and 12 min and 10,200 ft for the 37-ft, 80-rpm design. The advantage of the larger propeller diameter is obvious although not of any significance. On the other hand, for the application of a 30-ft CP propeller and assuming the total 100,000-hp ahead power available on each shaft in the reversed pitch mode, Figure 33 indicates a stopping time of 8 min and a distance of 6800 ft. Thus application of a CP propeller would improve braking of the catamaran module.

Table 11 compares stopping times and distances for different propulsion arrangements for the 1600-ft module and the 5000-ft ISUS derived from Figures 33 and 34. Also shown in the table are values for a 250,000-ton tanker that is representative of large tanker designs. Note that the stopping time and distance are smaller for the individual modules

than for the tanker. This, of course, is due to the much larger installed power per ton deadweight, a ratio which is 0.4 for the catamaran ship module but only 0.1 for the tanker. The stopping times and distances for the ISUS are roughly equivalent to values for supertankers.

Various braking devices such as flaps, parachutes, etc., could be considered in order to reduce the stopping time and distance for the ISUS. However, 30 percent appears to be the maximum reduction that can be realized with a practical system.¹⁸

CONTROL DURING BRAKING

Because of their fullness and beam-draft ratio, large tankers are generally either marginally stable or slightly unstable on course. A large tanker is directionally unstable during the stopping procedure because of the reversed flow from the astern running propeller over the after part of the hull. In practice then, the tanker steers off to one side, taking a curved track, and the assistance of tugs is necessary to accomplish a controlled stopping maneuver in confined waters.

The situation is much different for the ISUS. Each module will be stable, and the integrated supership will also be stable.¹⁹ Braking the catamaran should not result in loss of stability; thus, the supership can maintain its original straight line course without difficulty. It will be possible to actively control the ISUS by using the two propulsion units independently, and the control can be further improved by application of CP propellers.

Since control can be maintained during the stopping period, the problems associated with braking the supership (despite stopping distance and time) are considered to be completely different from what has been experienced with large tankers. Mating the catamaran ship modules to form the integrated supership can probably be performed without the need for tug assistance to provide control.

DIRECTIONAL CONTROL DURING STATIONKEEPING

The problem of stationkeeping at very low speeds must be approached through the use of side thrusters. Sizing of such thrusters is quite complex, and a true estimate cannot be made without knowledge of the ship geometry and the conditions under which it would be

¹⁹Schmitz, G., "Horizontal Forces and Moments Due to the Motion of Catamaran-Ships and Consideration of Their Dynamic Stability and Control," (in German) Schiffbauforschung, Vol. 9 (Feb 1970).

expected to keep station. Preliminary estimates can be made on the basis of rough ship geometry and the contributing environmental forces. These estimates are all made on the basis of a study by Stuntz and Taylor²⁰ correction factors and force coefficients are taken from their plots. The analysis is based entirely on turning moments. No attempt has been made to estimate the force necessary to hold the ship at an angle to the current or wind.

Wind, waves, and current all contribute to forces on a ship that is keeping station with no forward motion. Each force creates a turning moment with a lever arm equal to the distance from the center of pressure (of that force) to the center of buoyancy. The center of pressure, and hence the lever arm length, alters with changes in the angle of the ship to the wind. The magnitude of the force turning the ship also alters as the sine of the angle changes. This combination of magnitude changes creates a maximum moment when the angle to the wind is approximately 45 deg. For the purpose of sizing the bow thrusters, it will be assumed that a 40-knot wind and a 1-knot current act at an angle of 45 deg to the ship longitudinal axis.

The equation

$$F_c = C_{c\ell} (\rho/2) (V^2) (L) (H)$$

is based on model testing at NSRDC²⁰ and can be used to describe the current force. In the equation,

$C_{c\ell}$ = nondimensional lateral current force coefficient for $\phi_c = 90$ deg (a constant deep water value of $C_{c\ell} = 0.60$ also appears to be a reasonable assumption)

ϕ_c = direction of current relative to bow

F_c = lateral current force

V = current velocity

L = length of ship on waterline

H = mean draft of ship

ρ = mass density of salt water

Solving for the ISUS in a 1-knot current and $\phi_c = 90$ deg,

$$\begin{aligned} F_c &= (0.60) \left(\frac{64}{32.2 \times 2} \right) (1 \times 1.689)^2 (5000) (80) \\ &= 680,000 \text{ lb} \end{aligned}$$

²⁰Stuntz, G.R. and R.J. Taylor, "Some Aspects of Bow-Thruster Design," Trans. SNAME, Vol. (1964).

As the angle of current direction changes, however, this equation must be corrected.²⁰ The correction factor of 1.32 is based on testing; it is not calculated. The location of the center of force is about four-tenths of the length aft of the ship bow. Assuming that the center of buoyancy is at the midpoint of the ship, this creates a 500-ft lever arm. The turning moment is then

$$\begin{aligned} M_c &= (\text{lever}) (\sin \alpha) (\text{force}) (\text{correction factor}) \\ &= (500) (0.707) (680,000) (1.32) \\ &= 317,300,000 \text{ lb-ft} \end{aligned}$$

The wind force may be represented by the equation

$$F_w = \frac{C_{DW} (\rho'/2) V^2 (A \sin^2 \phi_w + B' \cos^2 \phi_w)}{\cos (a - \phi_w)}$$

where C_{DW} = wind drag coefficient in the direction of wind

F_w = resultant wind force

V = free stream wind velocity

ϕ_w = relative direction of wind, off bow

a = relative direction of resultant wind force

ρ' = mass density of air

A = longitudinal projected area of ship above waterline (broadside)

B' = transverse projected equivalent area of ship

If the true wind angle ϕ_w is 45 deg, the relative angle of the resultant force is 80 deg.²⁰ The coefficient of wind drag C_{DW} is approximately 0.72 for tankers and cargo ships. For the ISUS:

$$\begin{aligned} F_w &= \frac{0.72 (0.002378/2) (40 \times 1.698)^2 [5000 \times 80 \times (0.707)^2 + 260 \times 80 (0.707)^2]}{0.82} \\ &= 1.0 \times 10^6 \text{ lb} \end{aligned}$$

The center of wind force is also 40 percent of the length aft of the bow. This makes the turning moment due to wind force

$$\begin{aligned} M_{\text{wind}} &= (\text{lever}) (\sin \alpha) (\text{force}) \\ &= (500) (0.985) (1.0 \times 10^6) \\ &= 4.9 \times 10^8 \text{ lb-ft} \end{aligned}$$

The final contributing factor can be estimated only very grossly. Model tests by Spens and Lalangos²¹ indicate that the wave force on a 500-ft ship created a 19,000,000 lb-ft turning moment. Wave geometry was described as a wave height equal to 1/48 of the ship length and a wave length of 0.5 ship lengths. Extrapolating to the 5000-ft ISUS, the turning moment would be 190,000,000 lb-ft.

These three forces act to create a total turning moment on the order of 1.0×10^9 lb-ft. The bow and stern thrusters must be sized accordingly. The thrusters may be placed at the extreme forward and aft portions of the ship, allowing lever arms of 2500 ft. This means that when bow and stern thrusters are used at the same time, approximately 200,000 lb of thrust must be generated by each thruster.

Tests on a 4000-lb thruster indicate a required horsepower of 150, or roughly 25 lb thrust/hp. Application of this value to each module indicates a need for 8000 hp per side thruster, or a total of 32,000 hp for the entire ISUS.

Several factors may affect the sizing of the thrusters. Note from Figure 35 that running both forward thrusters in the same direction could affect the power requirement. The inflow to one thruster could be increased by the outflow of the other. It is equally possible that the reaction force between the hulls could negate any effect of one thruster on the other. Careful tests are needed to determine the feasibility of using side thrusters simultaneously.

CONCLUSIONS

The time and distance required for stopping the ISUS and its modules compare favorably with large tankers because of the larger power-displacement ratio. In contrast to large tankers, the supership is not expected to present control problems, since it remains stable during a stopping maneuver. Furthermore, the supership can be controlled by the two independent propulsion units.

The maneuvering problem can be reduced through the use of side thrusters. These thrusters have a high power requirement, about 32,000 hp. Although the estimates in this study are not precise, they do give a general idea of the magnitude of the problem.

The stopping and control of the ISUS and its modules is important to the success of the concept because joining the modules will depend on accurate control of motions. It is recommended that further studies be carried out in this area.

²¹Spens, P.G. and P.A. Lalangos, "Measurements of the Mean Lateral Force and Yawing Moment on a Series 60 Model in Oblique Regular Waves," Davidson Laboratory Report R-880 (Jun 1962).

CHAPTER 5: MODEL STUDY OF INTEGRATED SUPERSHIP

by

Grant A. Rossignol
Ship Performance Department

NOMENCLATURE

F_{AC}	Longitudinal force between after and center catamarans
F_{FC}	Longitudinal force between forward and center catamarans
F_{SHAC}	Horizontal (transverse) shear force between after and center catamarans
F_{SHFC}	Horizontal (transverse) shear force between forward and mid catamarans
F_{SVAC}	Vertical shear force between after and mid catamarans
F_{SVFC}	Vertical shear force between forward and mid catamarans
F_{x_1, y_1, z_1}	Longitudinal, transverse, vertical forces between forward and center catamarans on starboard side
F_{x_2, y_2, z_2}	Longitudinal, transverse, vertical forces between forward and center catamarans on port side
F_{x_3, y_3, z_3}	Longitudinal, transverse, vertical forces between center and aft catamarans on starboard side
F_{x_4, y_4, z_4}	Longitudinal, transverse, vertical forces between center and aft catamarans on port side
H	Draft
L	Total supership length
LBP	Length between perpendiculars (same as L)
LCG	Longitudinal center of gravity of individual catamaran
M_{LAC}	Longitudinal axial (roll) moment between after and center catamarans
M_{LFC}	Longitudinal axial (roll) moment between forward and center catamarans
M_{VAC}	Vertical axial (yaw) moment between after and center catamarans
M_{VFC}	Vertical axial (yaw) moment between forward and center catamarans
$S_f(\omega)$	Wave height spectral density ordinate
T	Wave period
$Z_A (Z_{AA})$	After catamaran heave displacement (amplitude)

$Z_C(Z_{AC})$	Center catamaran heave displacement (amplitude)
$Z_F(Z_{AF})$	Forward catamaran heave displacement (amplitude)
Δ	Displacement weight of Integrated Supership
ξ	Instantaneous wave elevation
ξ_A	Wave amplitude (single amplitude)
ξ_W	Wave height (trough to crest)
$\tilde{\xi}_{1/3}$	Significant double amplitude wave height
$\theta_A(\theta_{AA})$	After catamaran pitch angle (amplitude)
$\theta_{AC}(\theta_{AAC})$	Relative pitch angle (amplitude) between after and center catamarans
$\theta_C(\theta_{AC})$	Center catamaran pitch angle (amplitude)
$\theta_F(\theta_{AF})$	Forward catamaran pitch angle (amplitude)
$\theta_{FC}(\theta_{AFC})$	Relative pitch angle (amplitude) between forward and center catamarans
λ	Wavelength
$\phi(\phi_A)$	Supership roll angle (amplitude)
χ	Angle of ship heading relative to wave direction
ω	Angular wave frequency

Note: Symbols for forces and moments also represent amplitude values.

INTRODUCTION

Three existing catamarans were coupled together in tandem by means of hinge assemblies instrumented with block gages to form a model of the ISUS. The forward and center catamarans had symmetrical hulls but that of the aft catamaran was symmetrical from amidships aft and asymmetrical from amidships forward.

All tests were conducted at zero speed with the model moored to the carriage by shock cords. The small restoring forces provided by these cords prevented the model from drifting away from the carriage but did not influence the ship motions or force measurements. Tests were run in regular and irregular beam, head, and port bow waves. Sufficient motions and forces were measured to enable computation of all the required motions, forces, and moments.

MODEL PARTICULARS

The Integrated Supership model is shown in Figure 36. The forward catamaran is Model 5060, a symmetrical prototype of an ASR catamaran. The center catamaran is Model 5228, a symmetrical prototype of a conventional form CVA. The aft catamaran is Model 5061, an asymmetrical prototype of an ASR catamaran. The center catamaran was used without modification. However it was necessary to reduce the stern freeboard of the forward catamaran and the bow freeboard of the aft catamaran in order to mount the block gage assemblies parallel to the waterline. Characteristics of the model and full-scale ISUS are listed in Table 12. The ISUS model is a 1:120 scale model of the full-scale design.

PROCEDURE

INSTRUMENTATION AND TEST SETUP

The ISUS model was ballasted to the design waterline and centered under the carriage in the NSRDC Maneuvering and Seakeeping Facility. Four shock cords connected the center catamaran to the carriage as shown in Figure 37. The restraint allowed the model to undergo motion in all six degrees of freedom (pitch, heave, roll, surge, sway, and yaw) but kept it from drifting into the catwalk under the carriage.

The pitch and roll of the center catamaran were measured by means of a gyroscope; the relative pitch between any two forward and aft catamarans was measured by means of

a potentiometer. The heave acceleration of the forward catamaran was measured with a 1.0-g accelerometer, the heave of the center catamaran with ultrasonic probes, and the forces with block gages. The transducer locations and block gage assemblies are shown in Figures 38 and 39, respectively.

MEASURED VARIABLES AND DATA REDUCTION TECHNIQUES

Time histories of the signals of the model motions and forces at the joints between modules were recorded on analog tape and on Sanborn chart paper. These included heave (Z_C) and pitch (θ_C) of the midmodule and roll (ϕ) of the supership as well as relative pitch angles (θ_{AC} , θ_{FC}) between modules and the heave acceleration of the forward module at a specific wave height. At the same time, longitudinal, transverse, and vertical forces were also recorded at the joint between modules on both port and starboard sides.

From these recorded signals, the time histories of motions (Z_A , Z_F , θ_A , θ_F) of both forward and aft modules were calculated along with forces (F_{AC} , F_{FC}) and moments (M_{LAC} , M_{LFC} , M_{VAC} , M_{VFC}) generated at the joint.

Figures 40 and 41 are schematics showing the motions, forces, and moments. The equations used for the calculated time histories as functions of the experimental measurements are given in Appendix A.

Signals recorded on analog tape were written onto a digital tape by a Scientific Data Systems analog-to-digital converter. This digital tape was then used as input to a data reduction program which was run on an IBM 7090 computer. The first step in the program was to compute motion, force, and moment time histories from the measured signals. The program then performed a frequency domain analysis on both the computed and measured time histories.

In the frequency domain analysis, the regular and irregular wave data were processed separately. Fourier analyses were performed on the regular wave data to eliminate errors due to higher harmonics in the experimental data. The equations used for the computation of the Fourier coefficients are given in Appendix A. The Fourier coefficients of the responses were divided by the Fourier coefficients of the wave height to obtain the transfer functions. These transfer functions were nondimensionalized by the formulas given in Appendix A, and plotted against total ISUS length to wavelength ratio.

Power spectra were computed for the irregular wave data. The significant double amplitudes were then computed from the areas of these power spectra by the equation given in Appendix A.

Predicted significant double amplitudes of response were computed for States 3, 4, 5, 6, and 7 seas. The regular wave response amplitude operators (dimensional transfer functions squared) were multiplied point-for-point at the same frequency by the ordinates of the calculated Pierson-Moskowitz wave spectra to obtain predicted response spectra. The significant double amplitudes were then calculated from the areas of the response spectra.

TEST PROGRAM

Tests were conducted at heading angles of 225, 180, and 90 deg, all at zero speed. The convention used for heading angle was the angle from ship direction to wave direction proceeding in a counterclockwise manner (e.g., the 225-deg heading angle represents a wave approaching the port bow of the model). Tests were run in both regular waves and long-crested irregular seas. The irregular seas represented a State 7 sea. The regular wave tests were conducted in waves with model scale lengths ranging from 3.95 to 65.8 ft. In order to sufficiently define the transfer function, the number of wavelengths varied depending on the heading angle. The nominal wave steepness was $1/70$; a few tests were also conducted at nominal wave steepnesses of $1/100$ and $1/40$.

RESULTS

Figure 42 presents the experimental long-crested irregular wave spectra in State 7 beam, head, and port bow seas. The nominal significant wave height was 35 ft. Tests were requested in lower sea states, but this was beyond the capabilities of the wavemakers due to the large linear scale ratio of 120. Because such tests would require the generation of extremely low wave heights of high frequency content, it was decided to measure responses in regular waves and to estimate the results for the lower sea states.

Figures 43–46 present the nondimensional transfer functions of the motions for beam, head, and port bow regular waves at zero ship speed. These transfer functions are plotted against ISUS length to wavelength ratio and full-scale wave period. The transfer functions for the three heading angles (90, 180, and 225 deg) are superposed on the same figure for a given motion. Except for ISUS roll, the other motion transfer functions tend to indicate major resonance values for full-scale wave periods greater than 18 sec. For wave periods in the range of 15 to 18 sec the magnitudes seem to decrease substantially; however, they increase slightly for wave periods less than 15 sec. The significance of these results is that

wave periods greater than 18 sec are encountered less than 3 percent of the time.²²⁻²⁶ Wave periods greater than 18 sec will occur only in the most severe storms (e.g., hurricanes and typhoons). In the case of the ISUS roll transfer function, resonance values occur for wave periods less than 18 sec; this is also the case for a single ship module. Since the three modules are not free to roll relative to one another, the ISUS is essentially one long catamaran as far as roll is concerned, except for the possibility that the modules may have different natural periods. The multiple peaks of the pitch and heave transfer functions are partly explained by the fact that the ISUS has four more degrees of freedom than a conventional ship.

Figures 47-51 present the nondimensional transfer functions of the forces and moments for beam, head, and port bow regular waves at zero ship speed.

Figure 52 indicates Pierson-Moskowitz wave spectra for States 7, 6, 5, 4, and 3 seas, respectively. The equation for these spectra is given in Appendix A. These spectra were multiplied by the regular wave response amplitude operators (response squared/wave height squared) to obtain predicted motion, force, and moment spectra. The predicted significant double amplitude values obtained by using these spectra are given in Tables 13 and 14, in addition to the measured double amplitude values. The predicted significant values were increasingly less accurate as sea state decreased; the maximum wave frequency which could be generated in the basin was limited (as previously mentioned), and consequently the predicted response spectra for the lower sea states were not as well defined as were those for a State 7 sea. However, the predicted significant double amplitudes are considered to be reasonable estimates. As can be seen in Table 13, the motions decreased from moderate magnitudes in a State 7 sea to virtually zero in a State 3 sea. More importantly, as sea state decreased, the magnitudes of the forces and moments decreased by factors of 10^4 and 10^3 respectively.

²²“Oceanographic Atlas of the North Atlantic Ocean, Section IV—Sea and Swell,” U.S. Naval Oceanographic Office Publication 700 (1963).

²³“Oceanographic Atlas of the South Atlantic Ocean, Section IV—Sea and Swell,” U.S. Naval Oceanographic Office Publication 799B (1948).

²⁴“Oceanographic Atlas of the Northwestern and Southwestern Pacific Ocean, Section IV—Sea and Swell,” U.S. Naval Oceanographic Office Publication 799CE (1969).

²⁵“Oceanographic Atlas of the Indian Ocean, Section IV—Sea and Swell,” U.S. Naval Oceanographic Office Publication 799G (1965).

²⁶“Oceanographic Atlas of the Northeastern Pacific Ocean, Section IV—Sea and Swell,” U.S. Naval Oceanographic Office Publication 799D (1969).

Motion pictures were taken of the model tests in regular and irregular waves and two films were compiled.²⁷ One contains footage of the ISUS in typical sea and swell conditions. It includes tests in beam and head (State 7) seas for irregular waves and beam, head, and port bow tests for regular waves at a variety of wave steepnesses and wave periods. The second contains footage of the ISUS in swell conditions typical of those found in severe storms (e.g., hurricanes and typhoons). In this film the supership is seen in head and port bow regular waves. The actual wave steepnesses ranged from 1/32 to 1/70 and the wave periods from 20.75 to 31.72 seconds full-scale. The logs of the motion pictures are given in Appendix B.

CONCLUSIONS

The following conclusions are drawn for the ISUS on the basis of the model experiment:

1. ISUS motions were virtually nonexistent in States 3, 4, and 5 seas. There was considerable wave action between the two demihulls of an individual module in a State 7 sea at the port bow heading.
2. Significant values of both pitch and roll of the ISUS were considerably less than those for the single catamarans. Previous NSRDC experiments on the behavior of a single catamaran in waves had indicated that a significant wave height of 8 to 12 ft in head seas yielded significant pitch values between 4 to 6 deg. When these models were linked together (each as a module) to form an ISUS, the significant pitch values of the modules were between 1.7 to 3.2 deg for a significant wave height of 38 ft.
3. The significant pitch values were virtually the same for port bow and head seas, but significant roll values were consistently larger in beam than in port bow seas. Although the ship modules were not capable of rolling with respect to one another, the significant ISUS roll for both beam and port bow seas was considerably smaller than for a single catamaran. This reduction may be due to the combining of ship modules with different roll periods and to the fact that the connected modules had a distinctly different underwater geometry than a normal catamaran.
4. The significant forces and moments at the joints between the individual modules were larger in port bow seas than in either beam or head seas; their magnitudes were reduced by factors of about 10^4 and 10^3 respectively from State 7 to State 3 seas.

²⁷"Movies of Supership Model Tests in Waves: Part I—Normal Operating Conditions, Part II—Severe Storm Conditions," NSRDC Movie M-2301 (Jul 1971).

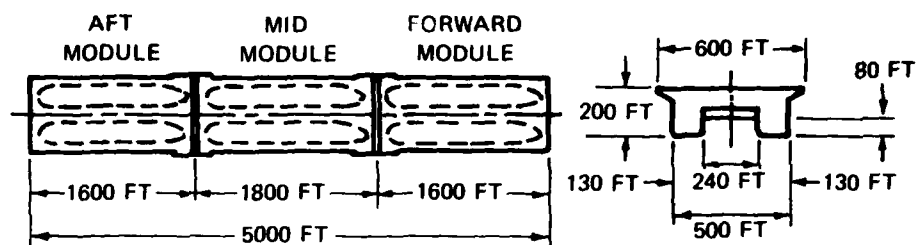
5. The largest response per unit wave height for both the motion and load data occurred at full-scale wave periods (> 18 sec) longer than those which are likely to be encountered.

6. Since the present tests covered only one configuration at zero ship speed, it is recommended that various configurations (e.g., hull separation and weight distribution) and ship speeds be investigated at different oblique sea headings. Such future tests should also measure the wave action between the demihulls in oblique seas and correlate these measurements with motions since this wave action could damage the bridging structure between hulls.

ACKNOWLEDGMENTS

This report is the collective effort of many who contributed expertise, knowledge, and time. The authors extend sincere appreciation to all who participated. Special thanks are due to Messrs. R.M. Stevens, G.D. Elmer, B. Wooden and many others who provided technical review and valuable comments to improve the contents of the report.

TABLE 1 - PRINCIPAL CHARACTERISTICS OF INTEGRATED SUPERSHIP SYSTEM



Characteristics	Aft Catamaran Module	Middle Catamaran Module	Forward Catamaran Module	Integrated Supership
Length/ft	1,600	1,800	1,600	5,000
Beam (at Waterline)/ft	500	500	500	500
Draft/ft	80	80	80	80
Displacement/tons	500,000	800,000	500,000	1,800,000
Speed/knots	18	18	18	12
Power/shp	200,000	240,000	200,000	200,000

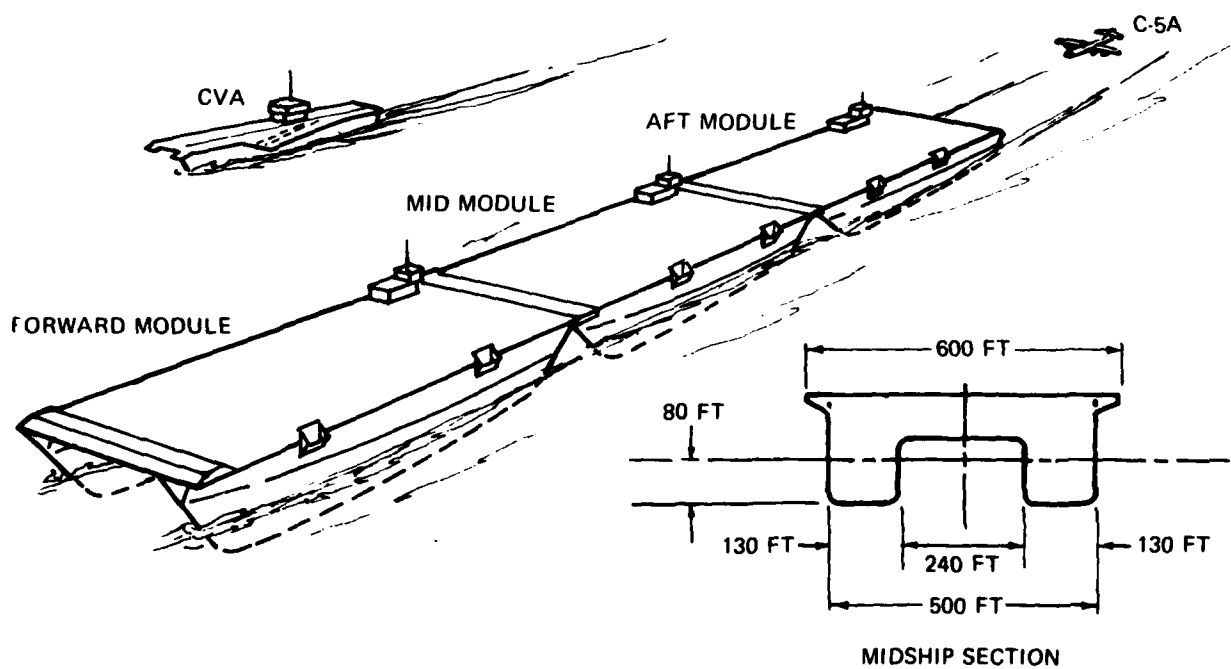


Figure 1 - Air-to-Sea Interface, Integrated Supership System

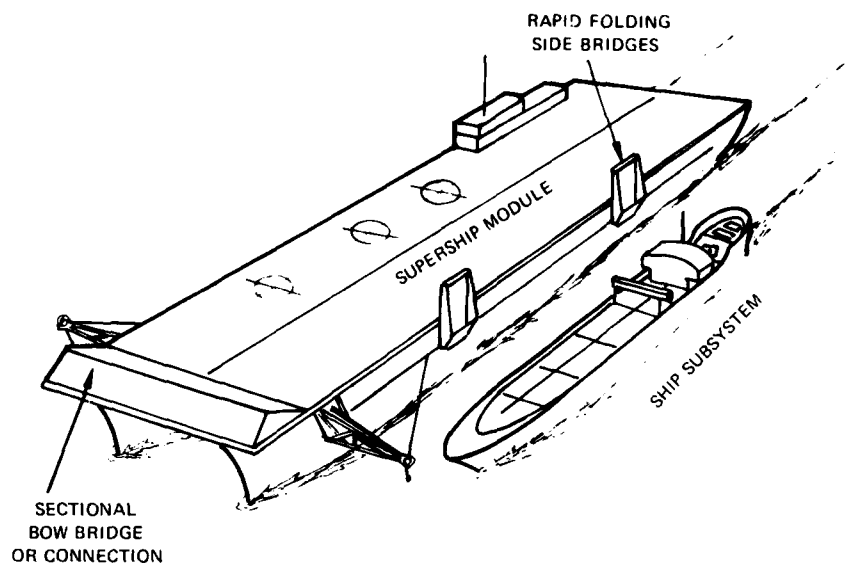


Figure 2 – Supership Modules

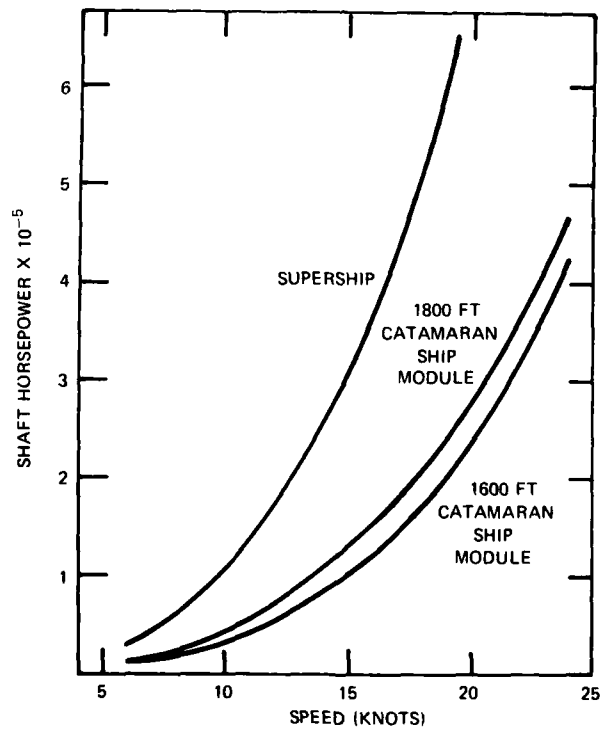


Figure 3 – Estimated Power for the Supership and Its Catamaran Ship Modules

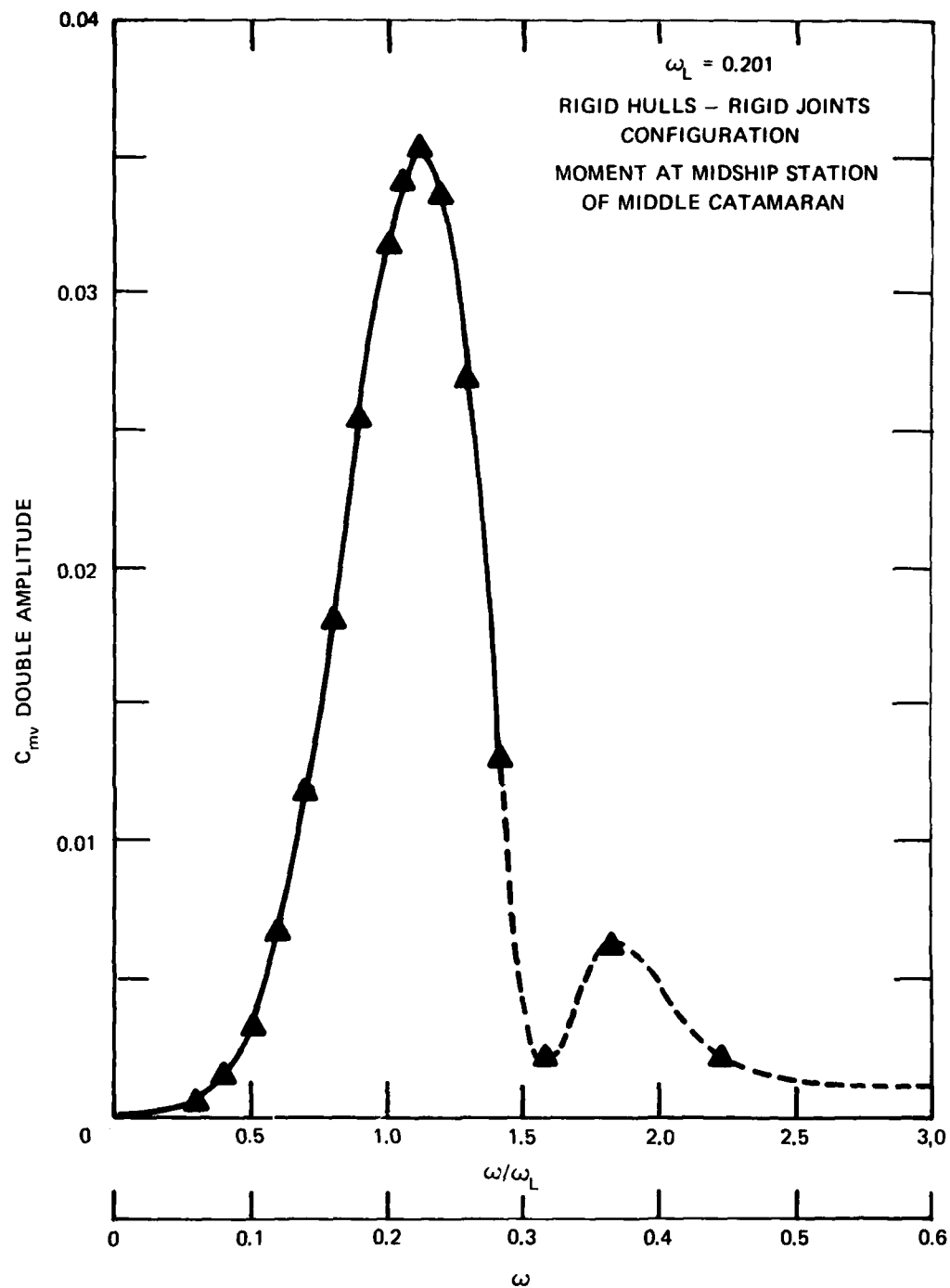


Figure 4 - Vertical Bending Moment Nondimensional Transfer Function for Rigid ISUS

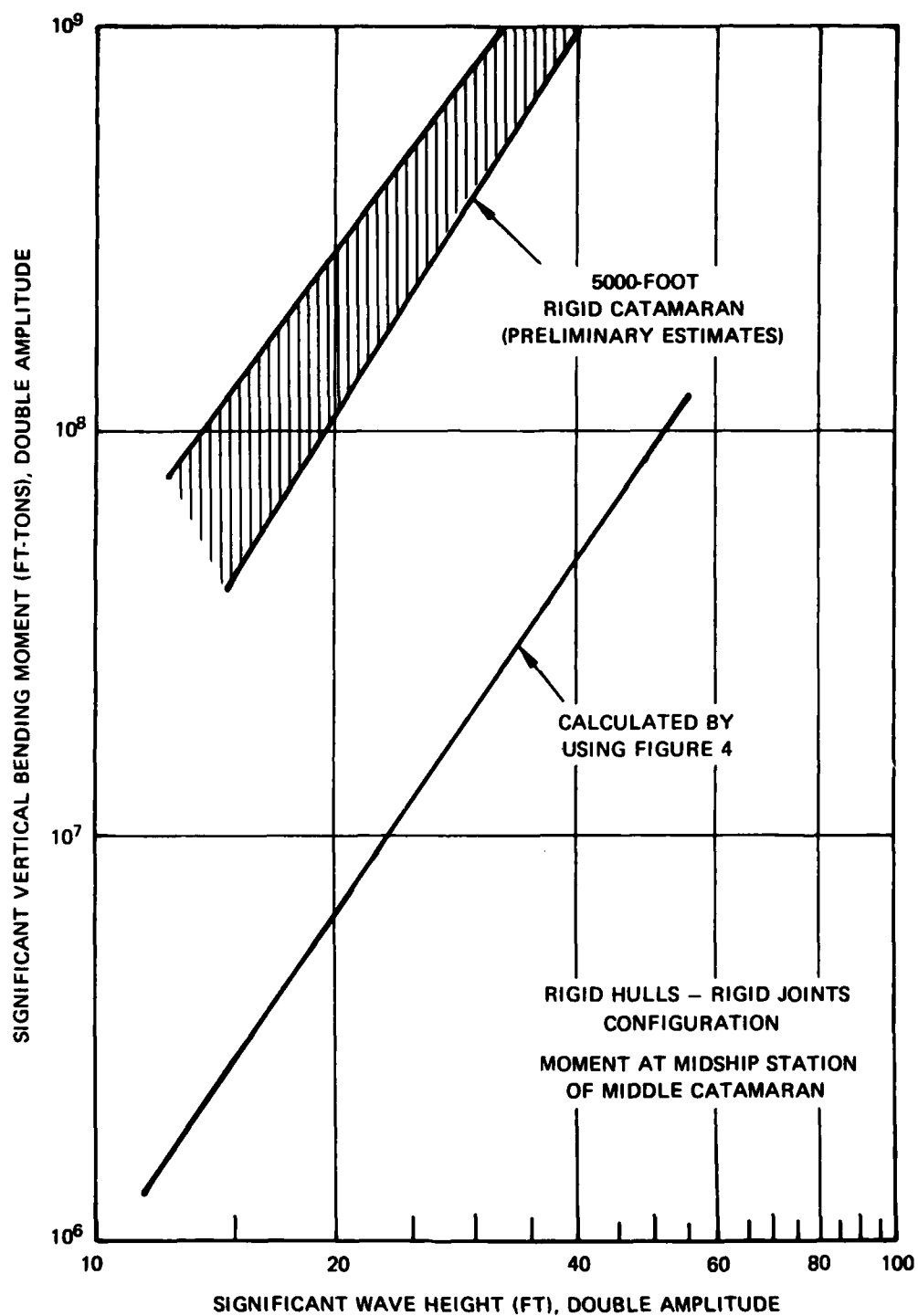


Figure 5 – Significant Vertical Bending Moment versus Significant Wave Height for Rigid ISUS

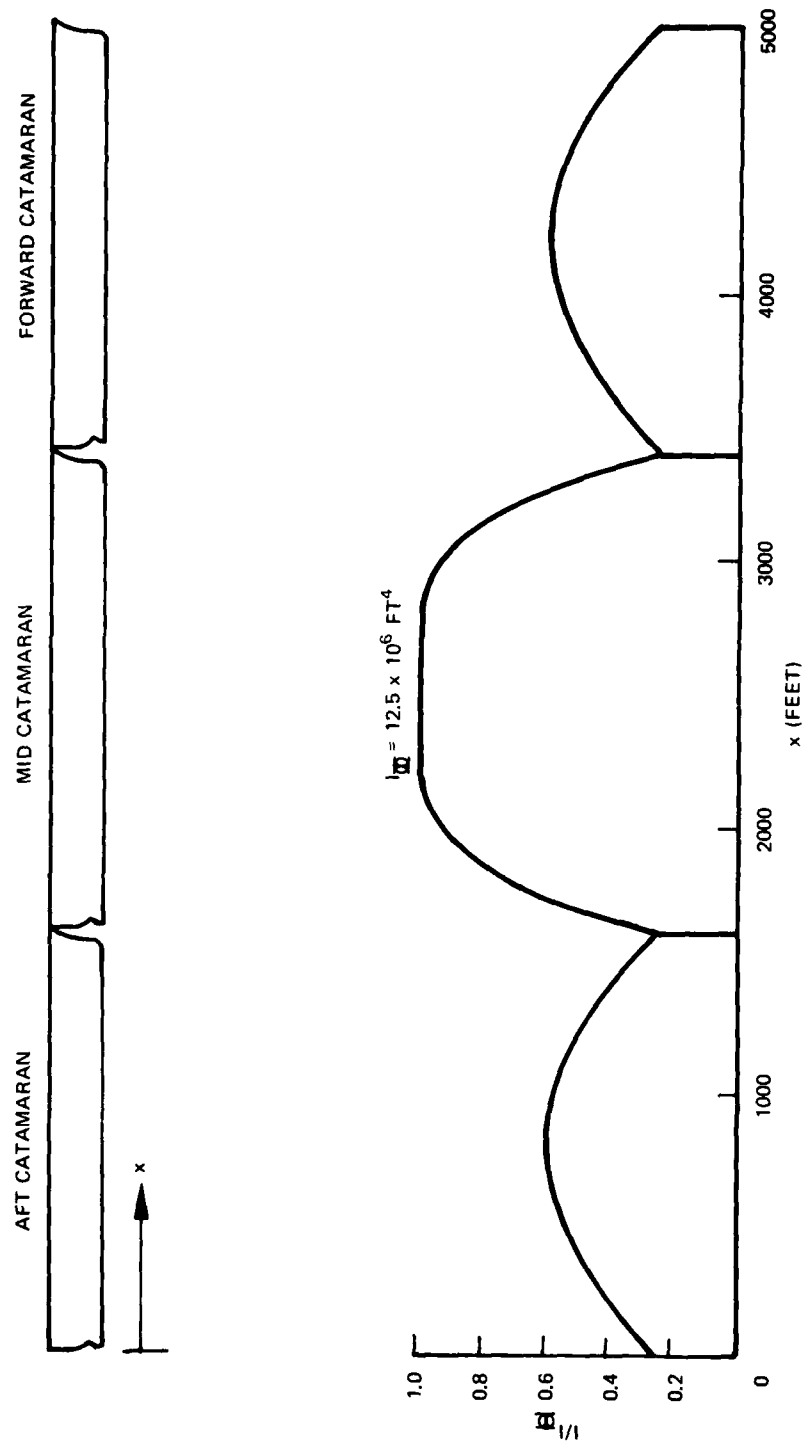


Figure 6 — Hull Moment of Inertia Distribution for Rigid ISUS

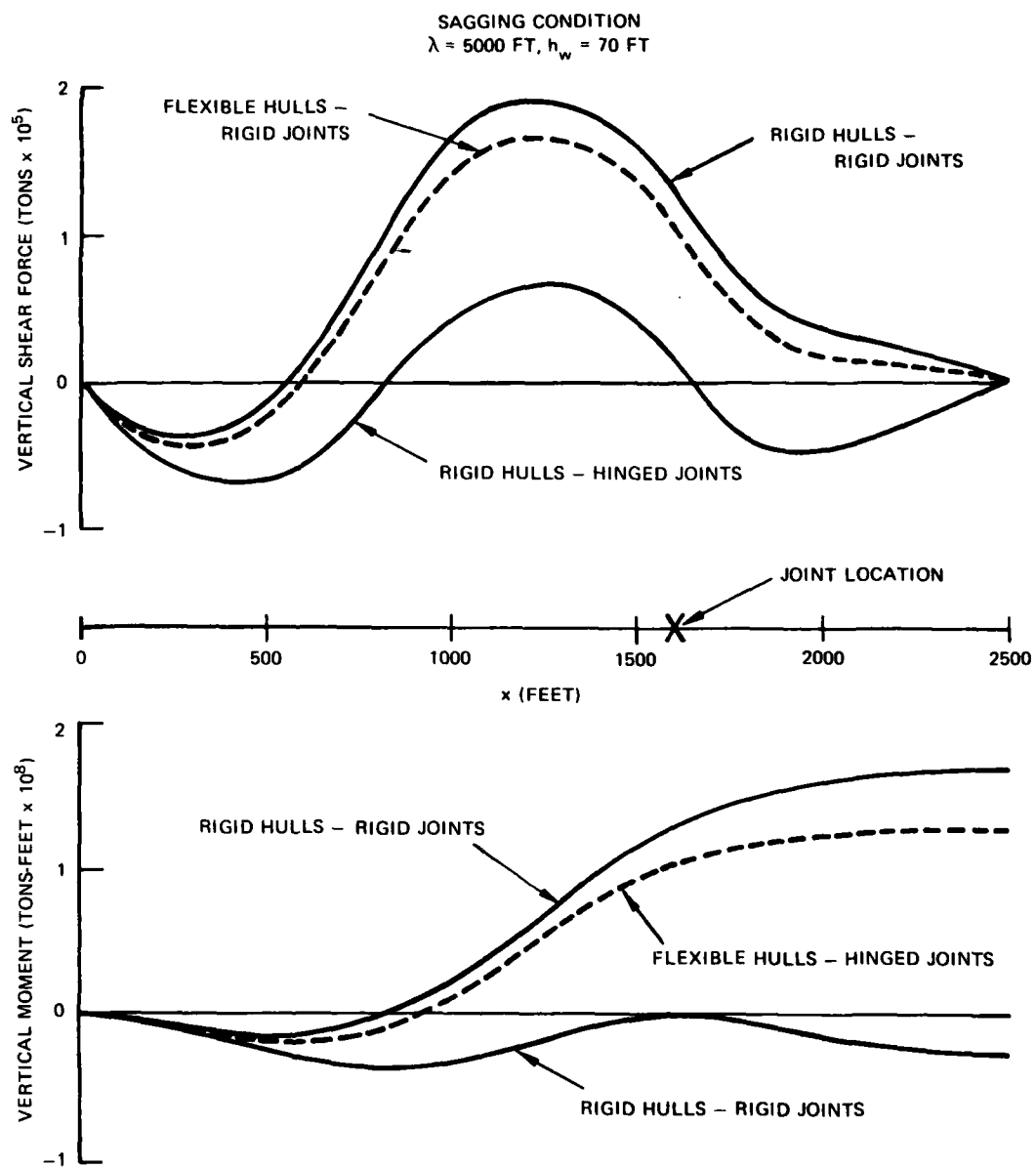


Figure 7 - Sagging Load Distribution on the ISUS

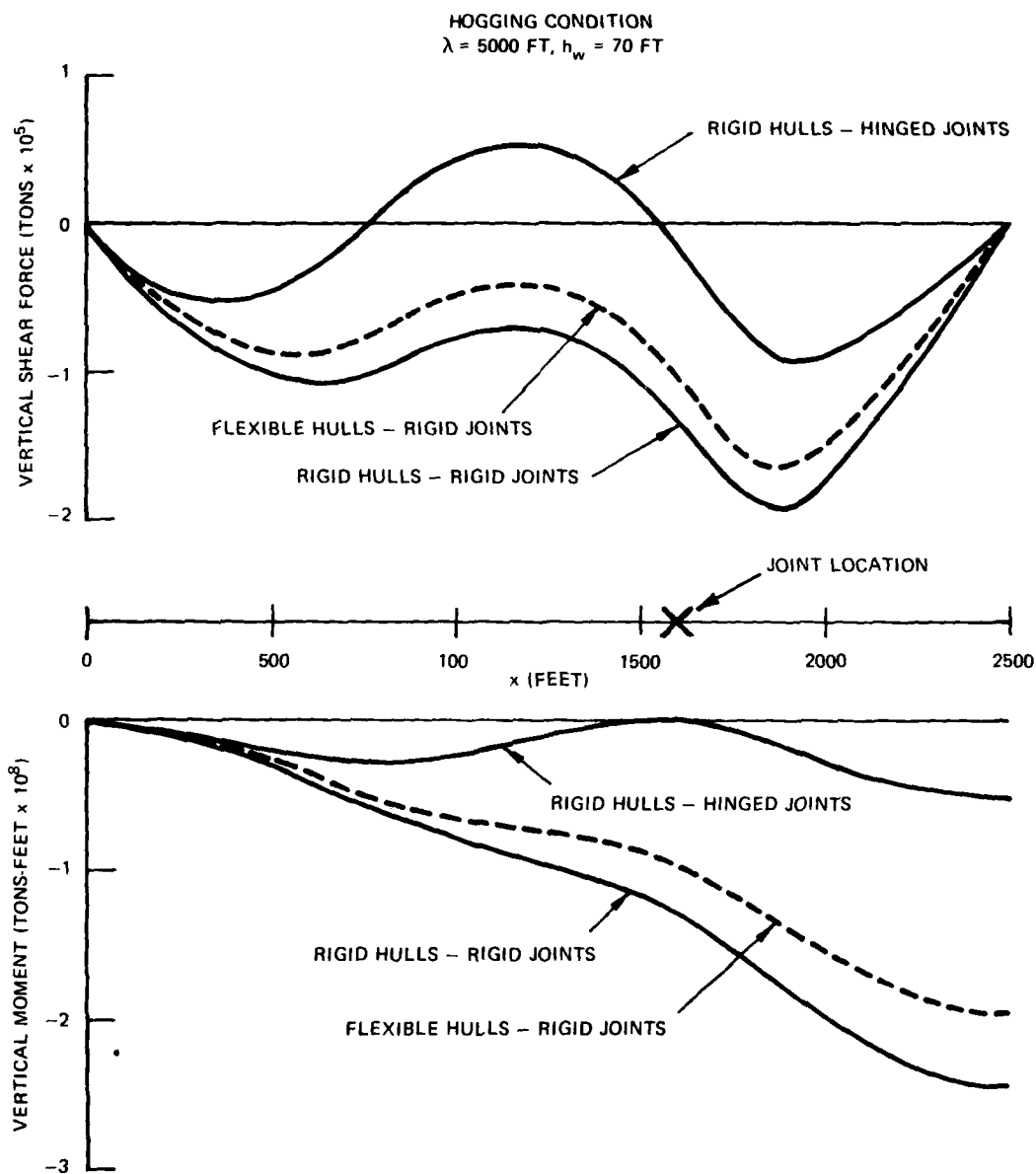


Figure 8 - Hogging Load Distribution on the ISUS

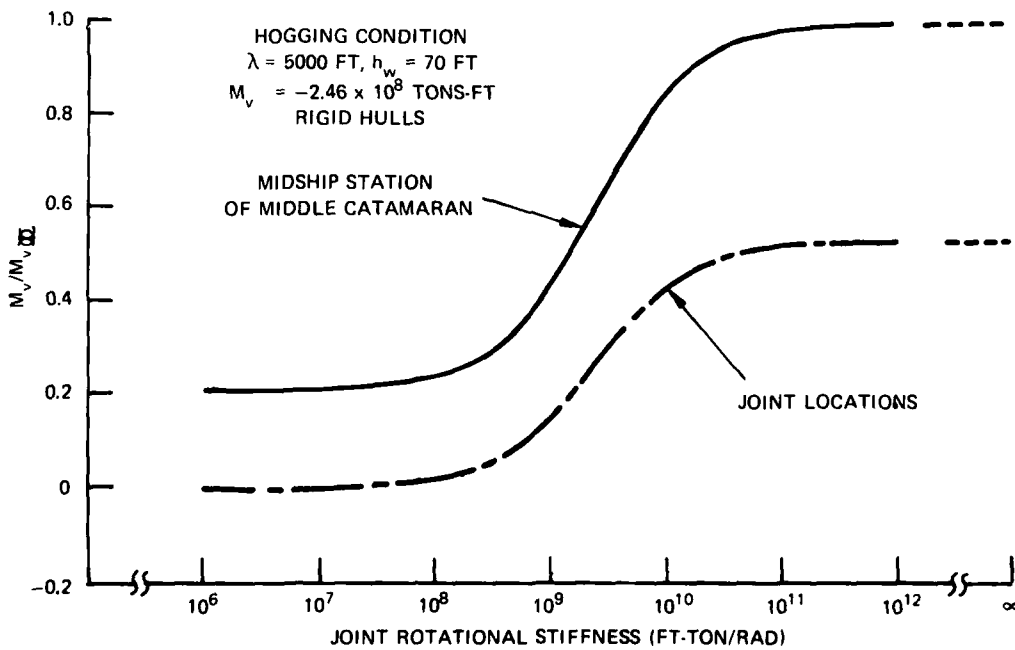
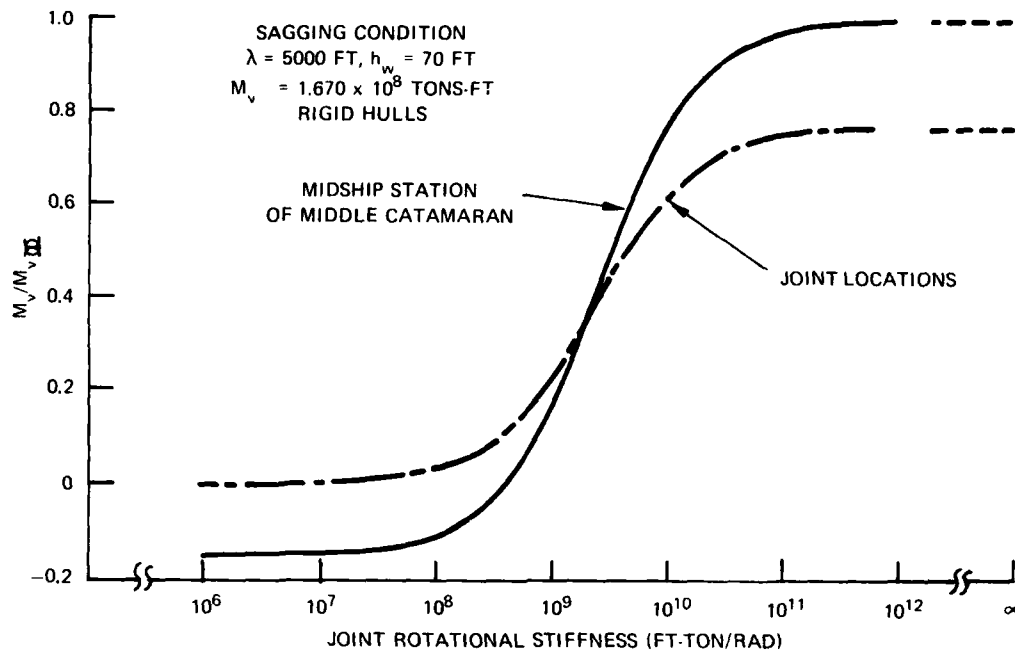


Figure 9 – Influence of Joint Stiffness on Vertical Bending Moment

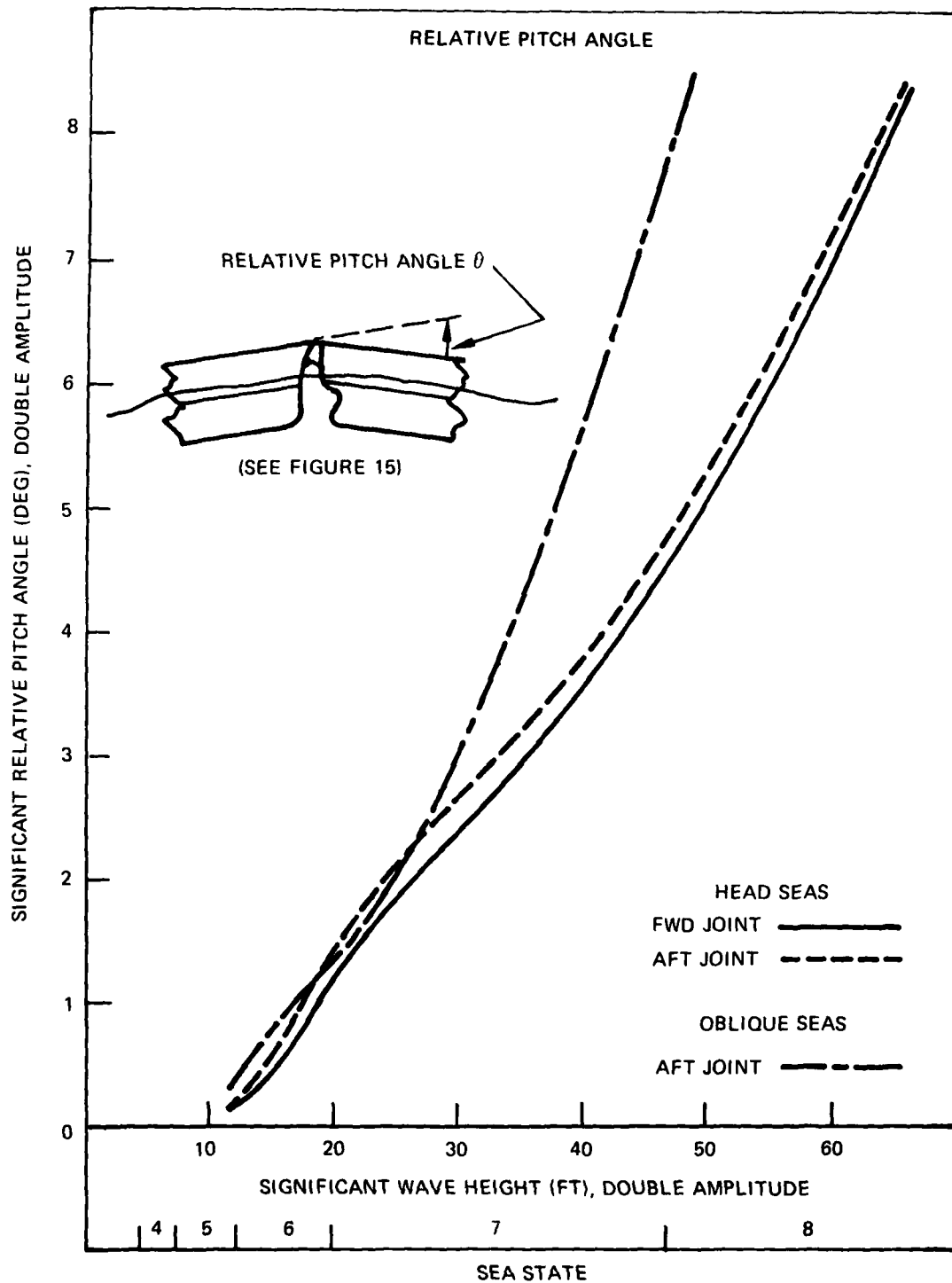


Figure 10 – Significant Relative Pitch Angle as a Function of Significant Wave Height for Hinged ISUS

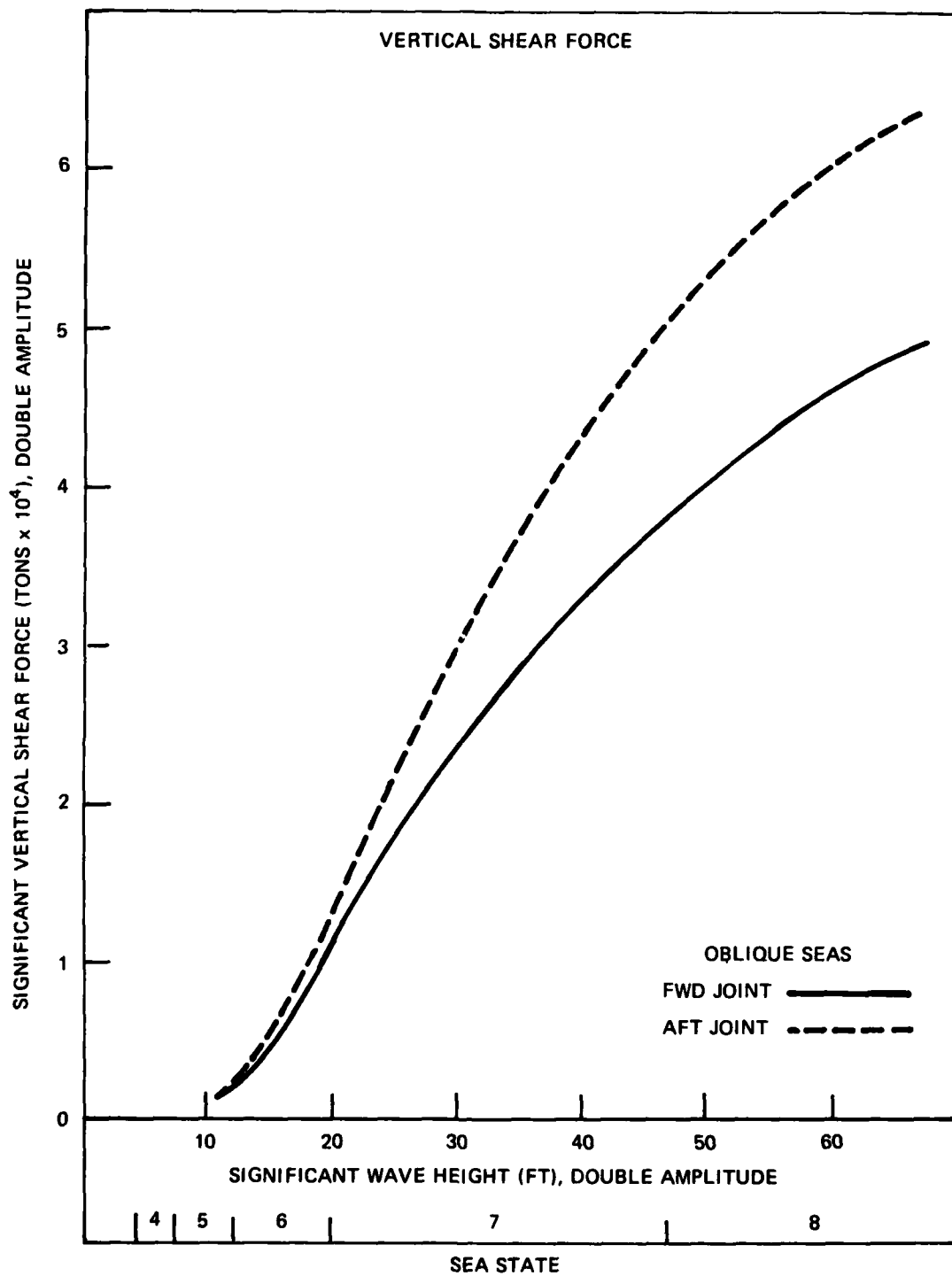


Figure 11 – Significant Vertical Shear Force as a Function of Significant Wave Height for Hinged ISUS

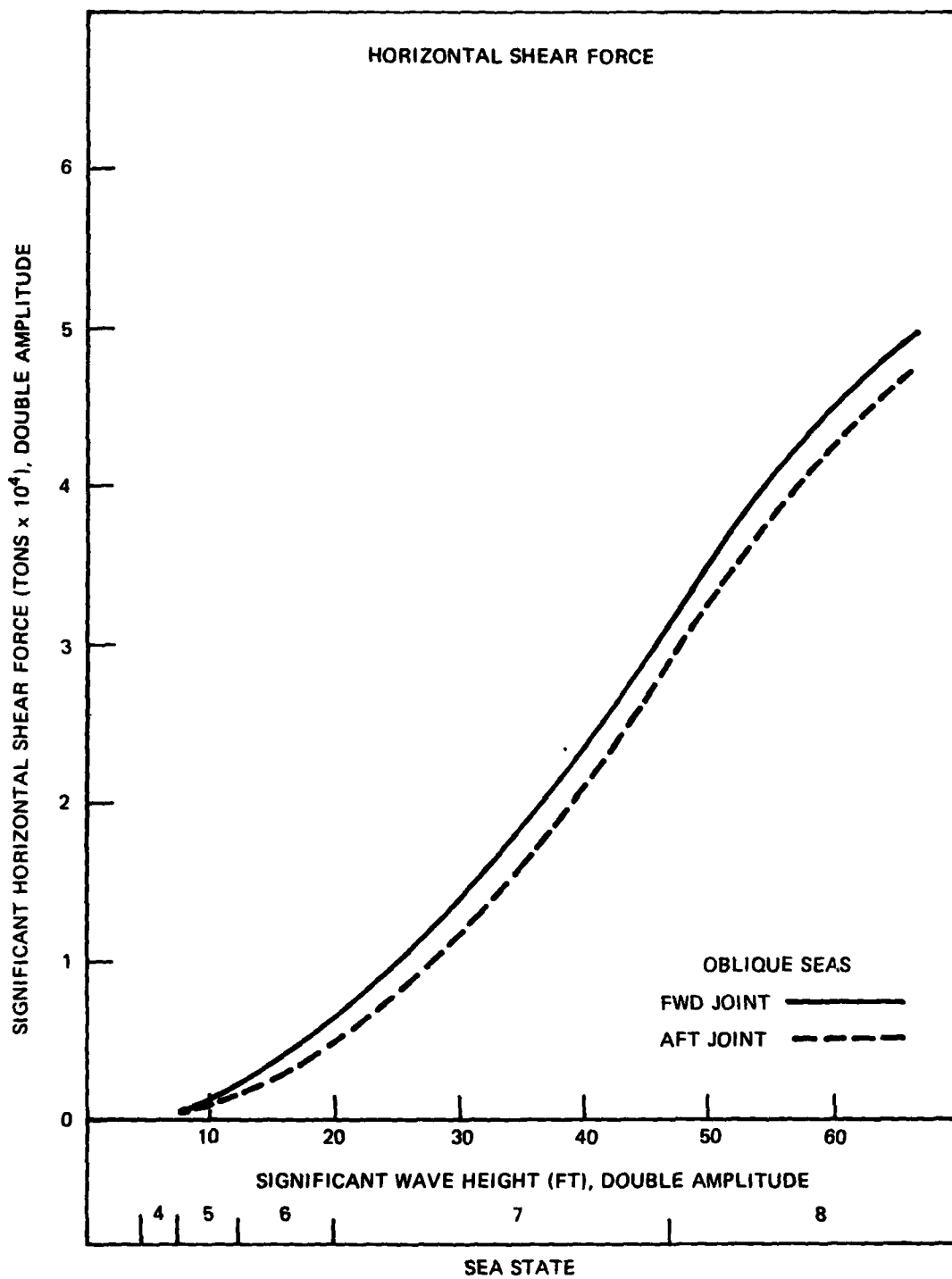


Figure 12 – Significant Horizontal Shear Force as a Function of Significant Wave Height for Hinged ISUS

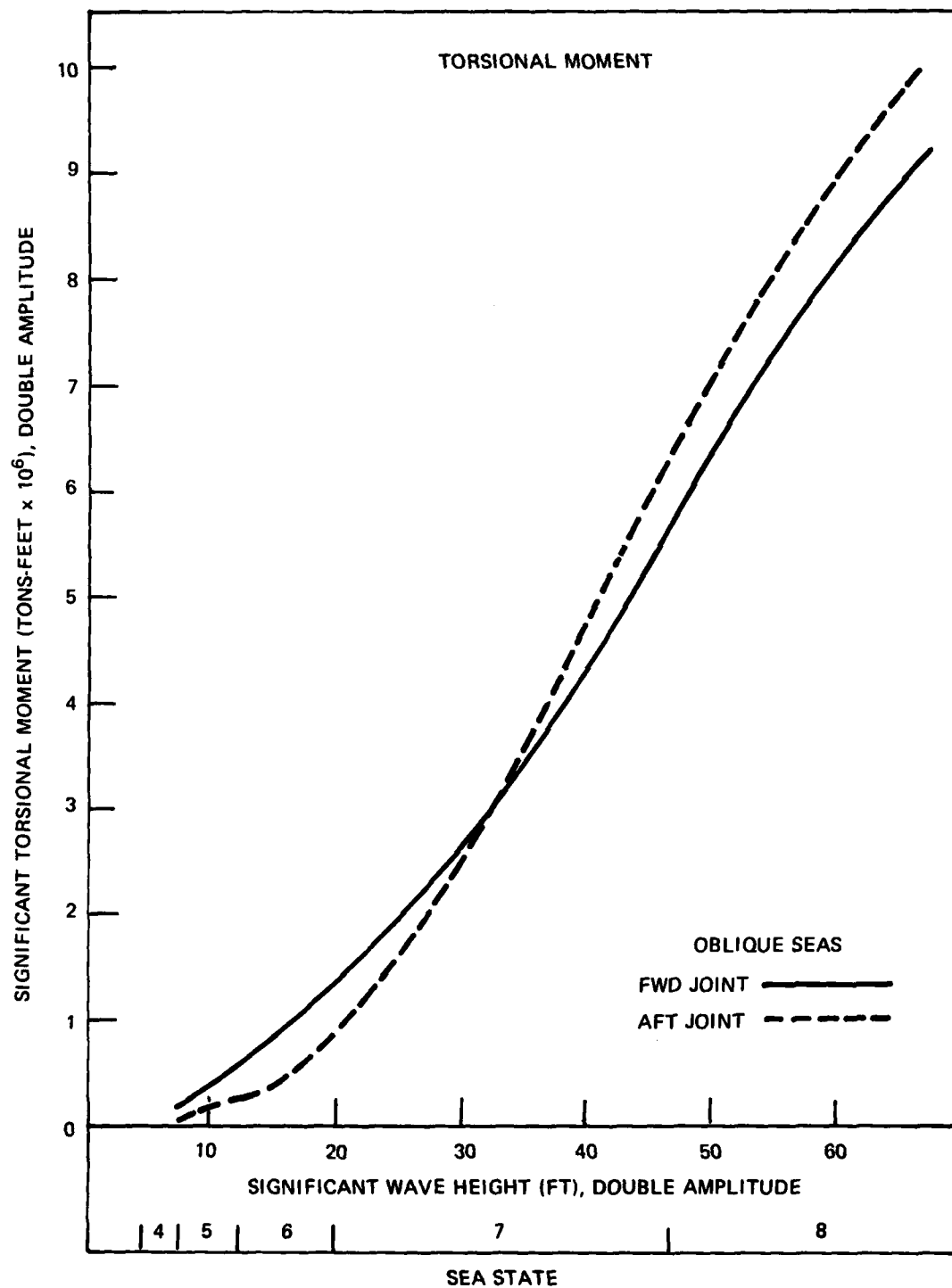


Figure 13 – Significant Torsional Moment as a Function of Significant Wave Height for Hinged ISUS

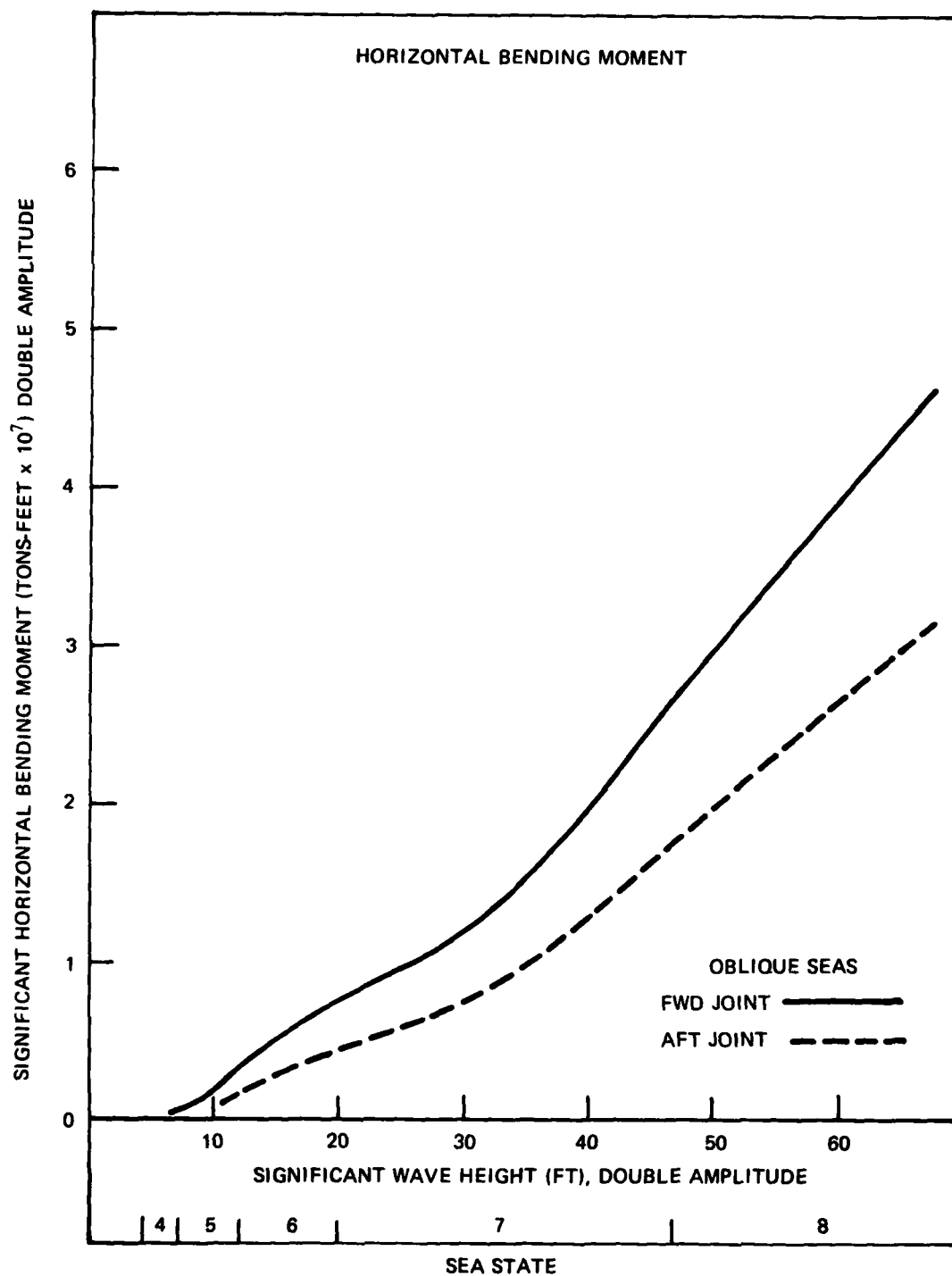


Figure 14 -- Significant Horizontal Bending Moment as a Function of Significant Wave Height for Hinged ISUS

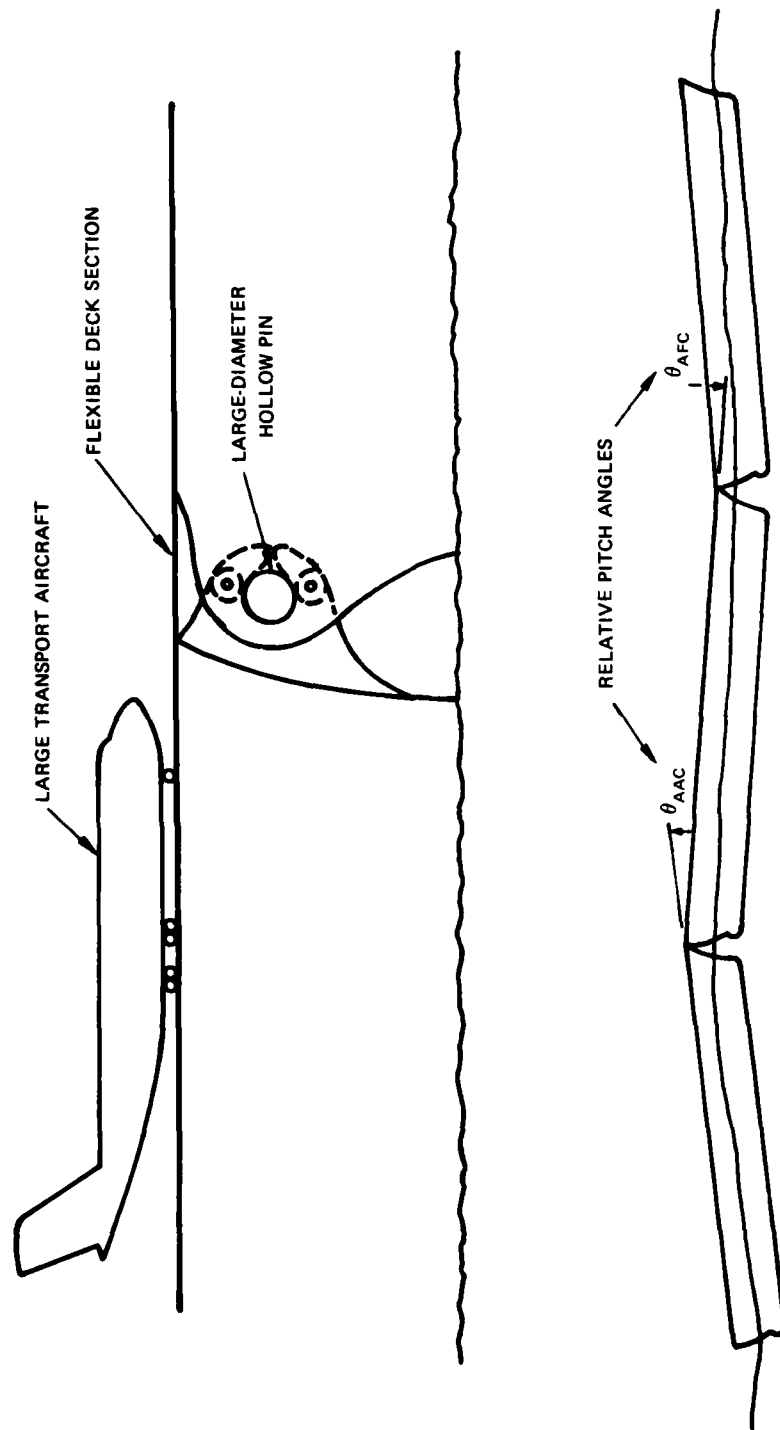


Figure 15 – Hinged Joining Mechanism Concept

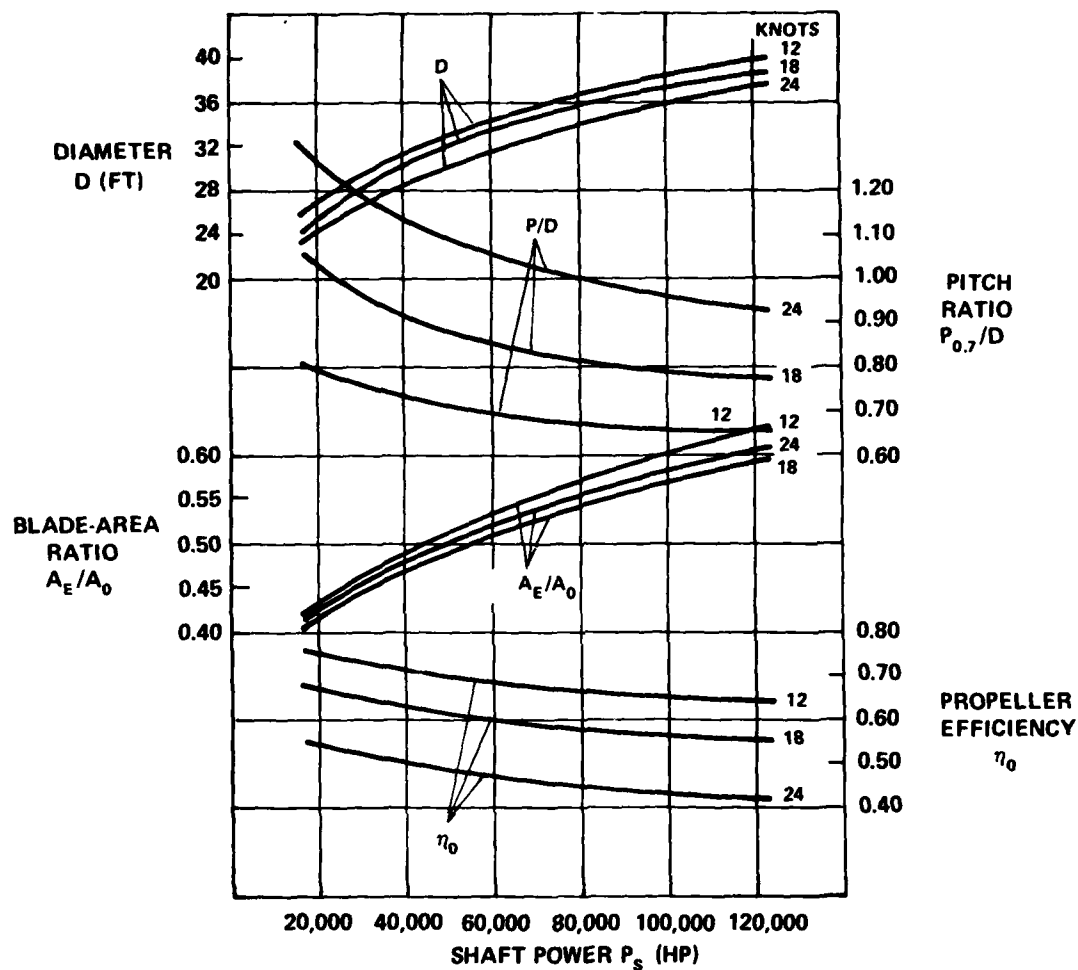


Figure 16 – Characteristics of Propellers Optimized for Shaft Speed of 80 RPM as a Function of Delivered Shaft Power for Various Ship Speeds

(Blade number $Z = 5$, wake $w = 0.20$, shaft submergence $h = 60$ ft)

Figure 17 - Weight of Optimum Fixed-Bladed and Built-up Propellers of Different Materials

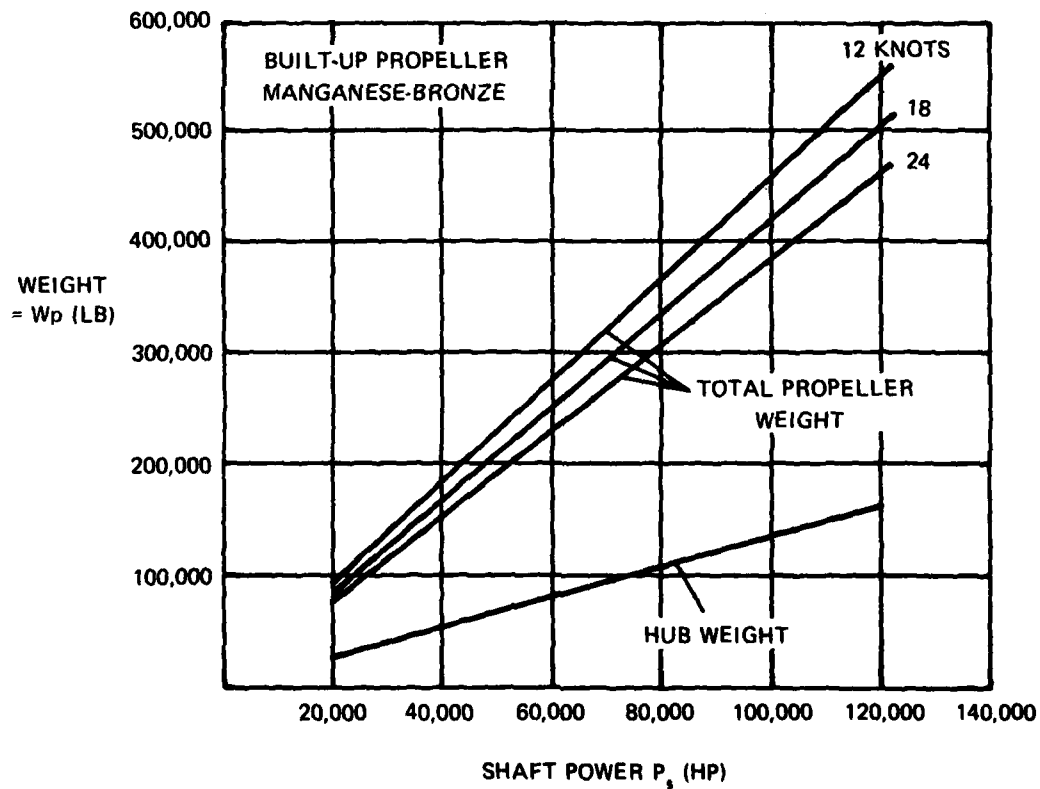
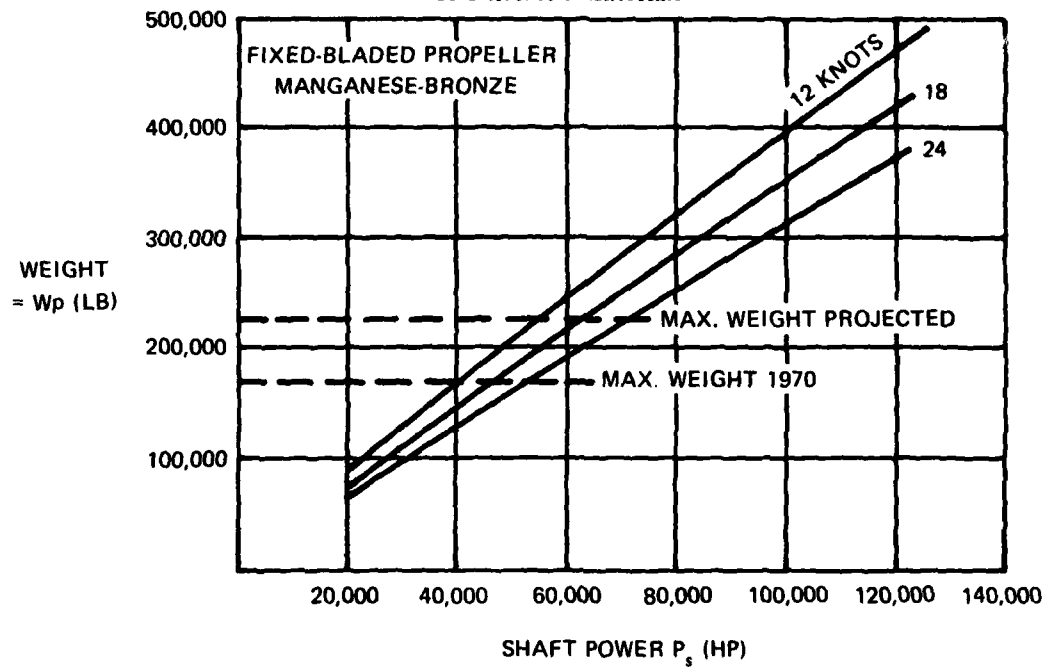
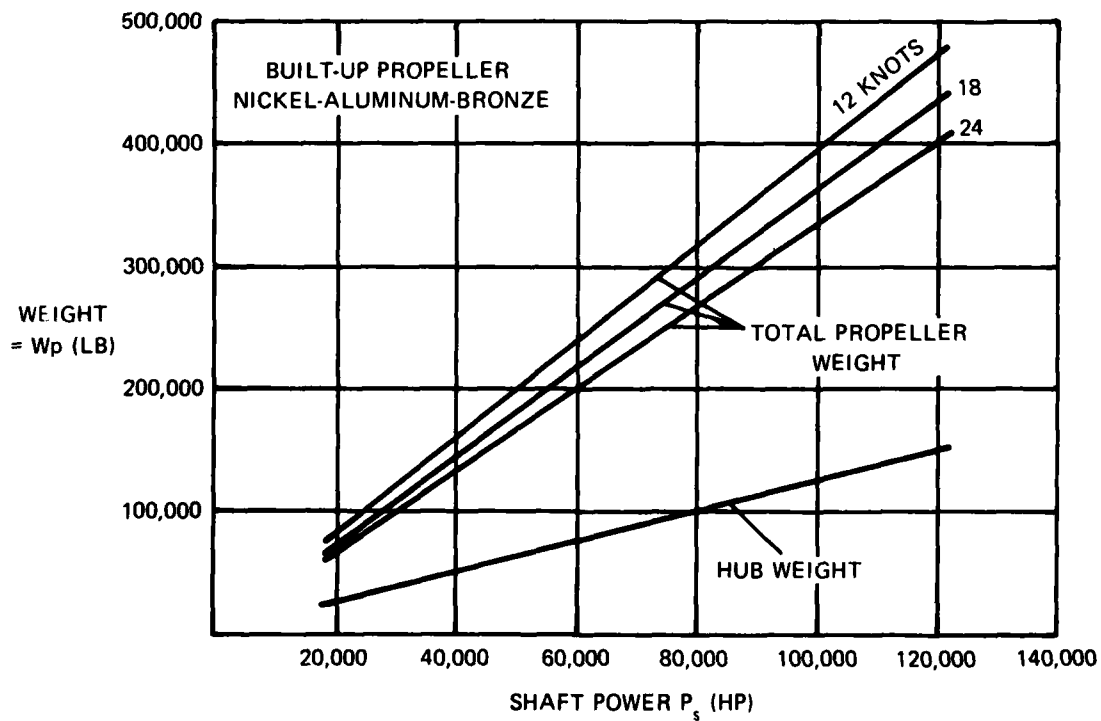
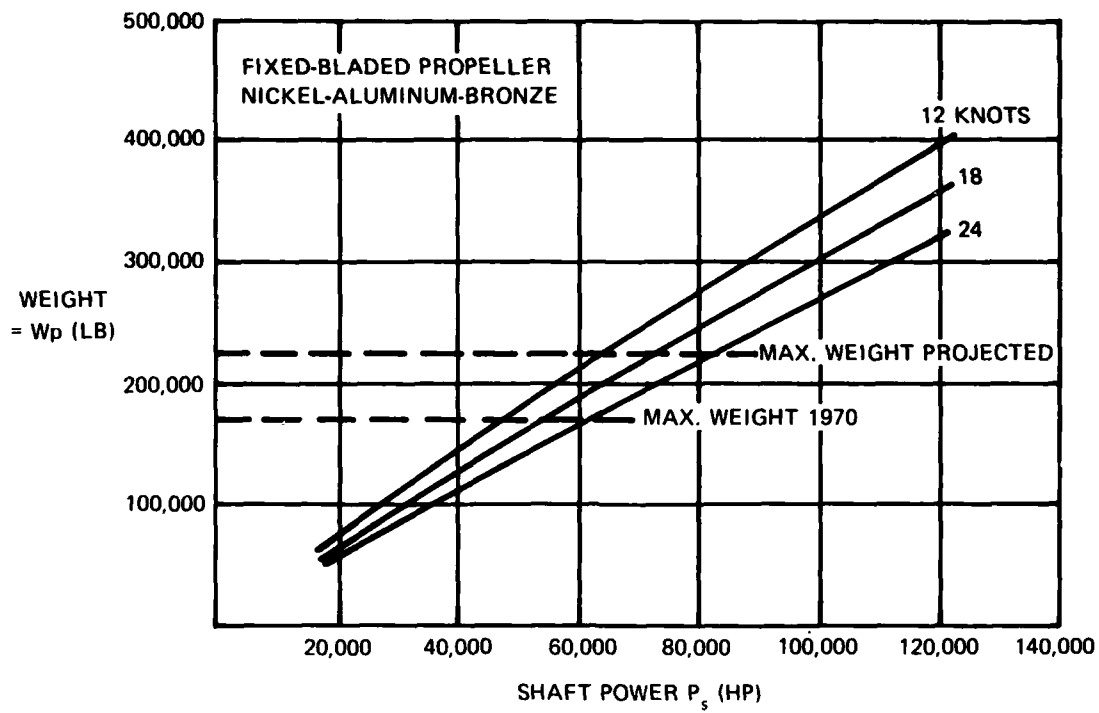


Figure 17 (Continued)



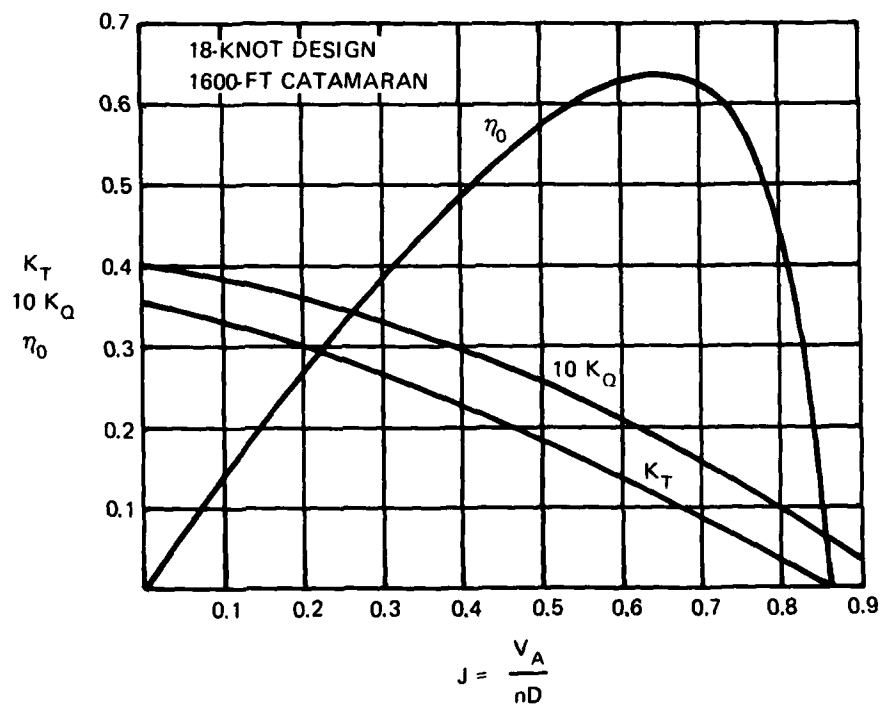
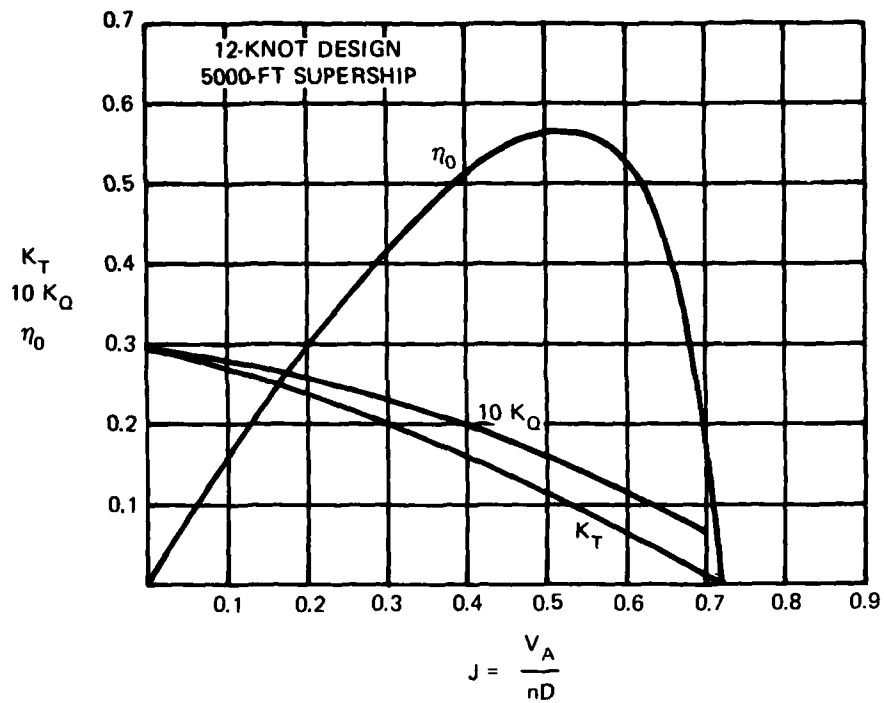


Figure 18 – Open Water Characteristics for Propellers Designed to Absorb 100,000 SHP at 80 RPM

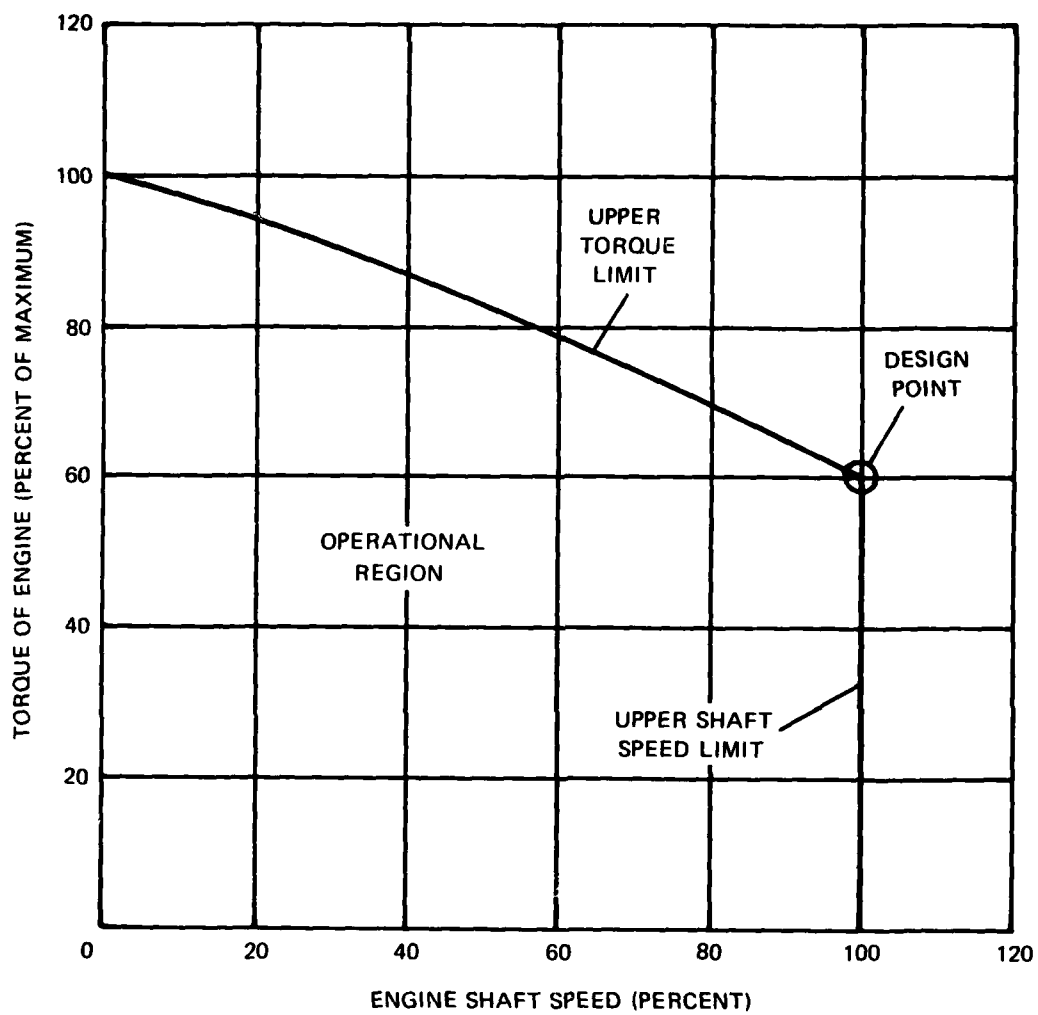


Figure 19 – Performance Curve of Steam Turbine

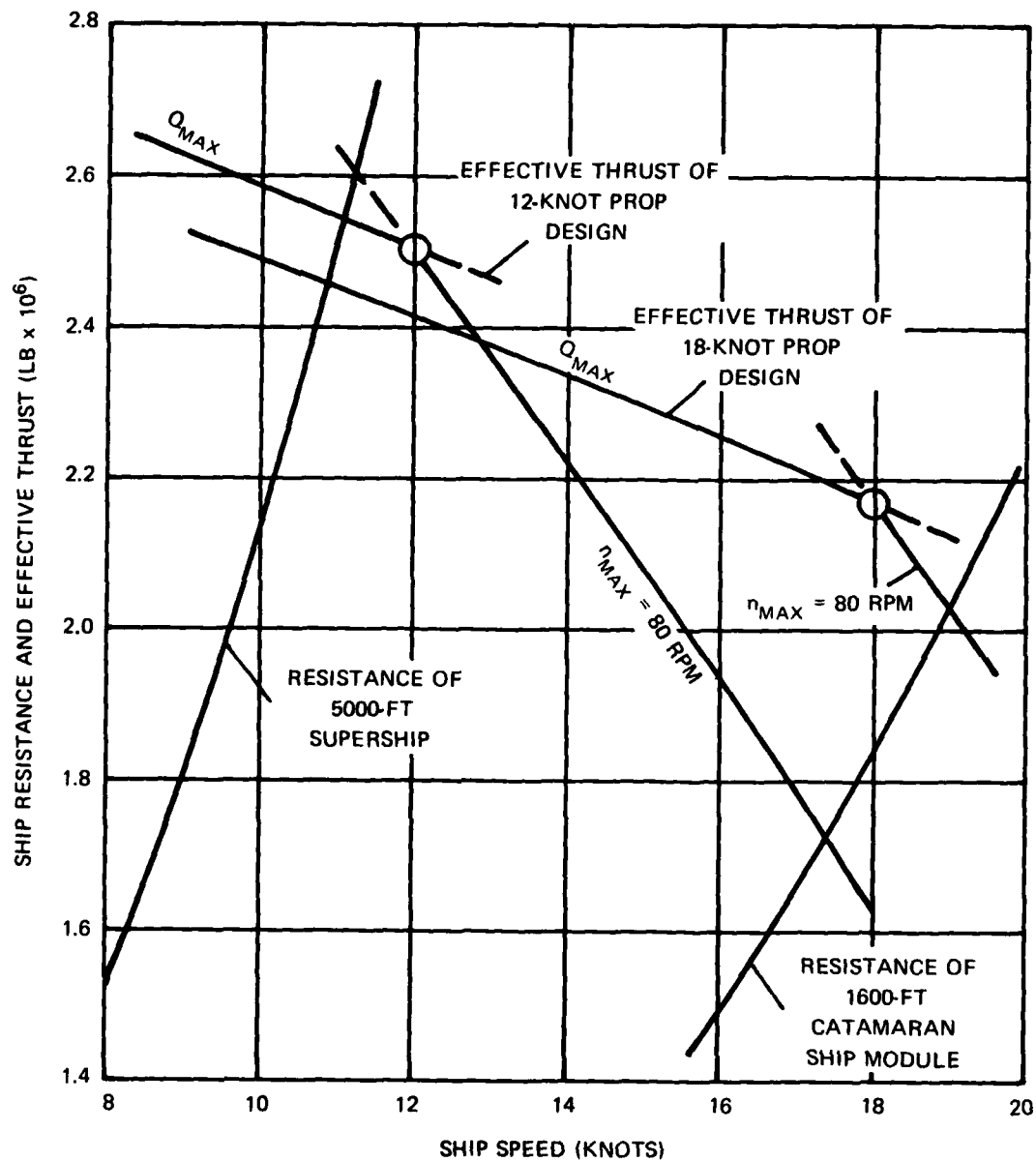


Figure 20 – Off-Design Performance of Twin-Screw Propulsion Arrangement with Propellers Designed as Optimum for 12 and 18 Knots

(thrust deduction $t = 0.15$)

Figure 21 — Characteristics of Propellers Optimized at a Specific Speed
for Given Diameter as a Function of Delivered Shaft Power

(Blade number $Z = 5$, wake $w = 0.20$)

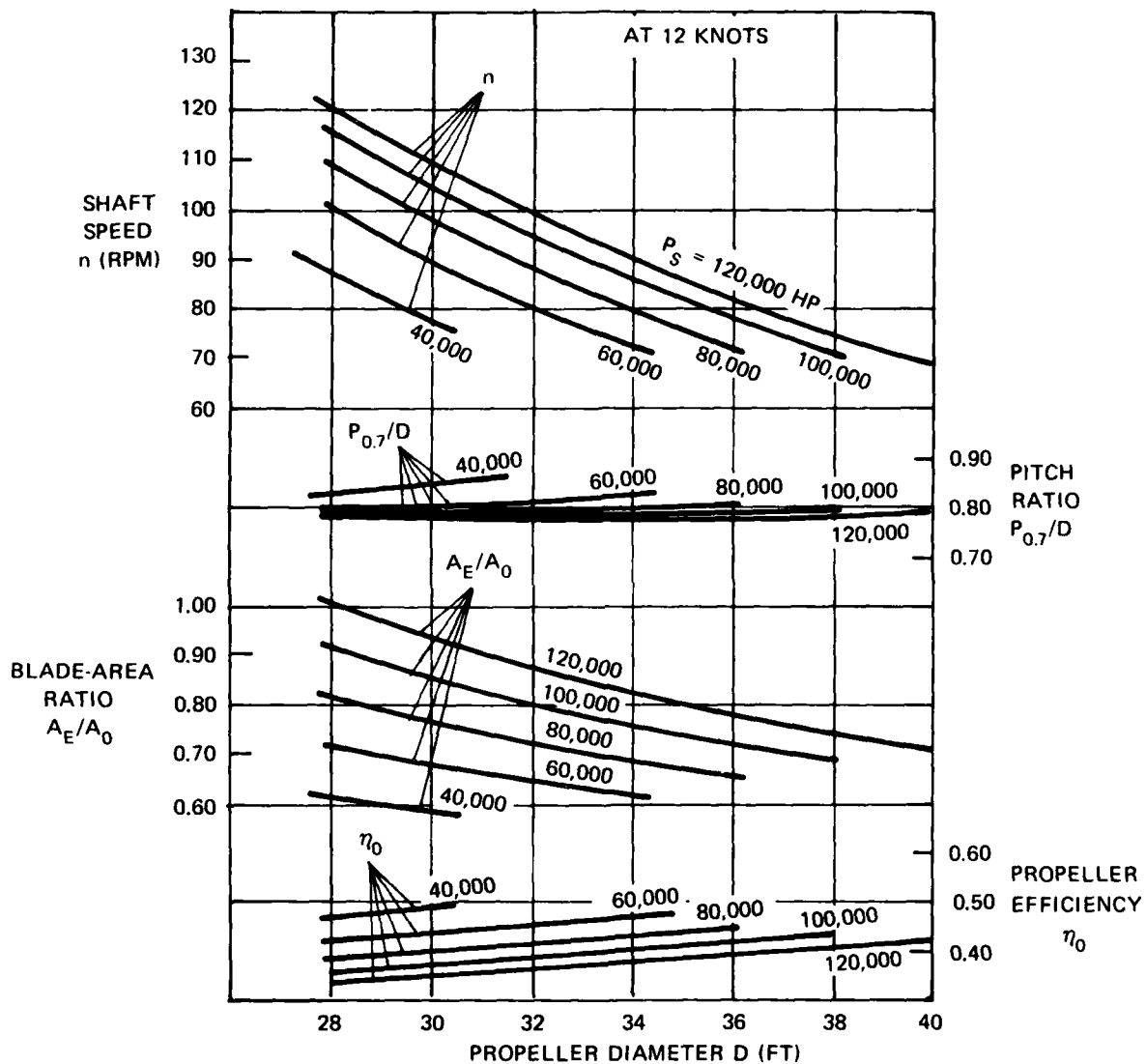


Figure 21 (Continued)

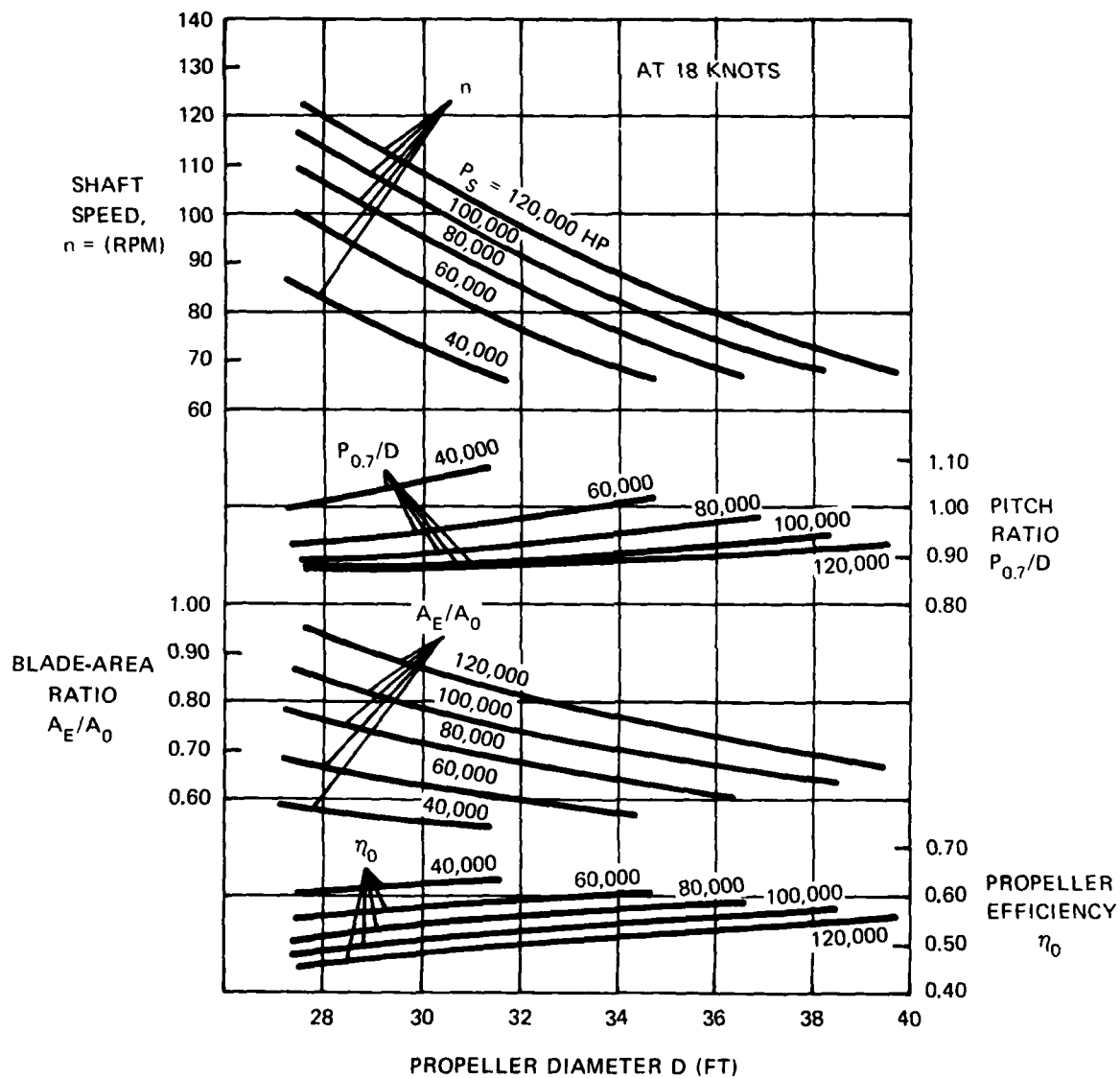


Figure 22 Weights of Optimum Fixed-Bladed and Controllable-Pitch Ni-Al-Bronze Propellers Designed for Specific Ship Speeds

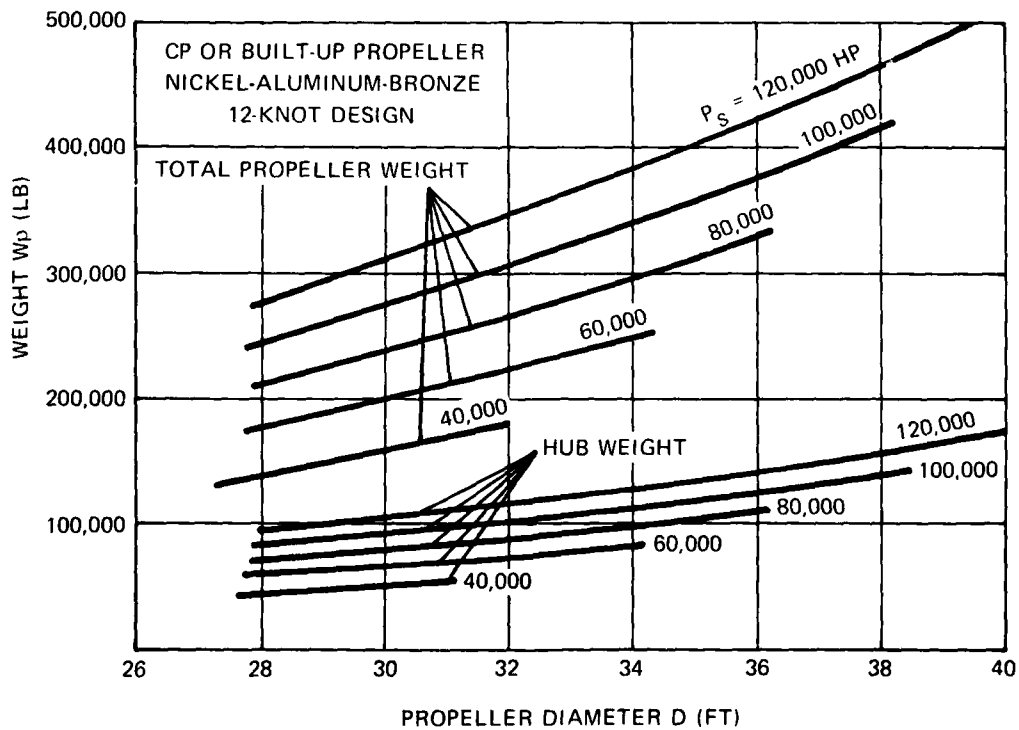
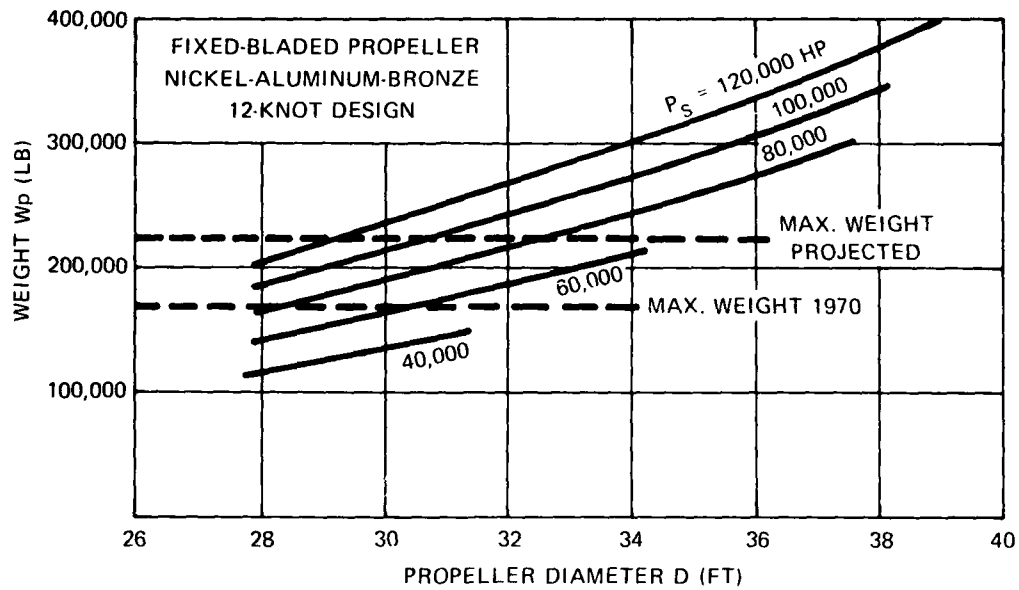
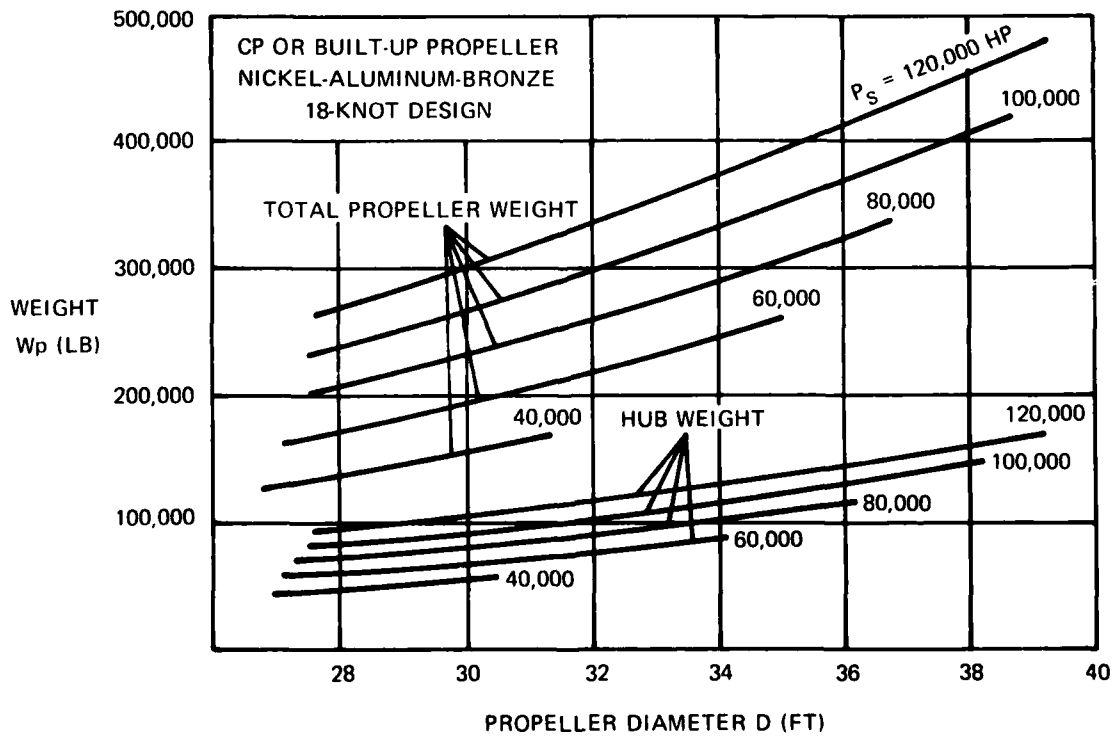
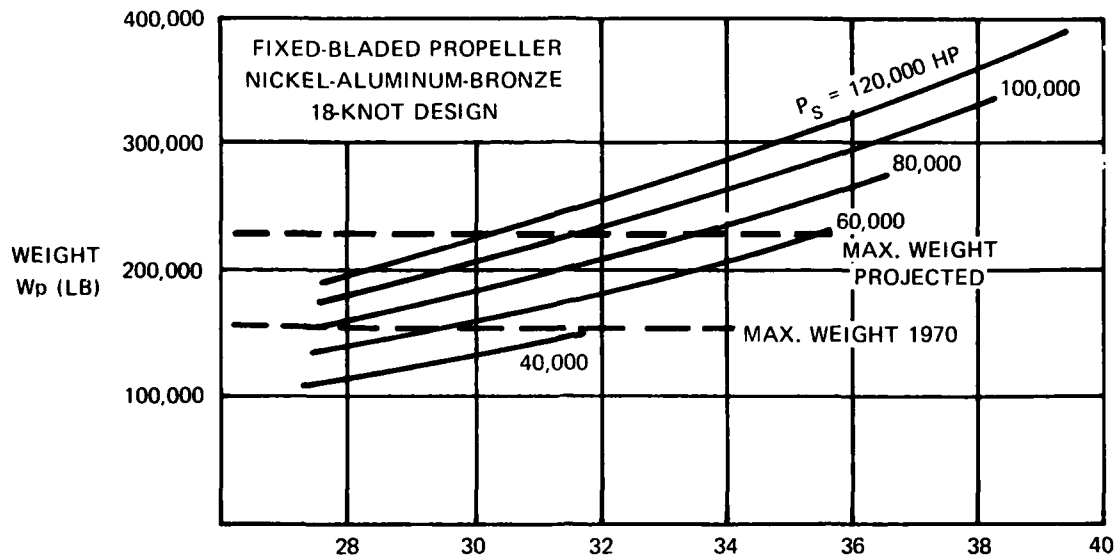


Figure 22 (Continued)



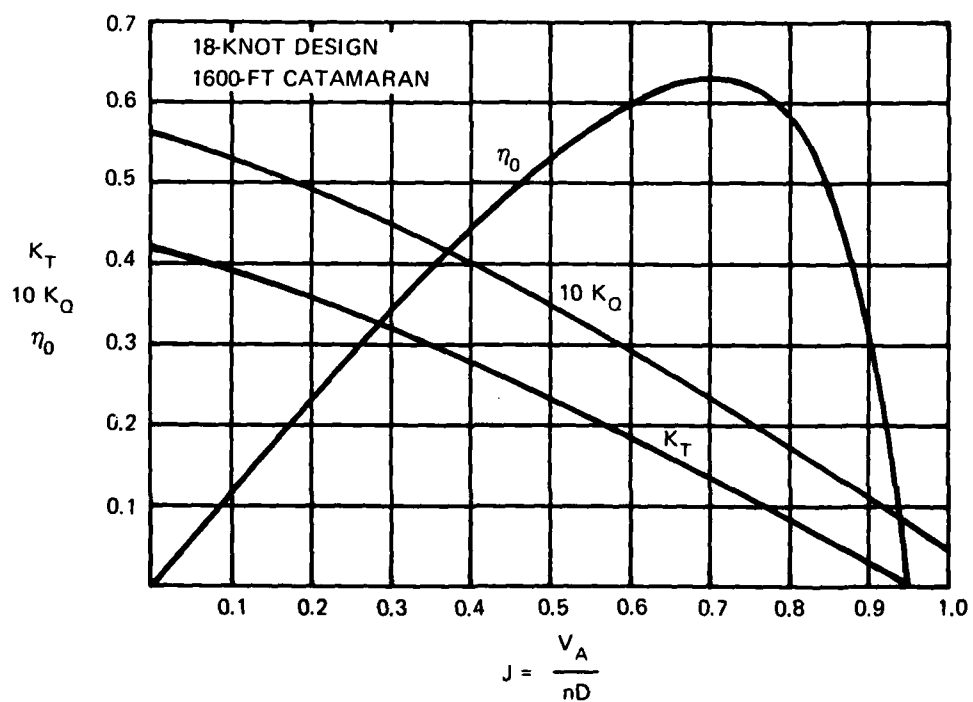
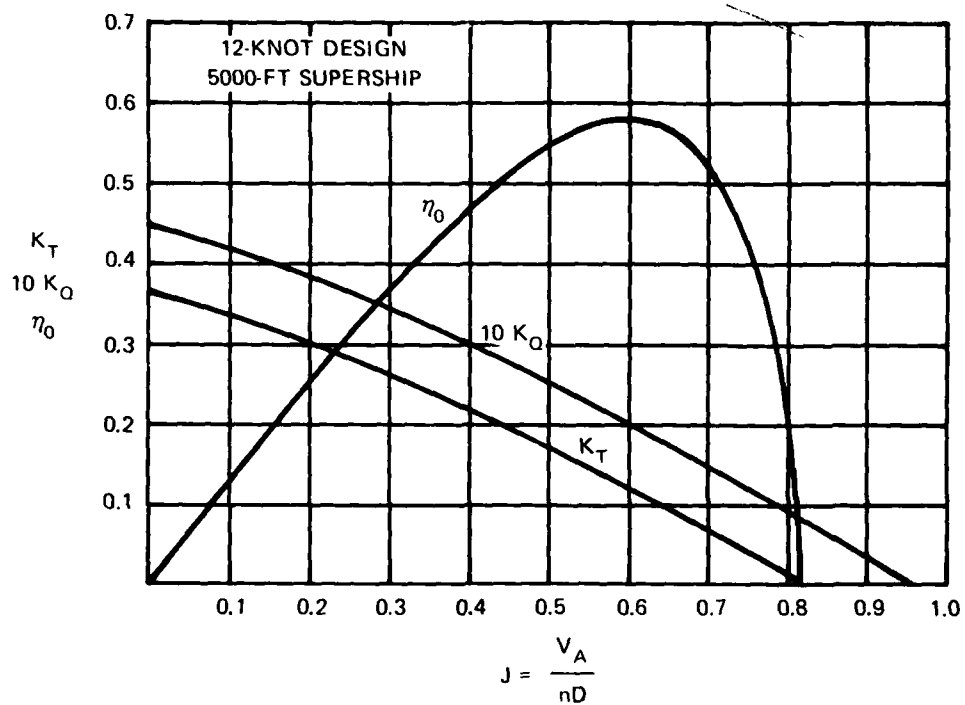


Figure 23 – Open Water Characteristics for Propellers Designed to Absorb 100,000 SHP on 30-Foot Diameter

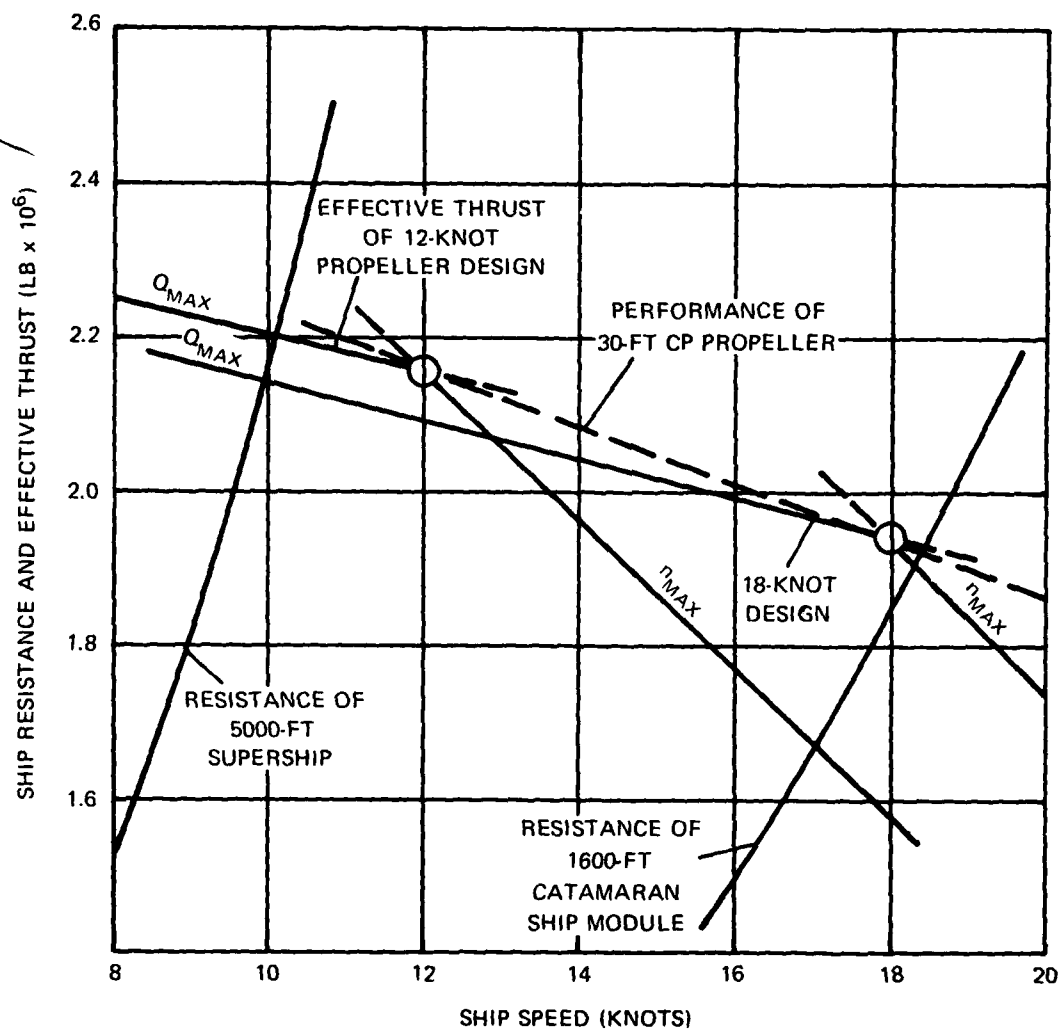


Figure 24 – Off-Design Performance of Twin-Screw Propulsion Arrangements with 30-Foot-Diameter Propellers Optimized for 12 and 18 Knots

(Thrust deduction $t = 0.15$)

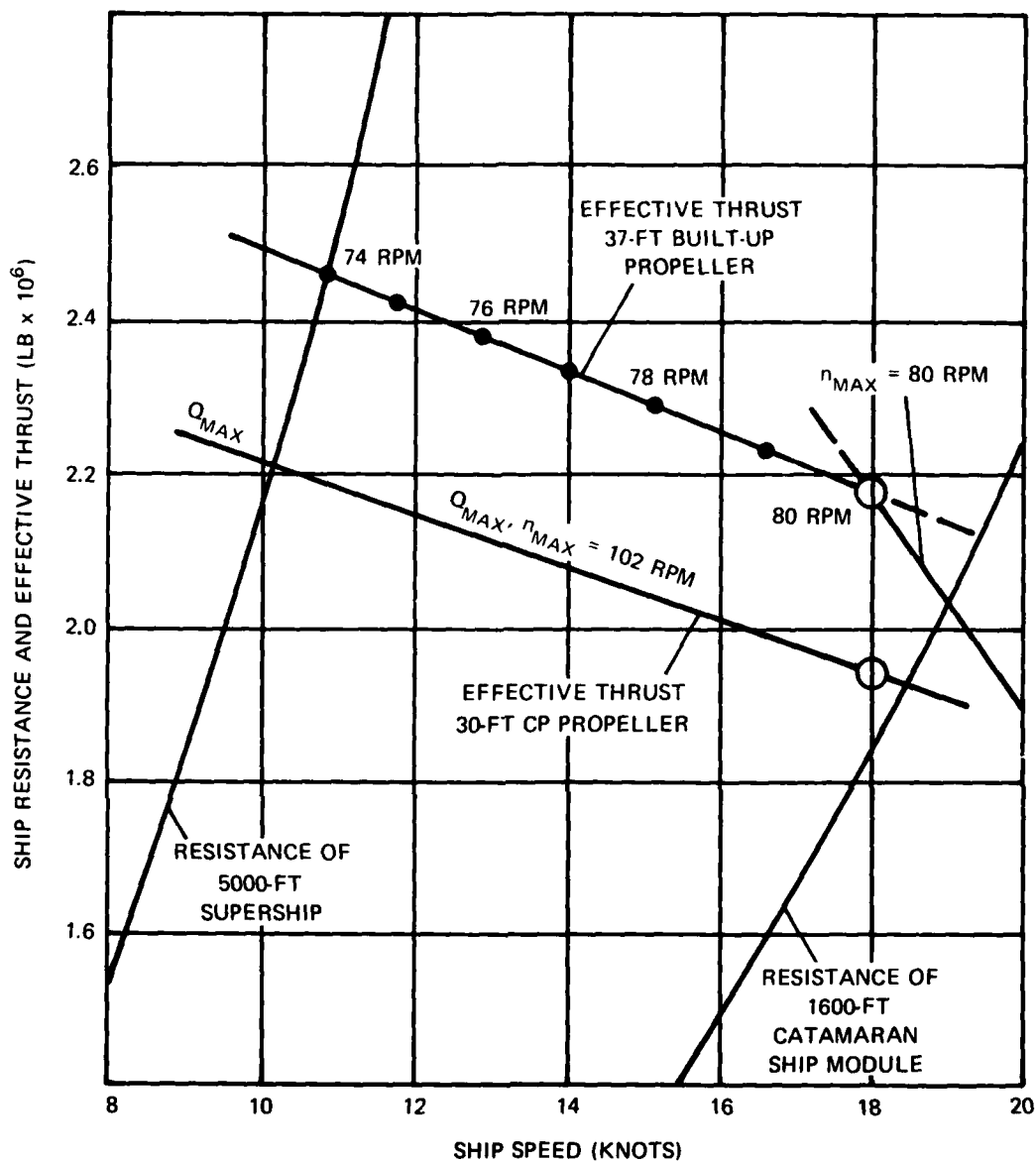


Figure 25 – Propulsion Study Results for Performance of 37-Foot, 80-RPM Built-up Propeller and 30-Foot, 102-RPM CP Propeller

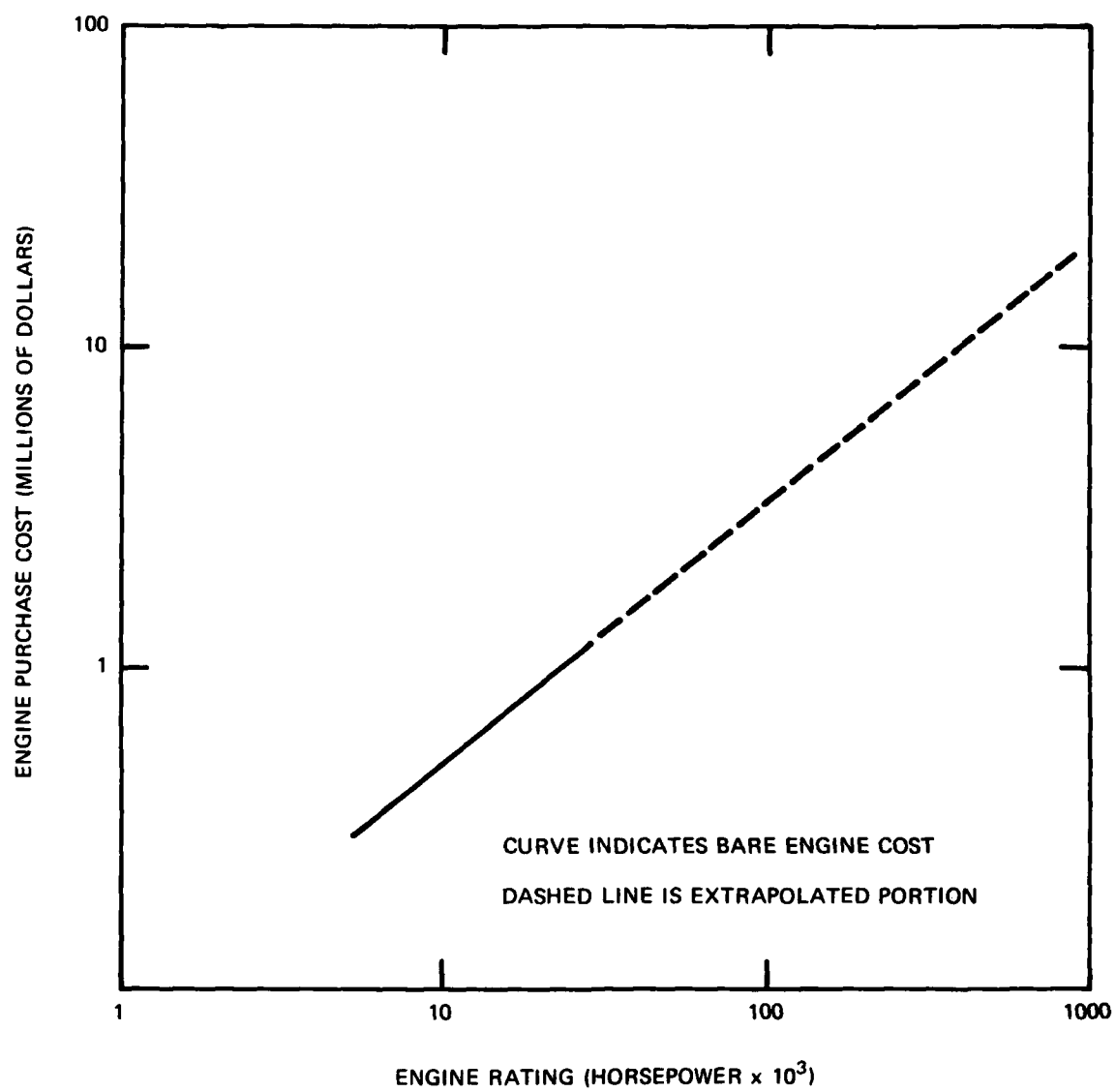


Figure 26 – Diesel Engine Procurement Cost

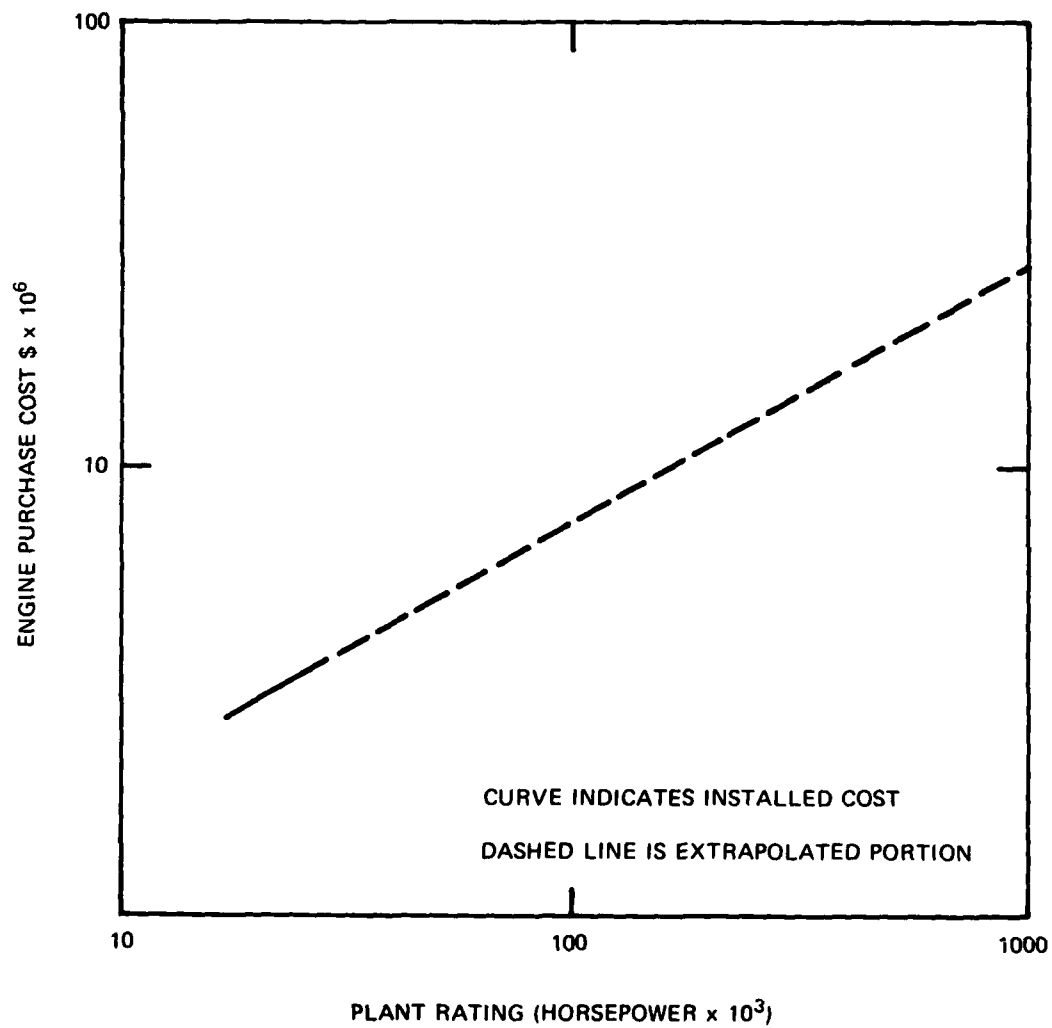


Figure 27 – Steam Plant Installation Cost
(Based on MST-14 reheat plant)

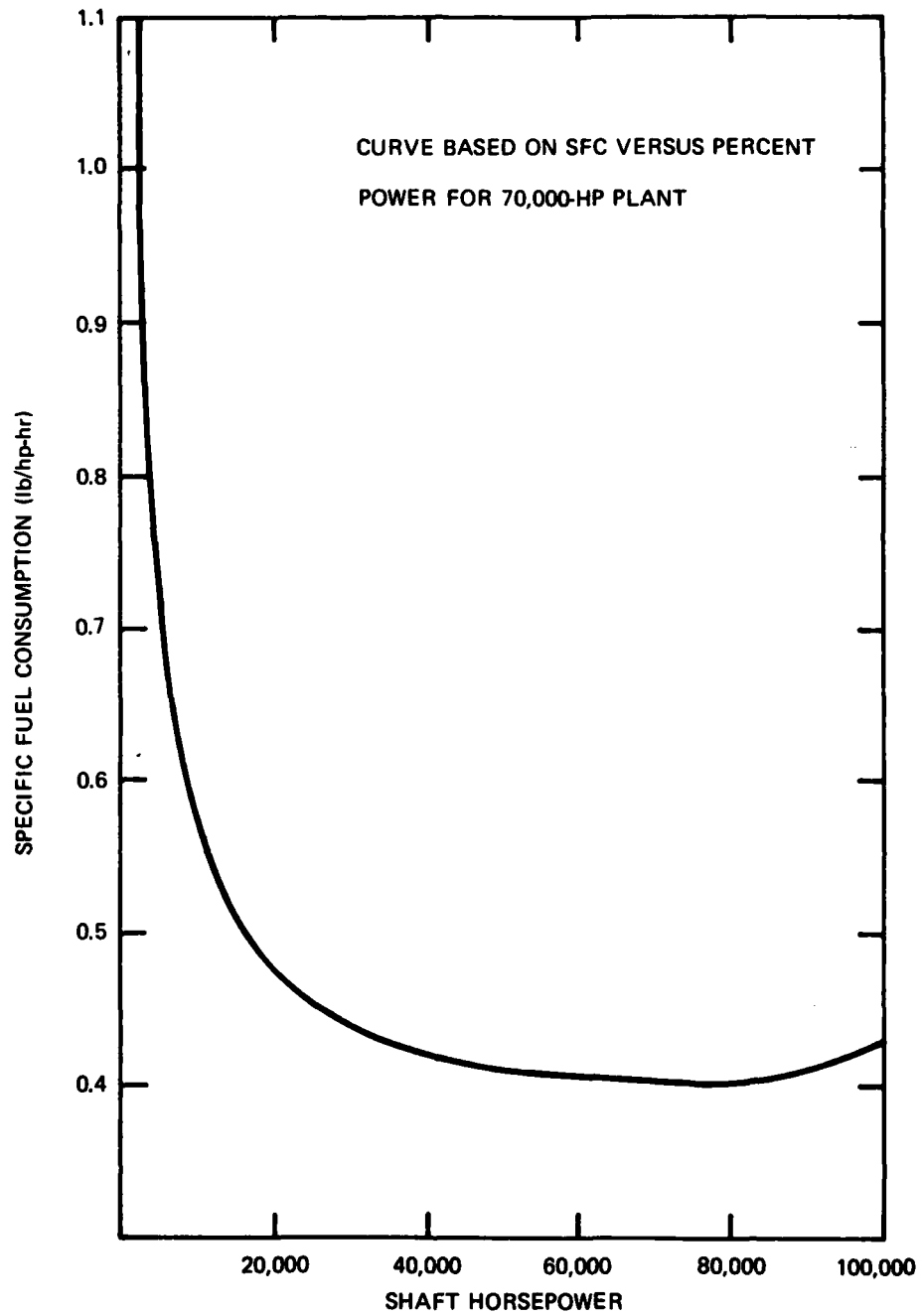


Figure 28 – Typical Fuel Consumption for a 70,000-HP Steam Turbine

Figure 29 – Fuel Consumption as a Function of Speed for ISUS
with Oil-Fired Steam Plant

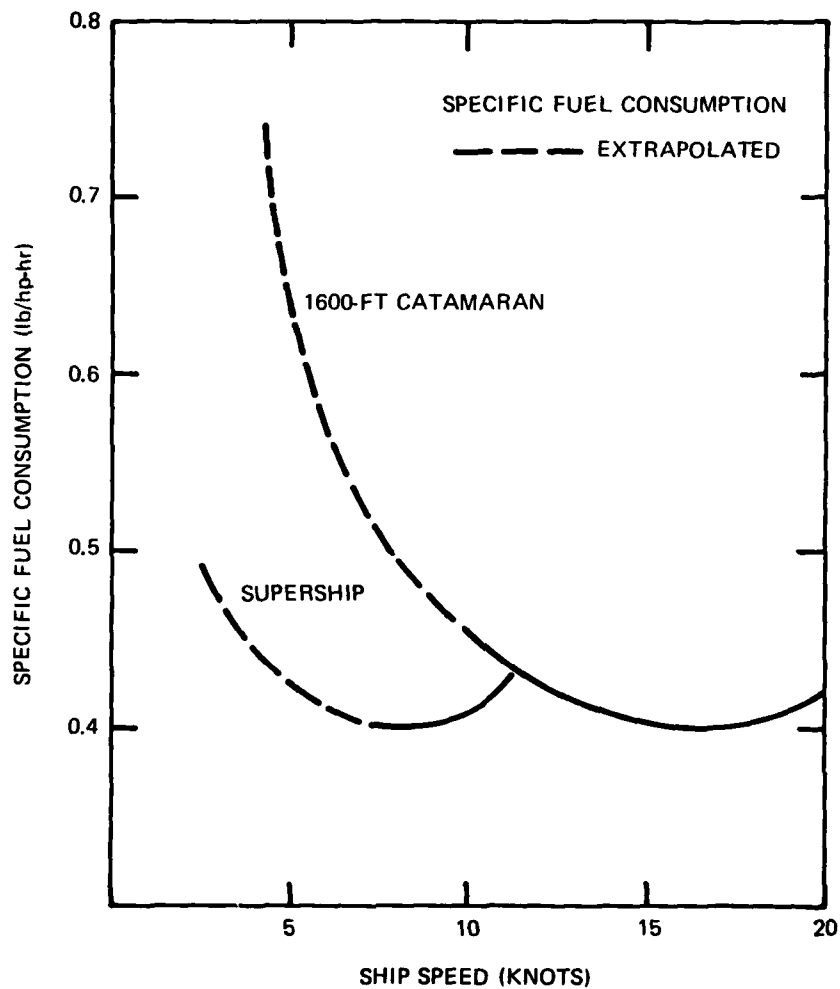
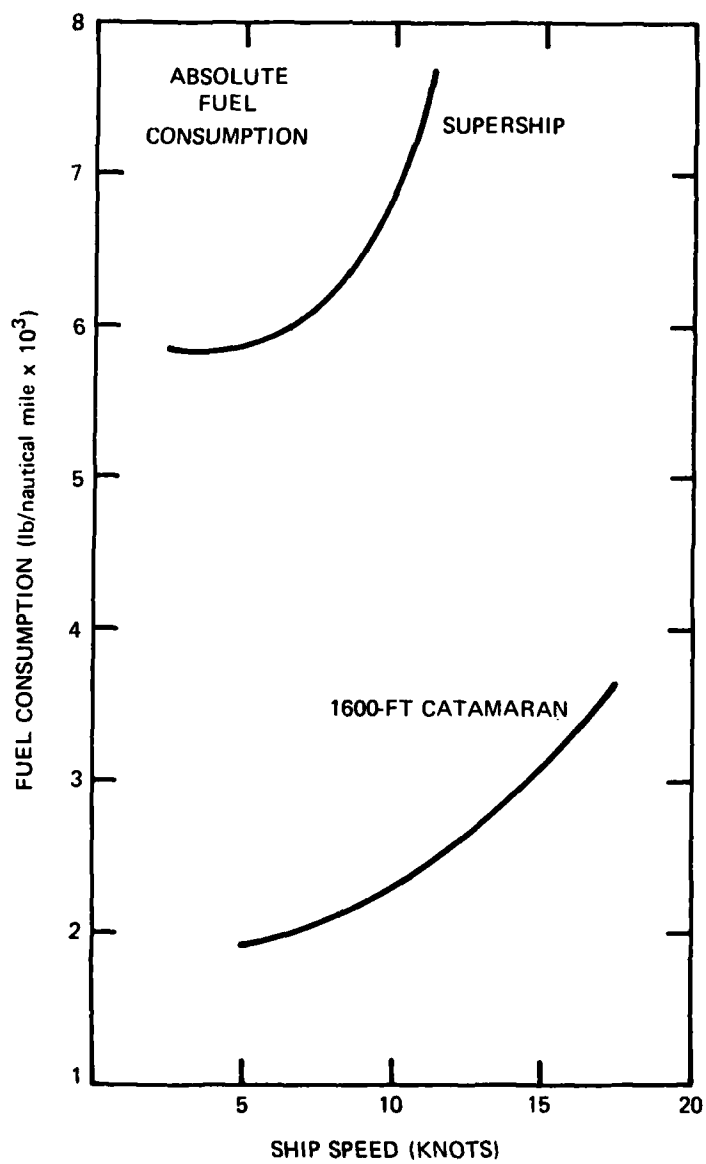


Figure 29 (Continued)



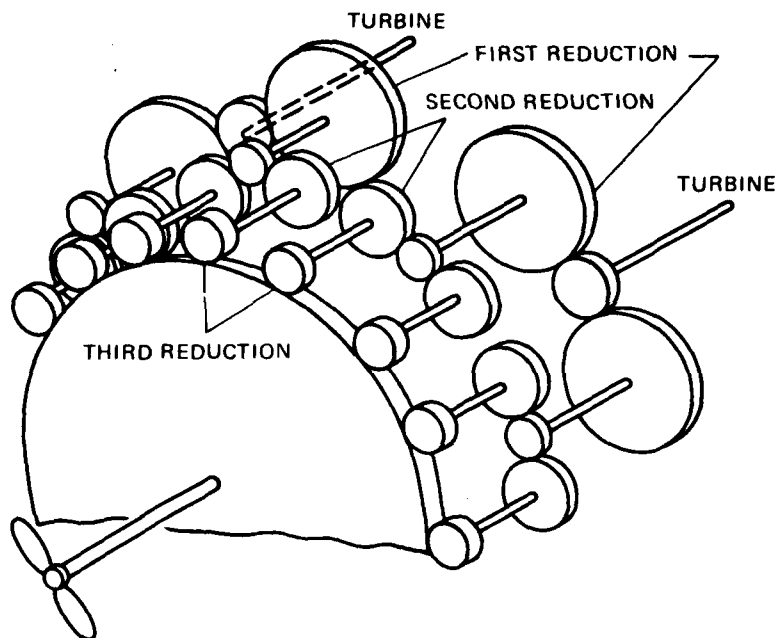


Figure 30 – Triple-Reduction, Parallel-Torque Path Gear

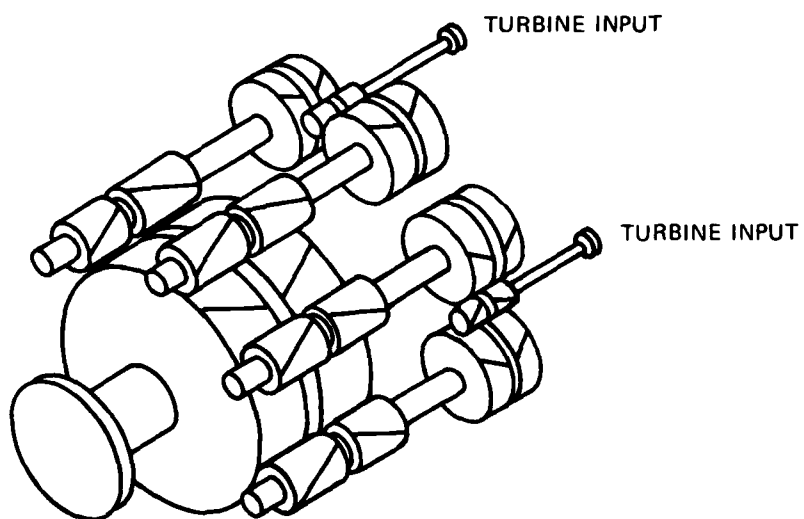


Figure 31 – Double-Reduction Gears

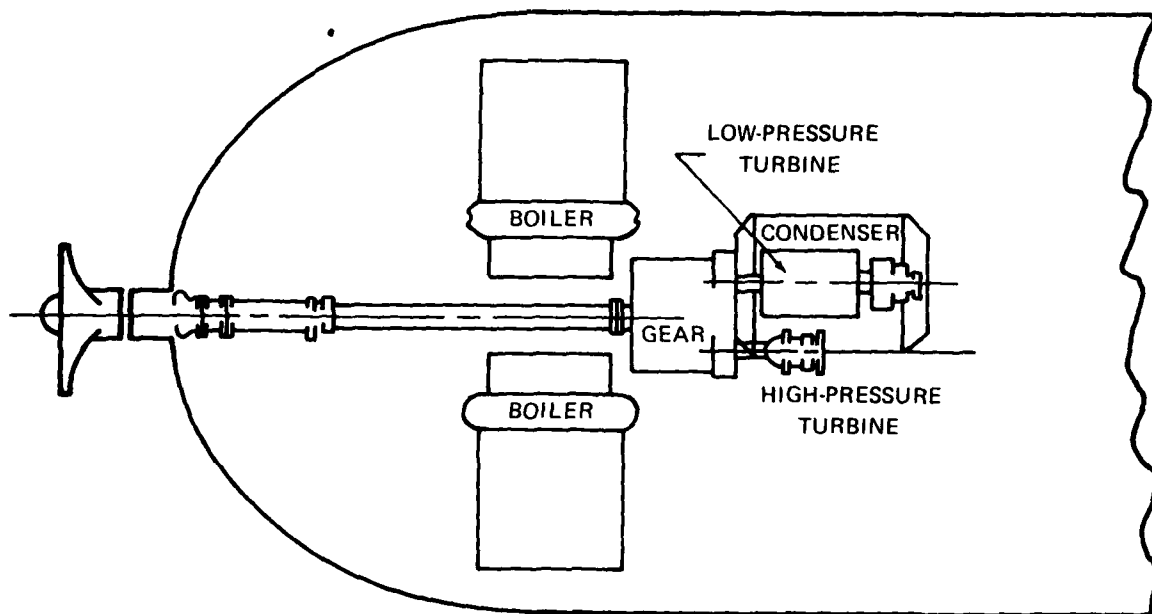


Figure 32a - Plan View

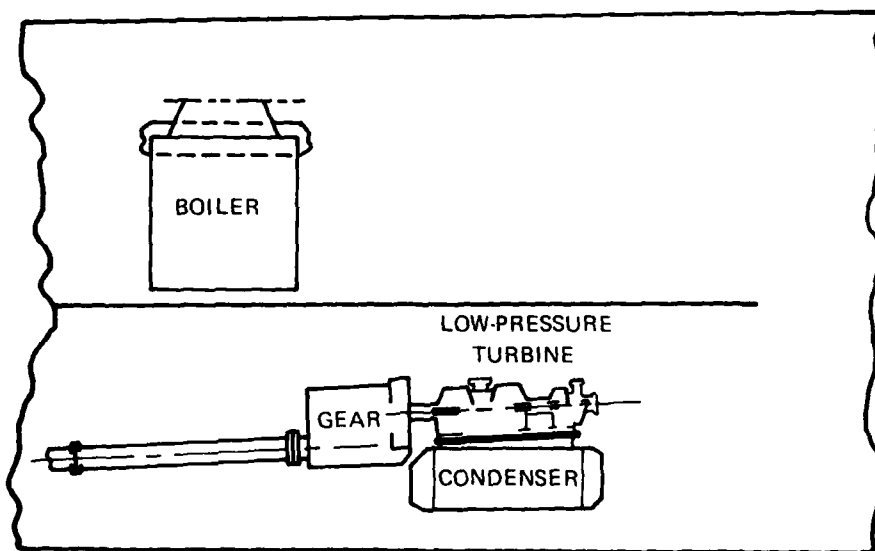


Figure 32b - Elevation

Figure 32 - Propulsion Machinery Arrangement for ISUS

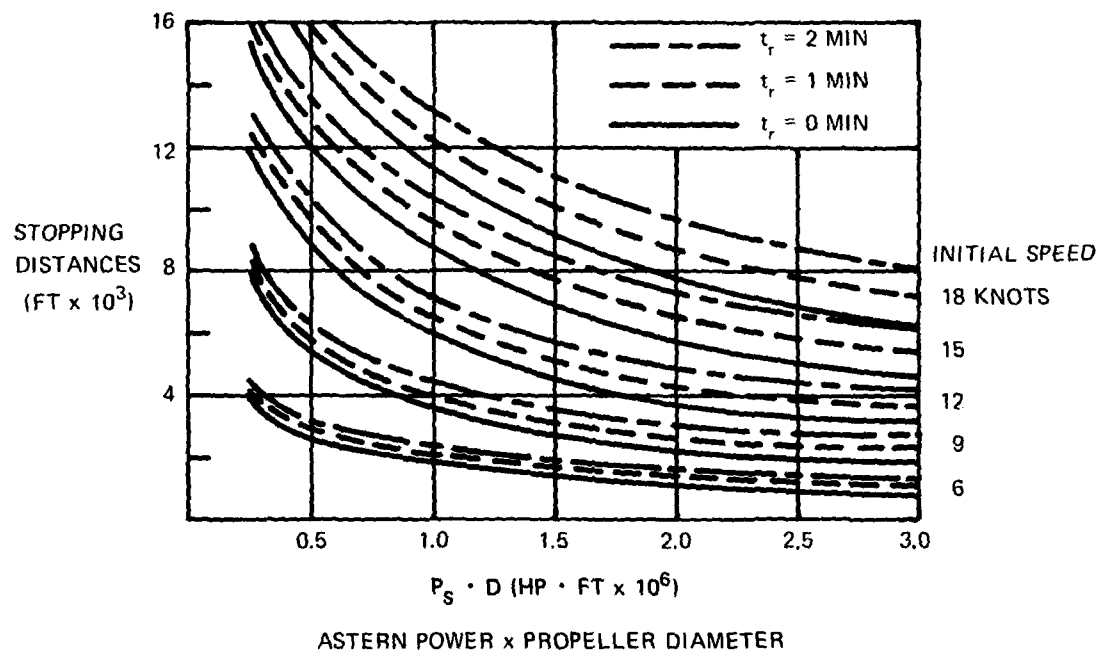
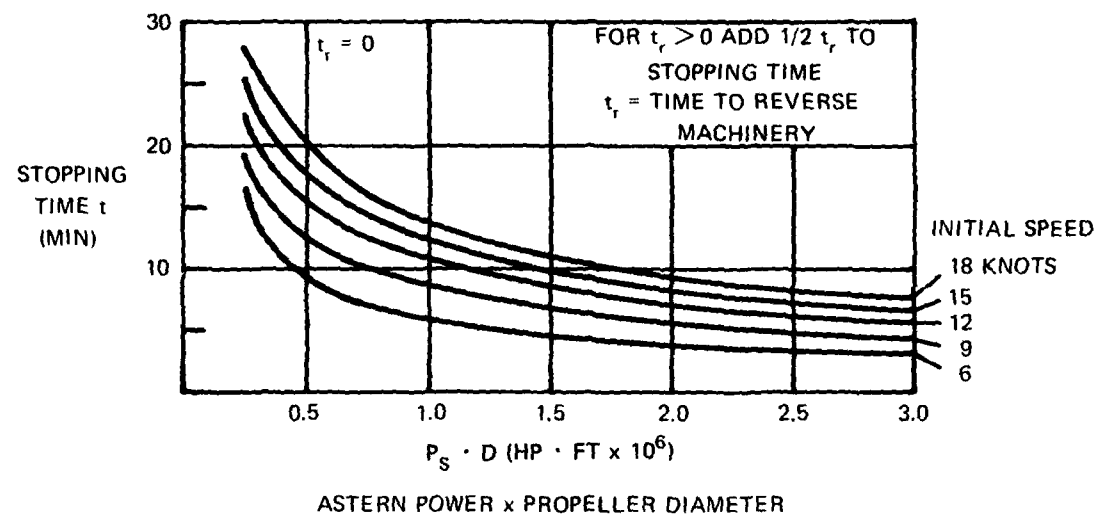


Figure 33 – Stopping Distance and Time for the 1600-Foot Module as a Function of Astern Power Times Propeller Diameter of Each Shaft

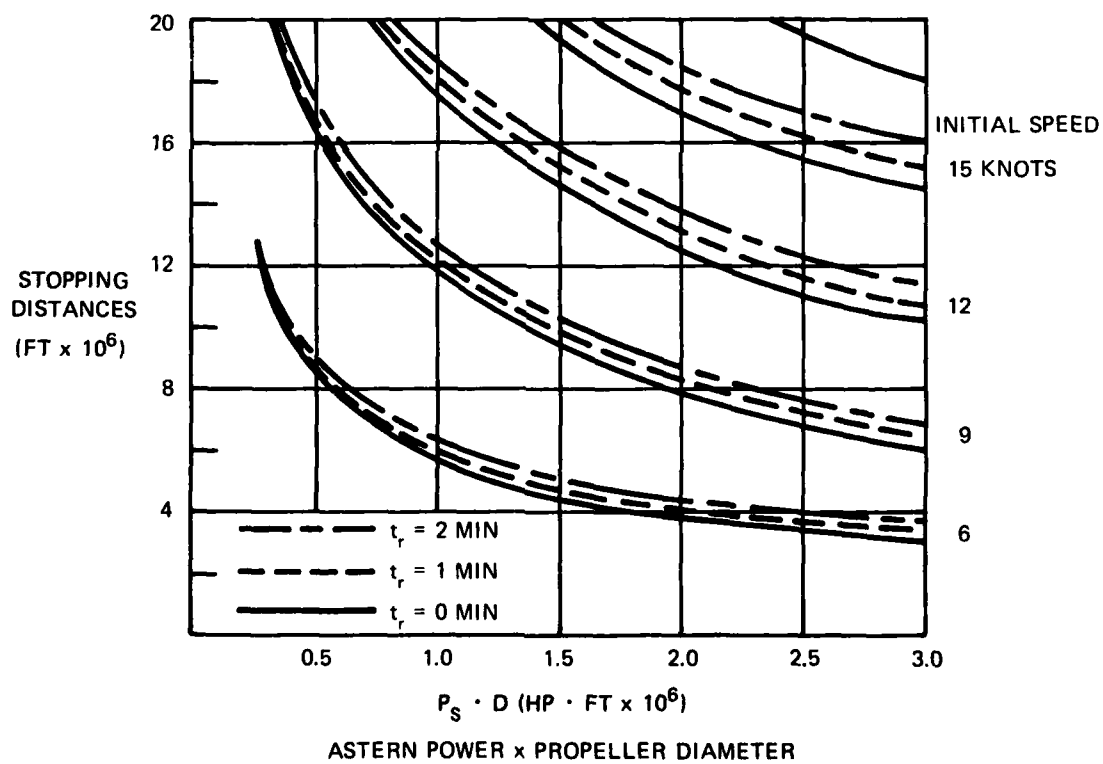
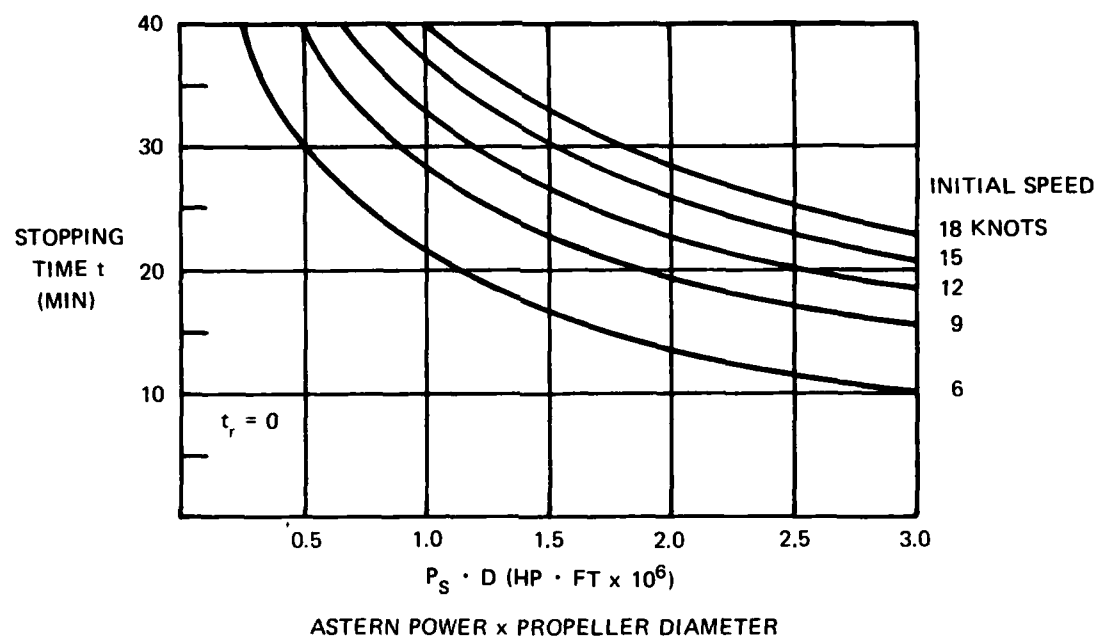


Figure 34 – Stopping Distance and Time for 5000-Foot ISUS as a Function of Astern Power Times Propeller Diameter of Each Shaft

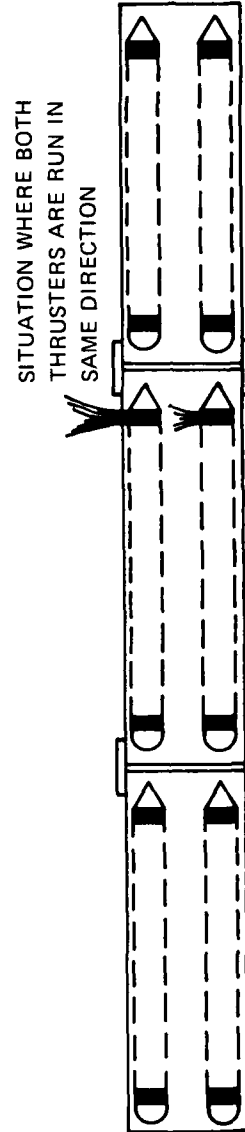


Figure 35 -- Side Thruster Arrangement for ISUS

AD-A081 435


















































DAVID W TAYLOR NAVAL SHIP RESEARCH AND DEVELOPMENT CE--ETC F/G 13/10
ADVANCED CONCEPT DEVELOPMENT OF AN INTEGRATED SUPERSHIP SYSTEM.--ETC(U)
AUG 74 S T LIANG, J C ADAMCHEK, J S TEJSEN

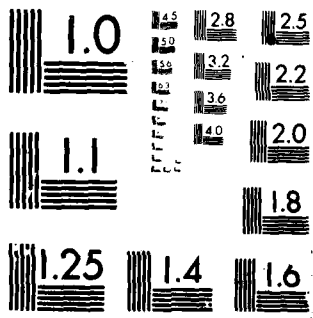
UNCLASSIFIED

NSRDC-3788-VOL-2

NL

2 of 2
ALL
PAGE(S)

														
														
														
						<div>END DATE FILMED 4-80 DTIC</div>								



MICROCOPY RESOLUTION TEST CHART
NATIONAL BUREAU OF STANDARDS-1963-A



Figure 36 -- Integrated Supership Model



Figure 37 — Shock Cord Hookup of Model to Carriage

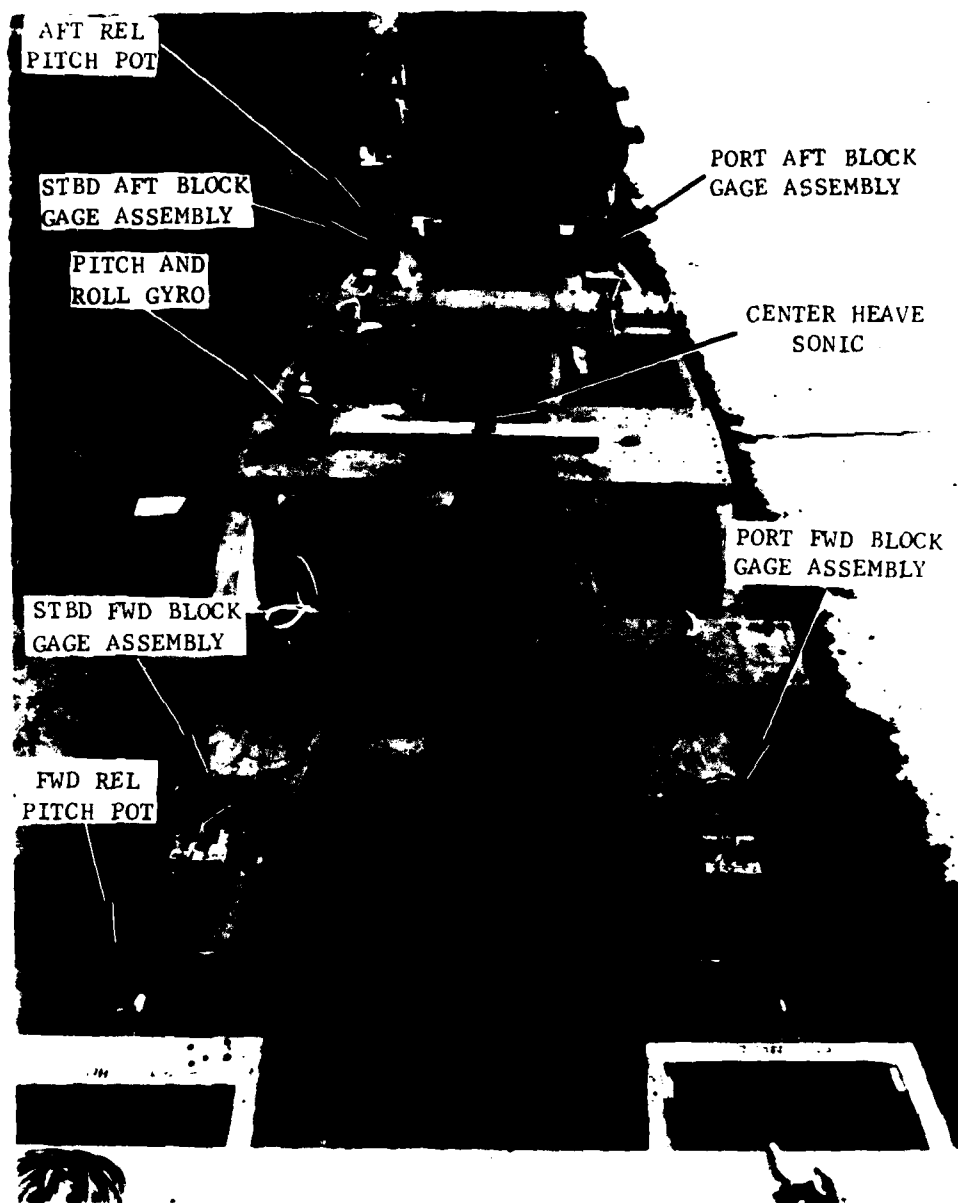


Figure 38 - Transducer Locations on ISUS Model

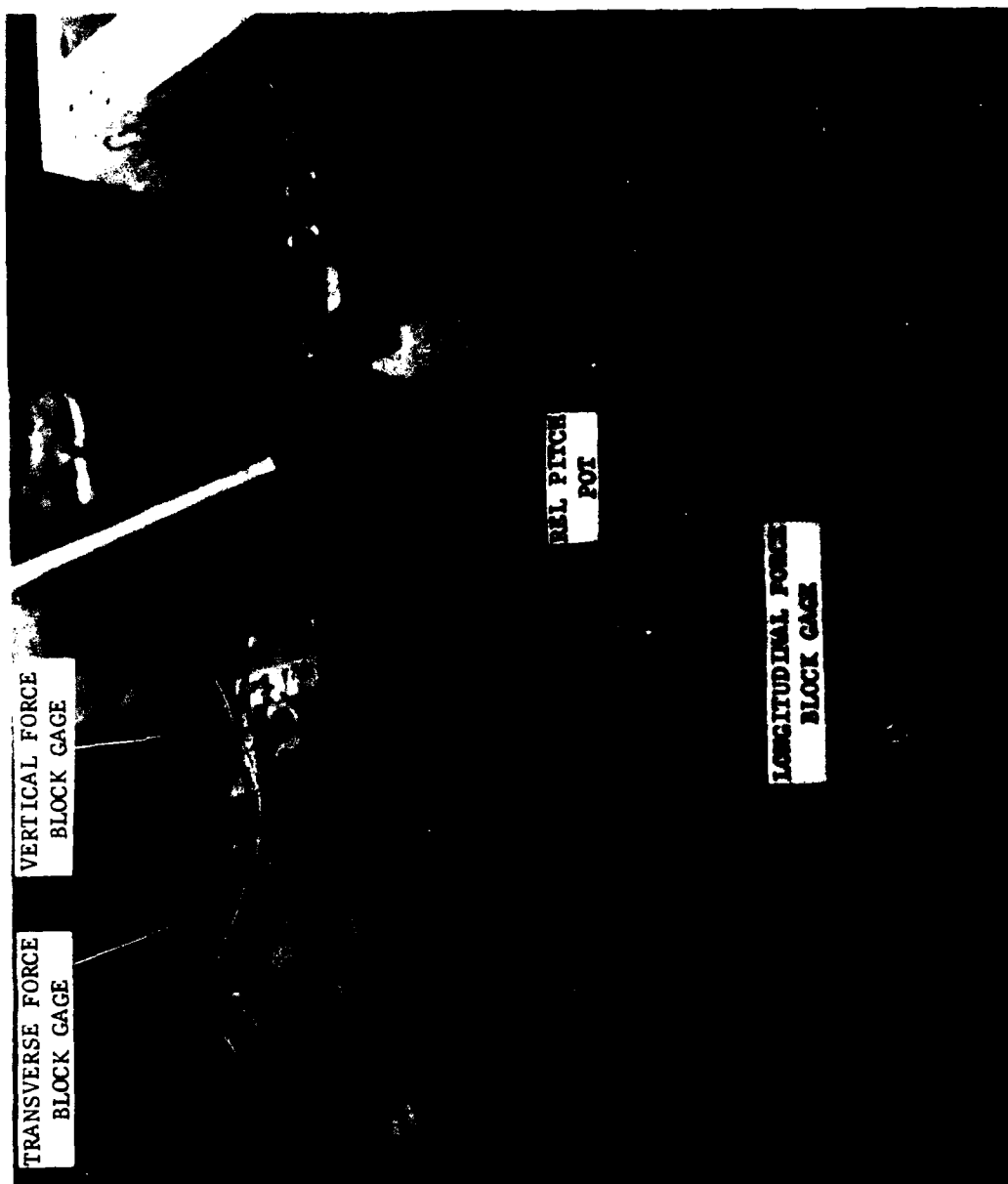


Figure 39 - Details of Block Gage Assembly

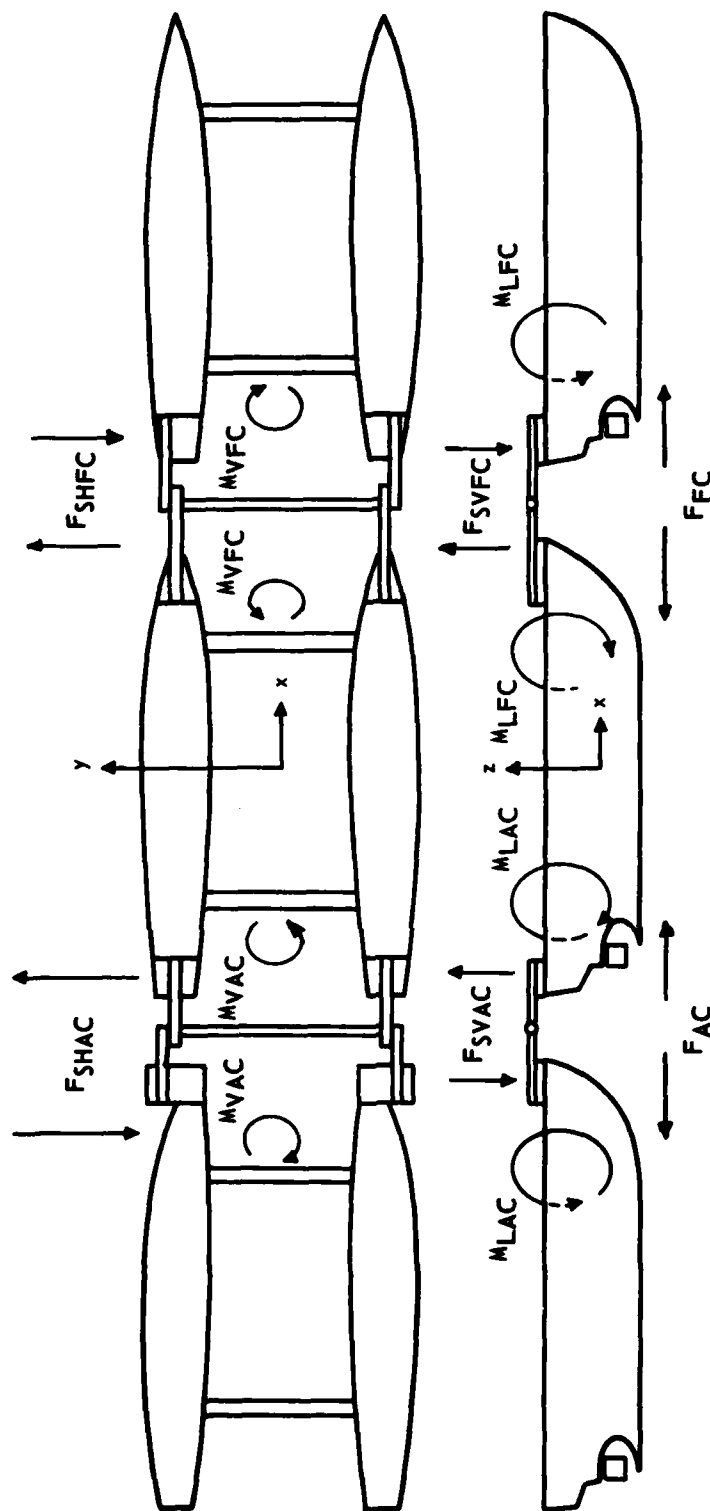


Figure 41 – Positive Directions of ISUS Model Forces and Moments

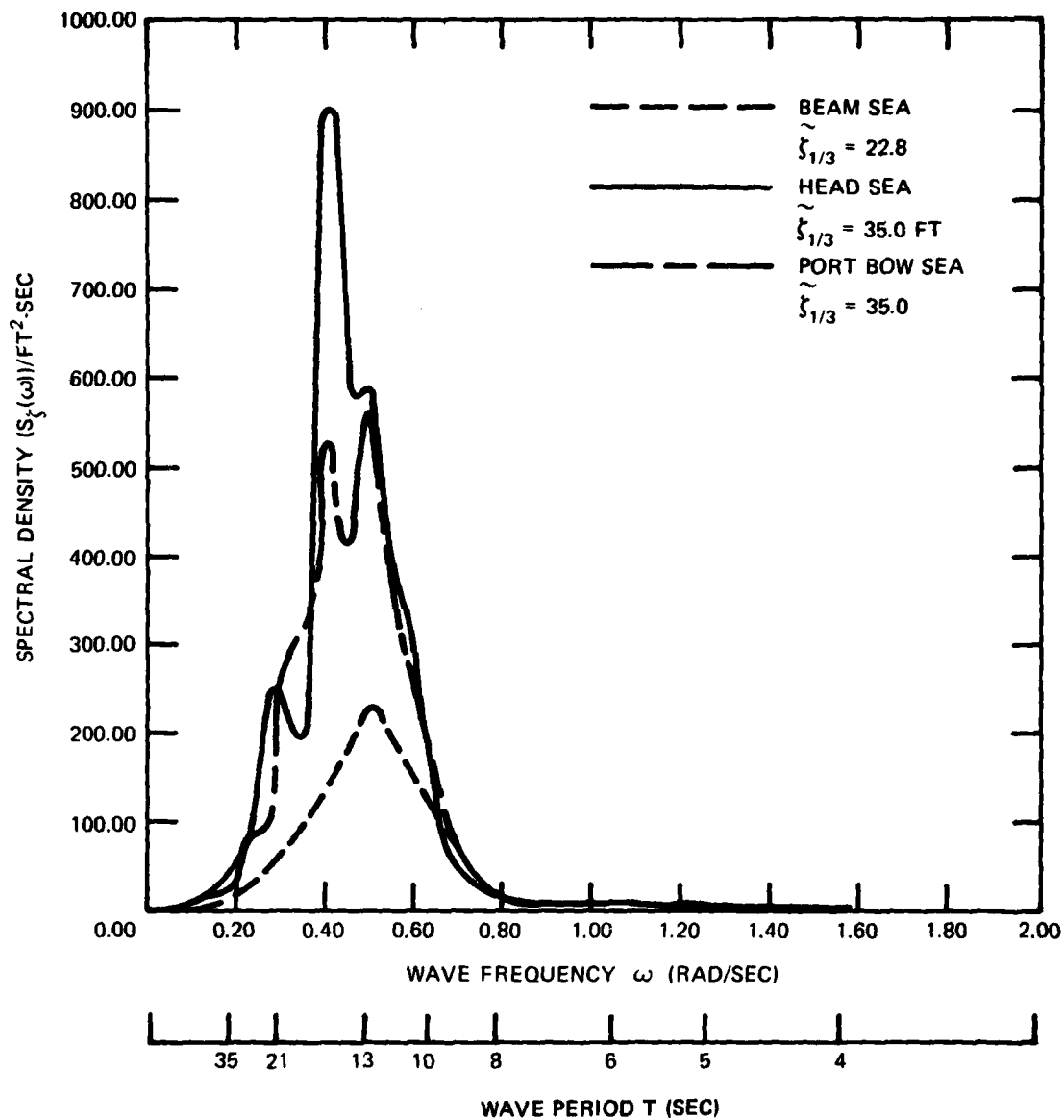


Figure 42 – Experimental Long-Crested Irregular Wave Spectra in State 7 Sea

Figure 43 - Pitch Amplitude/Wave Slope of the Individual Modules versus Total ISUS Length/Wave Length

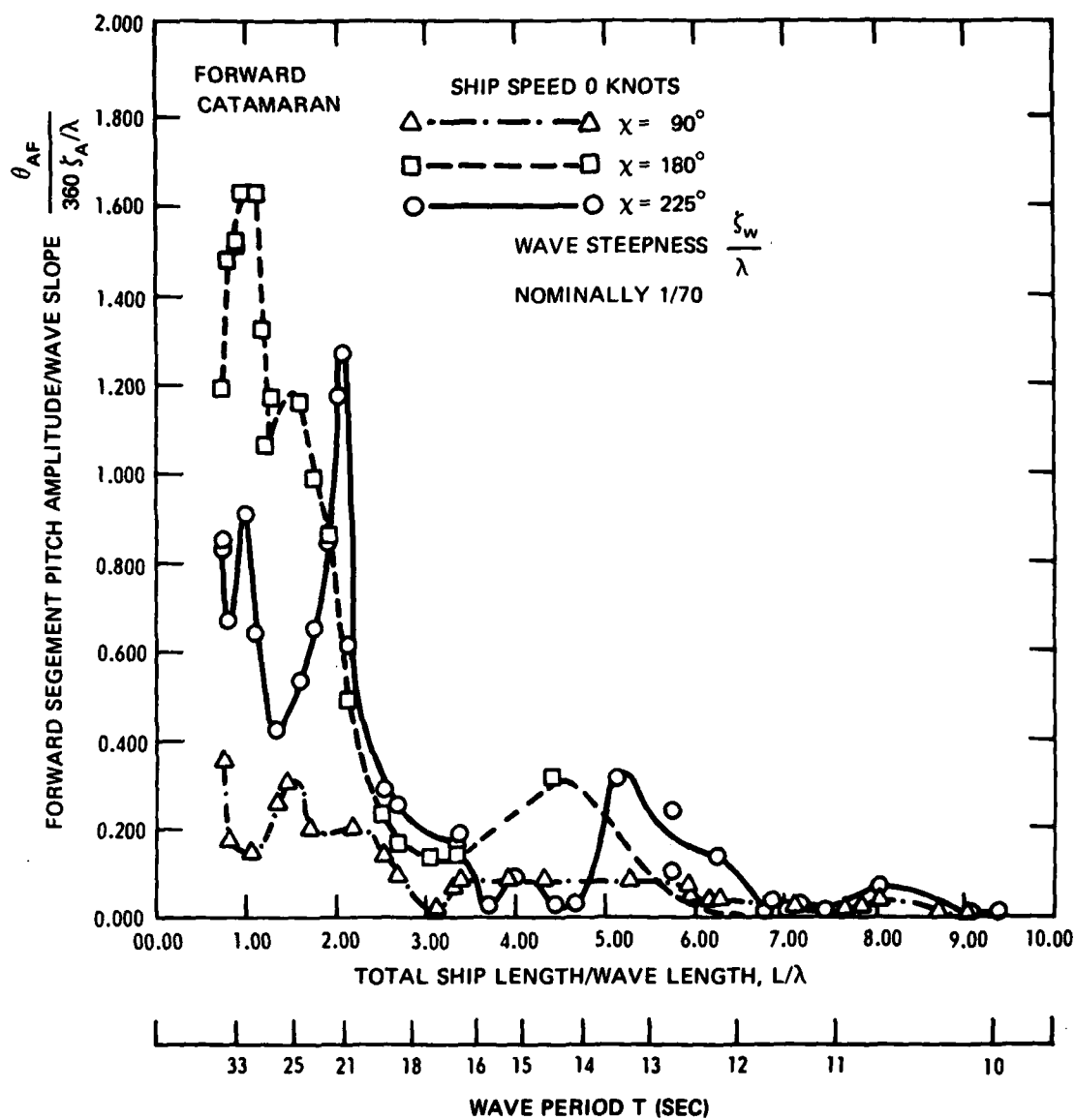


Figure 43 (Continued)

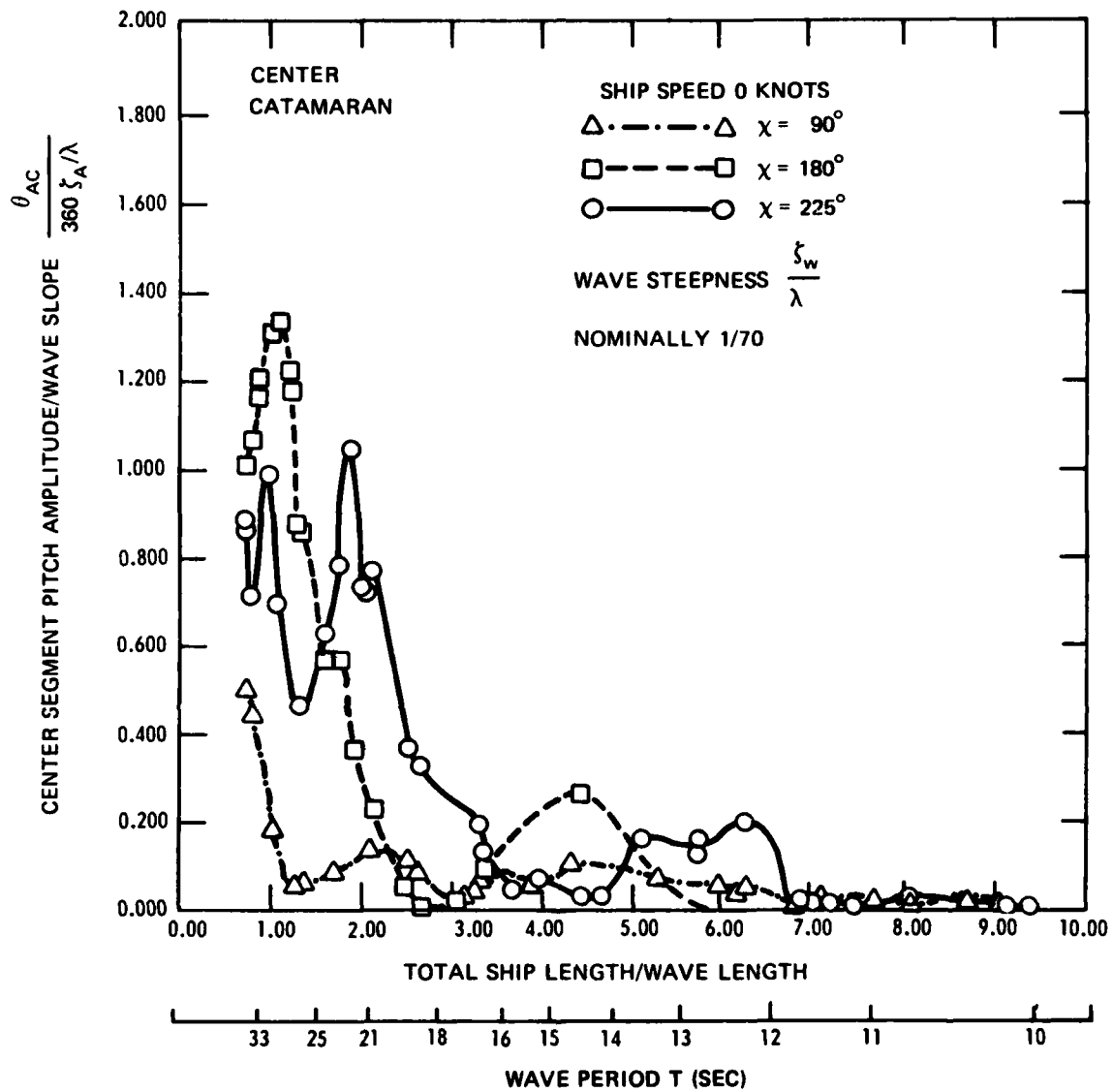


Figure 43 (Continued)

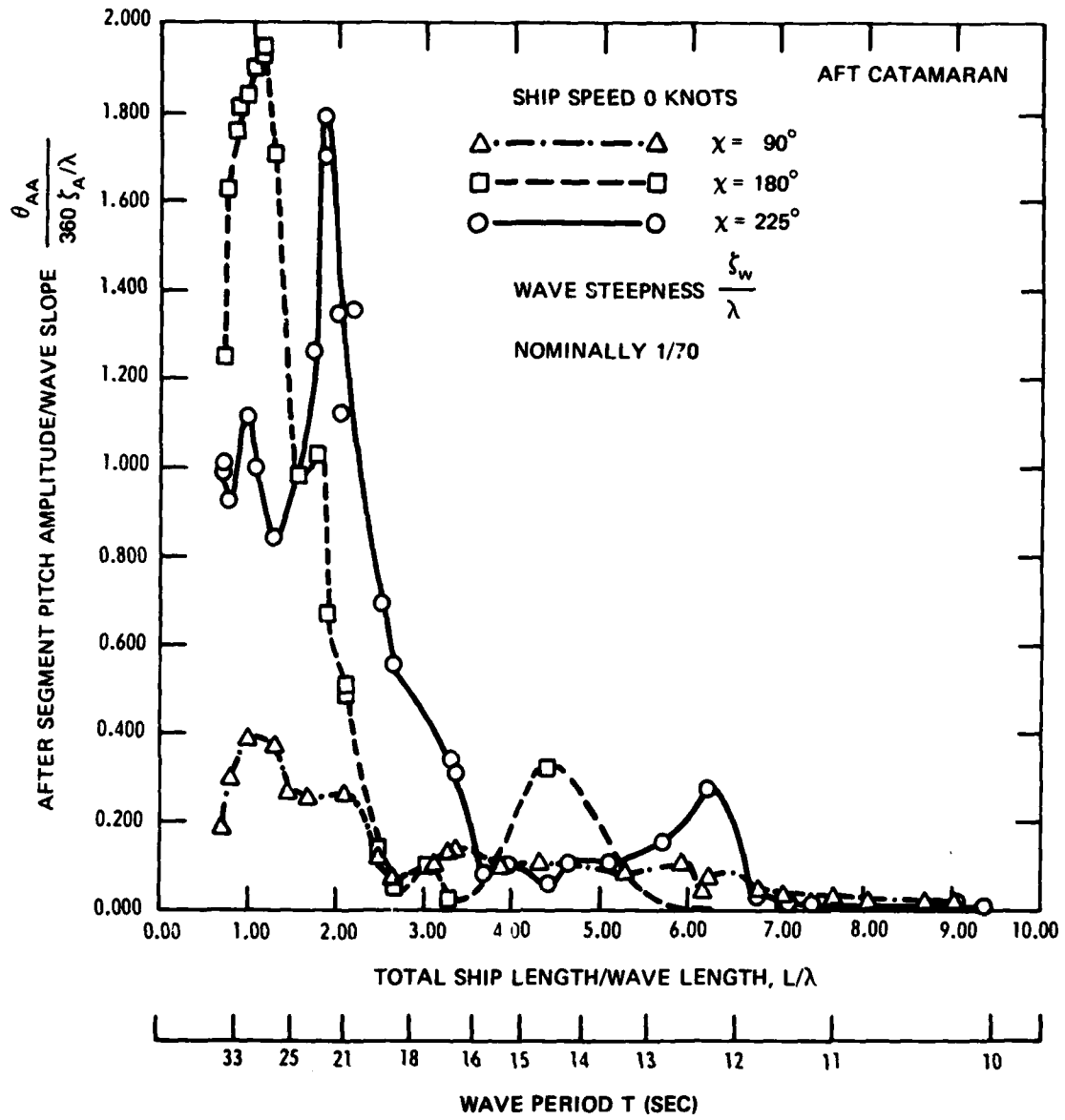


Figure 44 – Heave Amplitude/Wave Amplitude of the Individual Modules versus Total ISUS Length/Wave Length

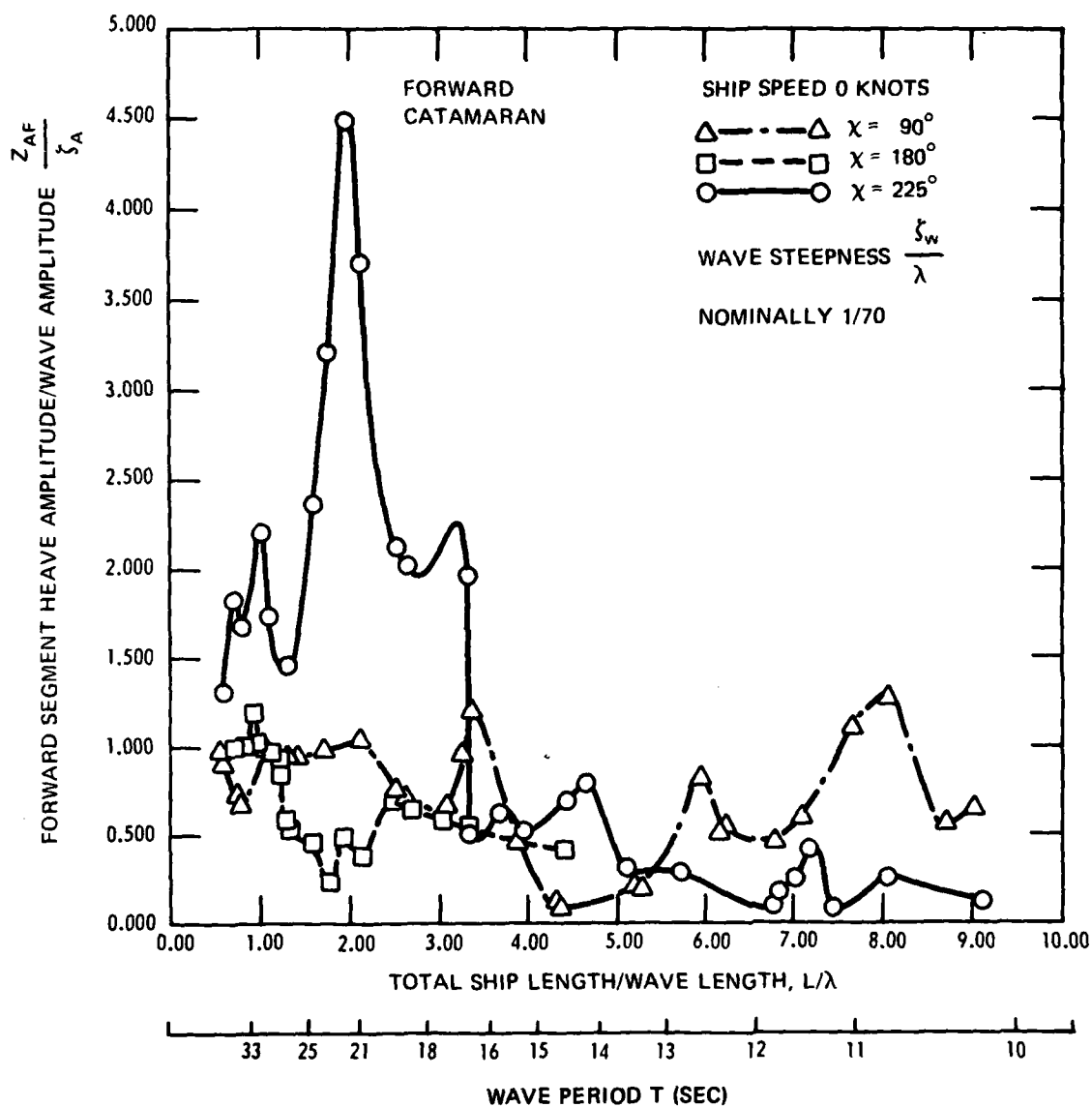


Figure 44 (Continued)

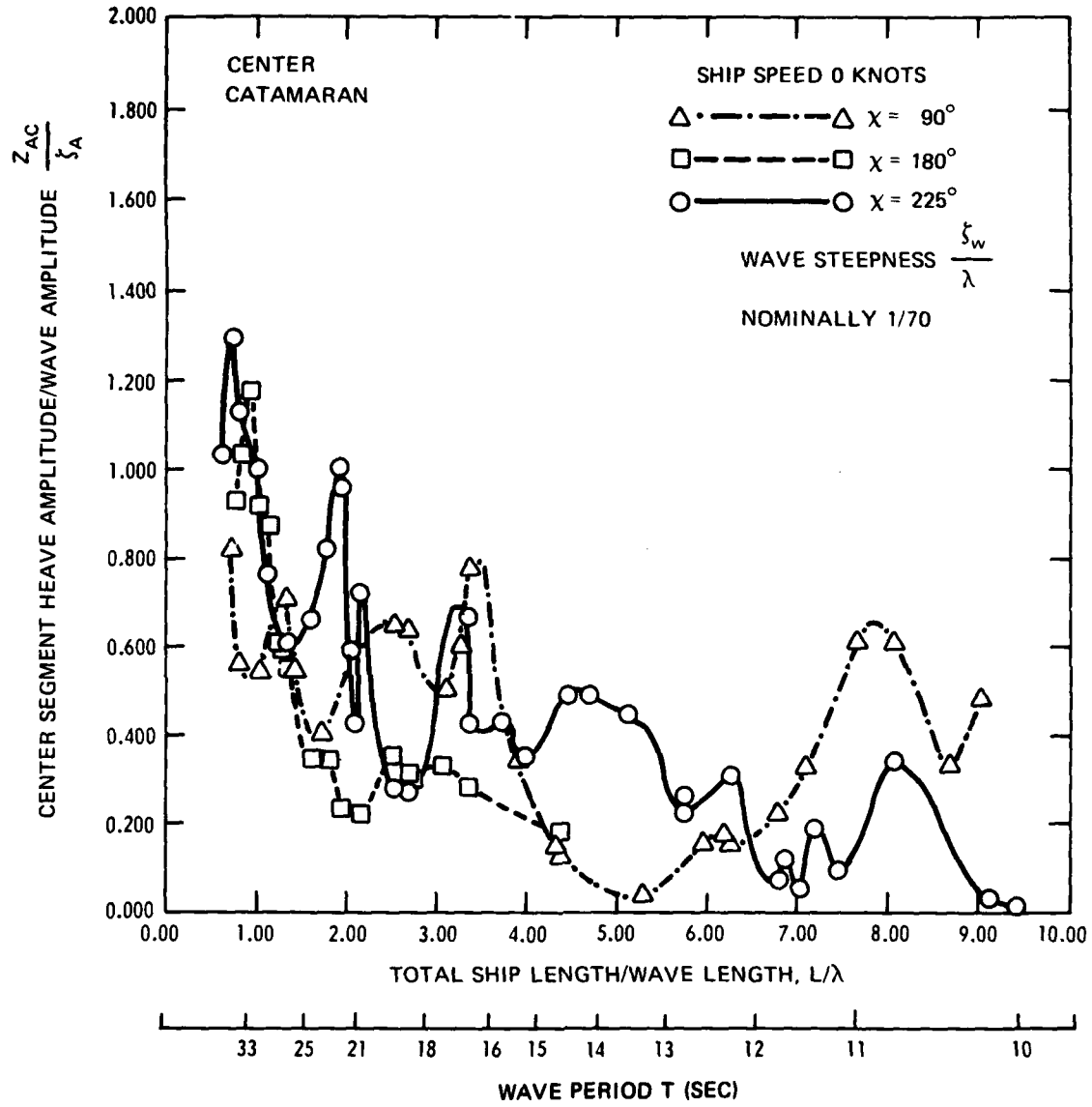


Figure 44 (Continued)

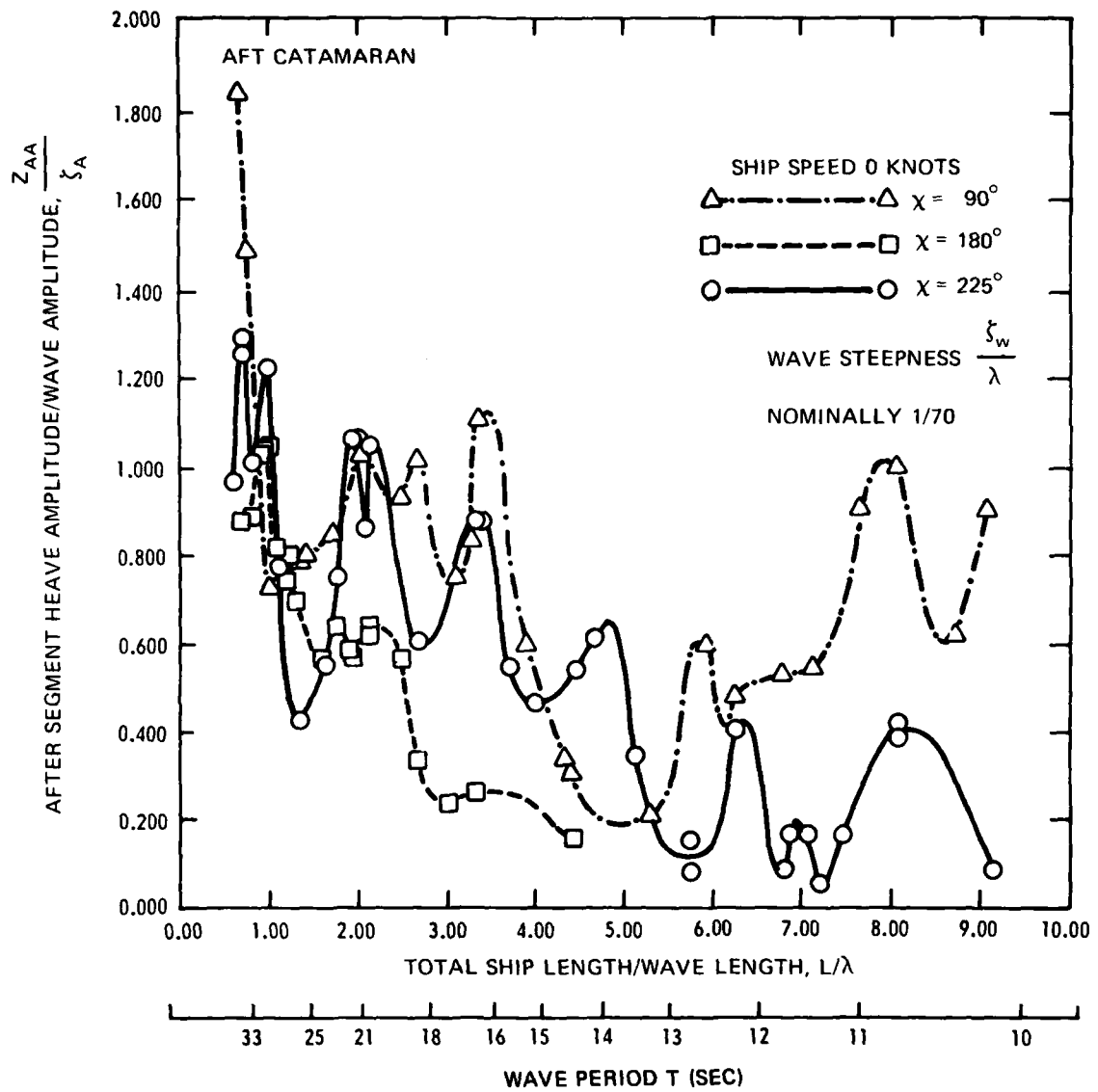


Figure 45 – Relative Pitch Amplitude between Wave Slope of Two Modules versus Total ISUS Length/Wave Length

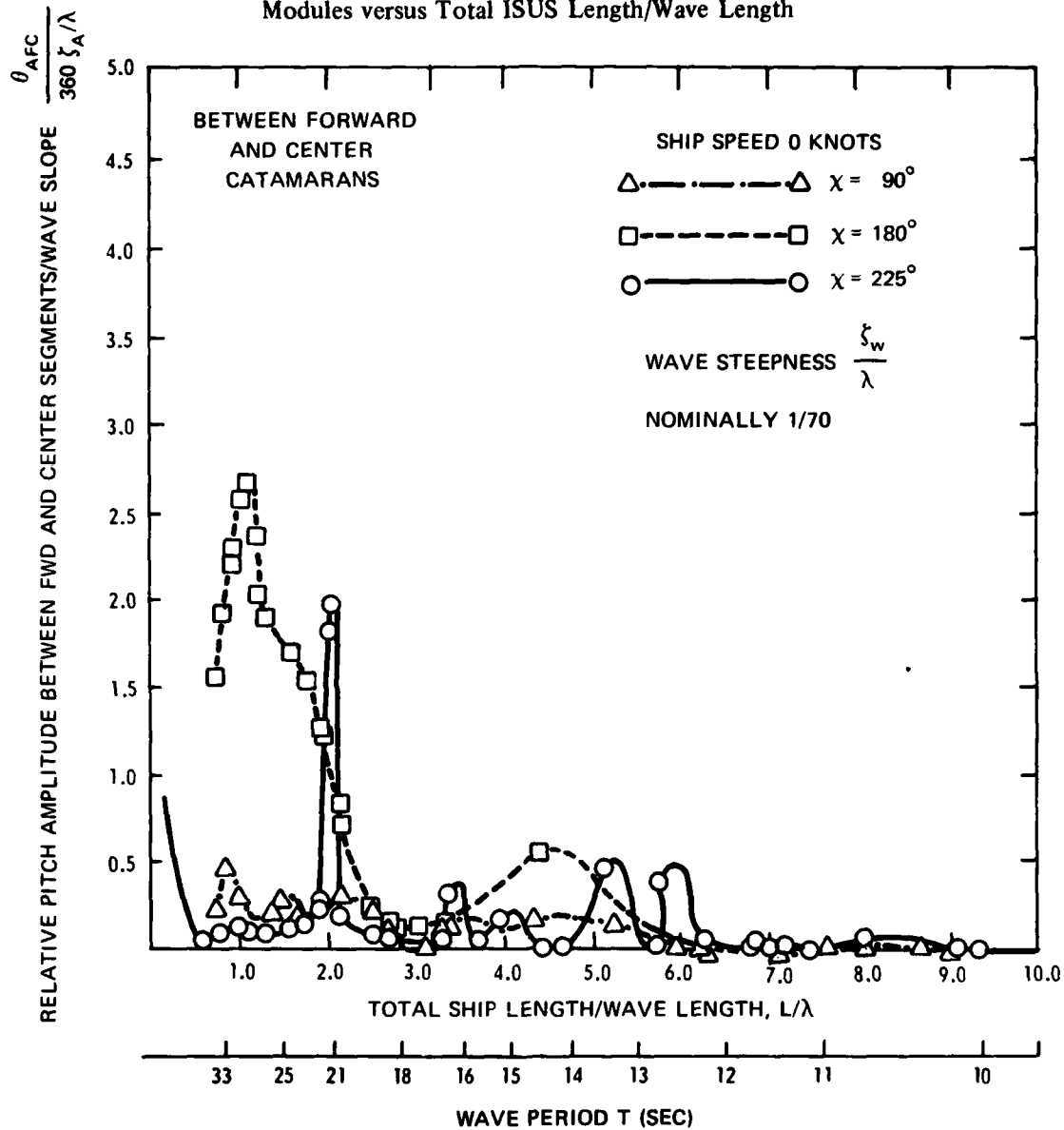
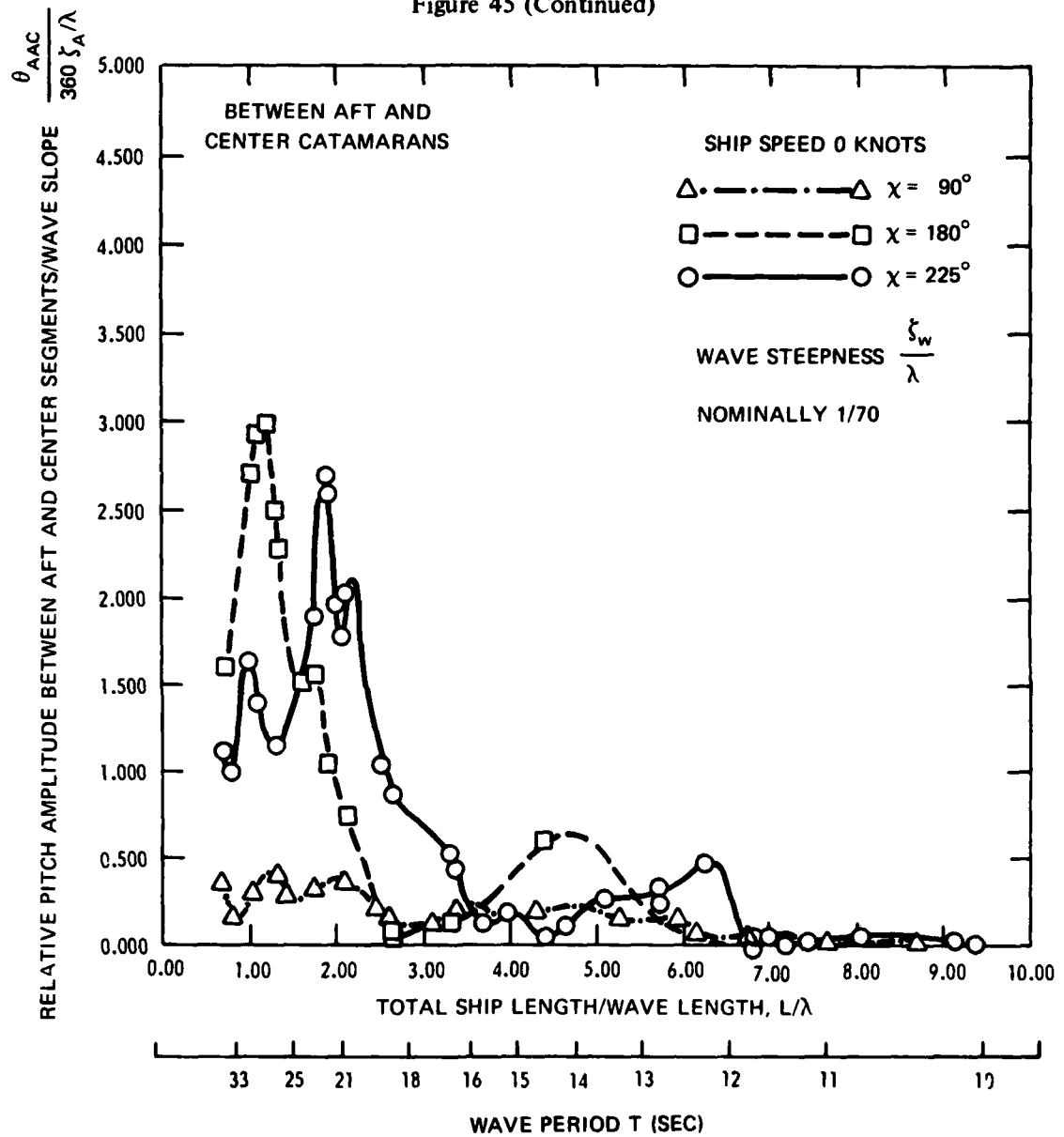


Figure 45 (Continued)



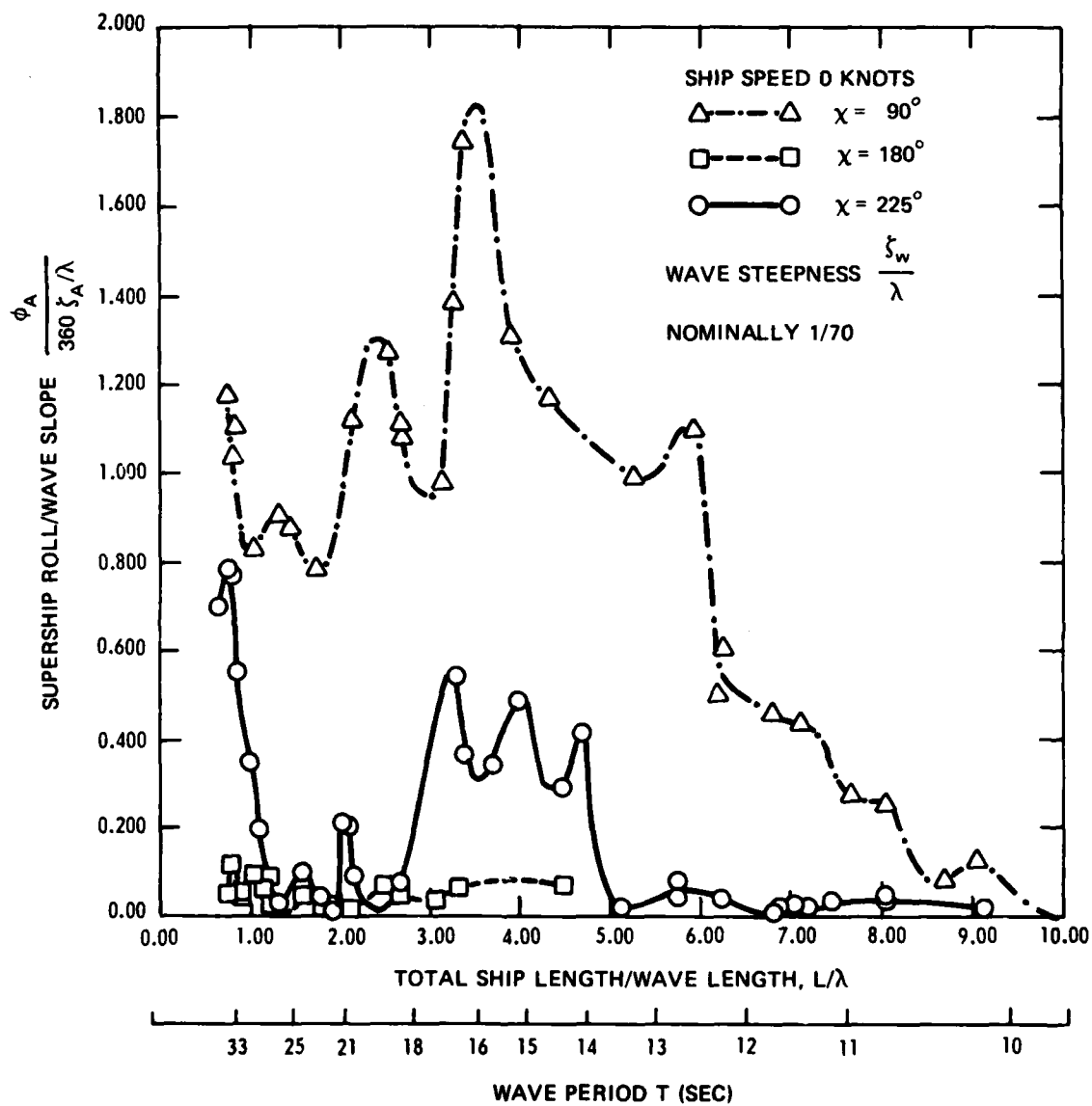


Figure 46 – ISUS Roll/Wave Slope versus Total ISUS Length/Wave Length

Figure 47 — Nondimensional Transfer Function of Vertical Shear Force between the Modules versus Total ISUS Length/Wave Length

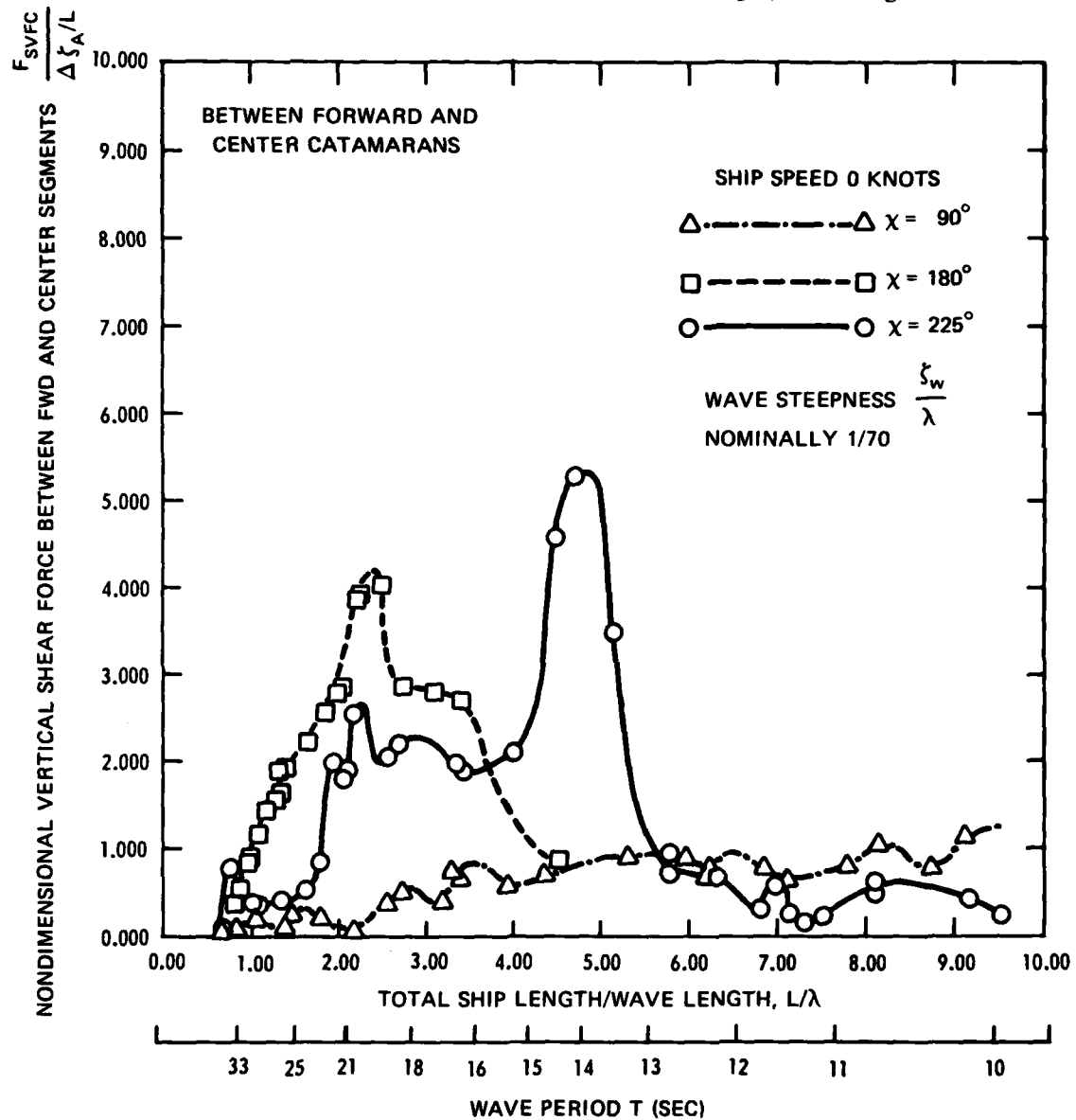


Figure 47 (Continued)

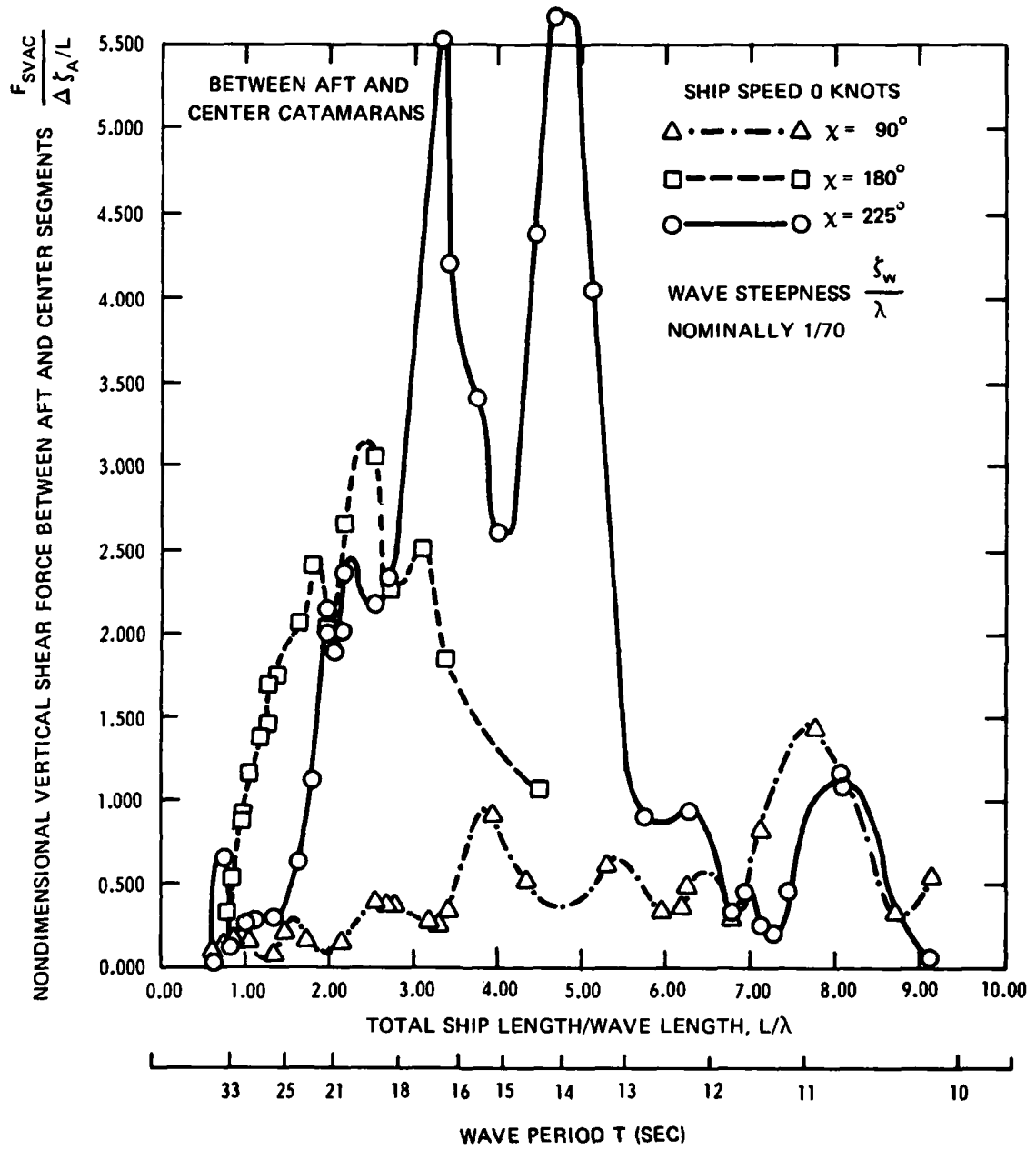


Figure 48 – Nondimensional Transfer Function of Horizontal Shear Force between the Modules versus Total ISUS Length/Wave Length

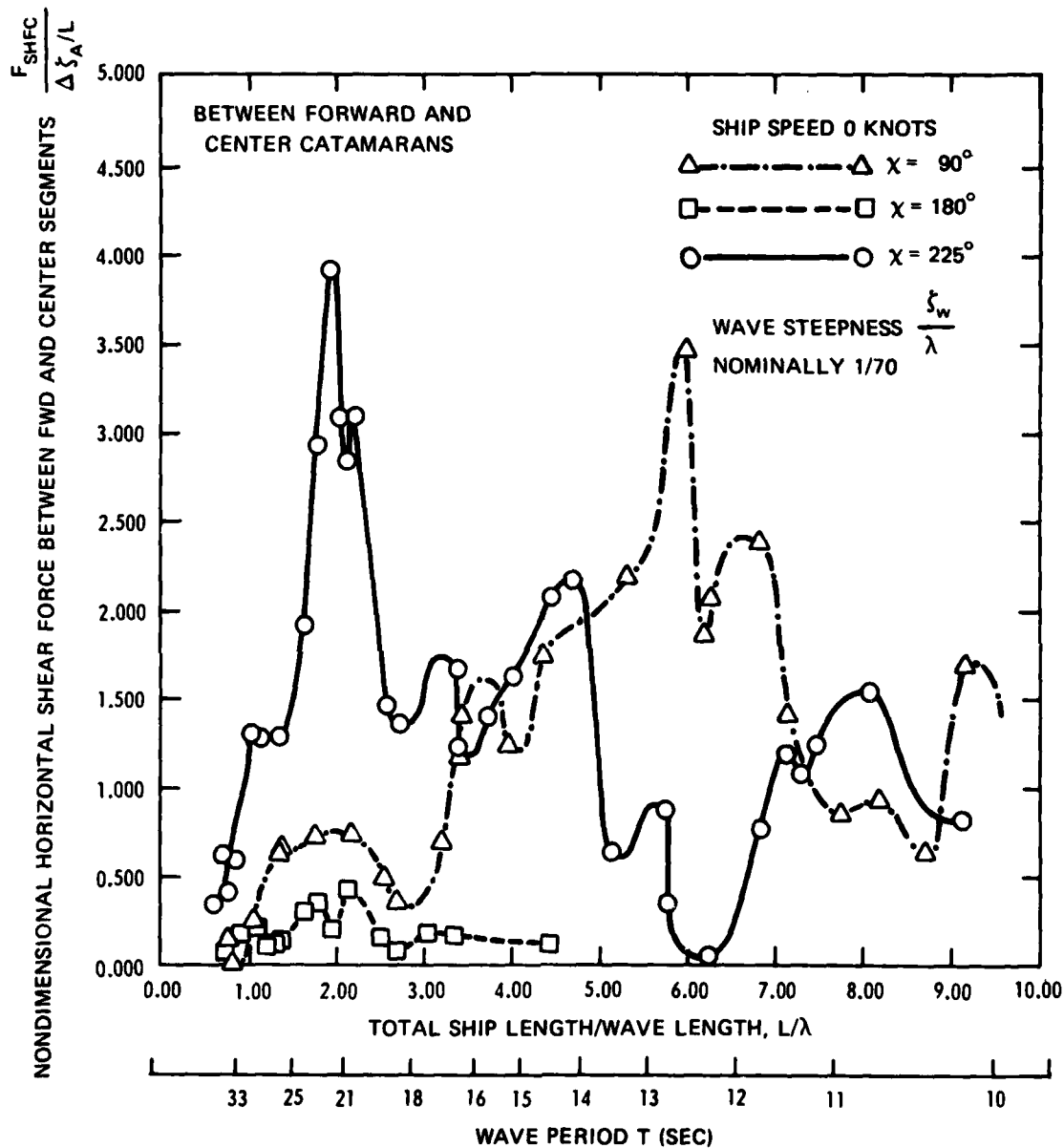


Figure 48 (Continued)

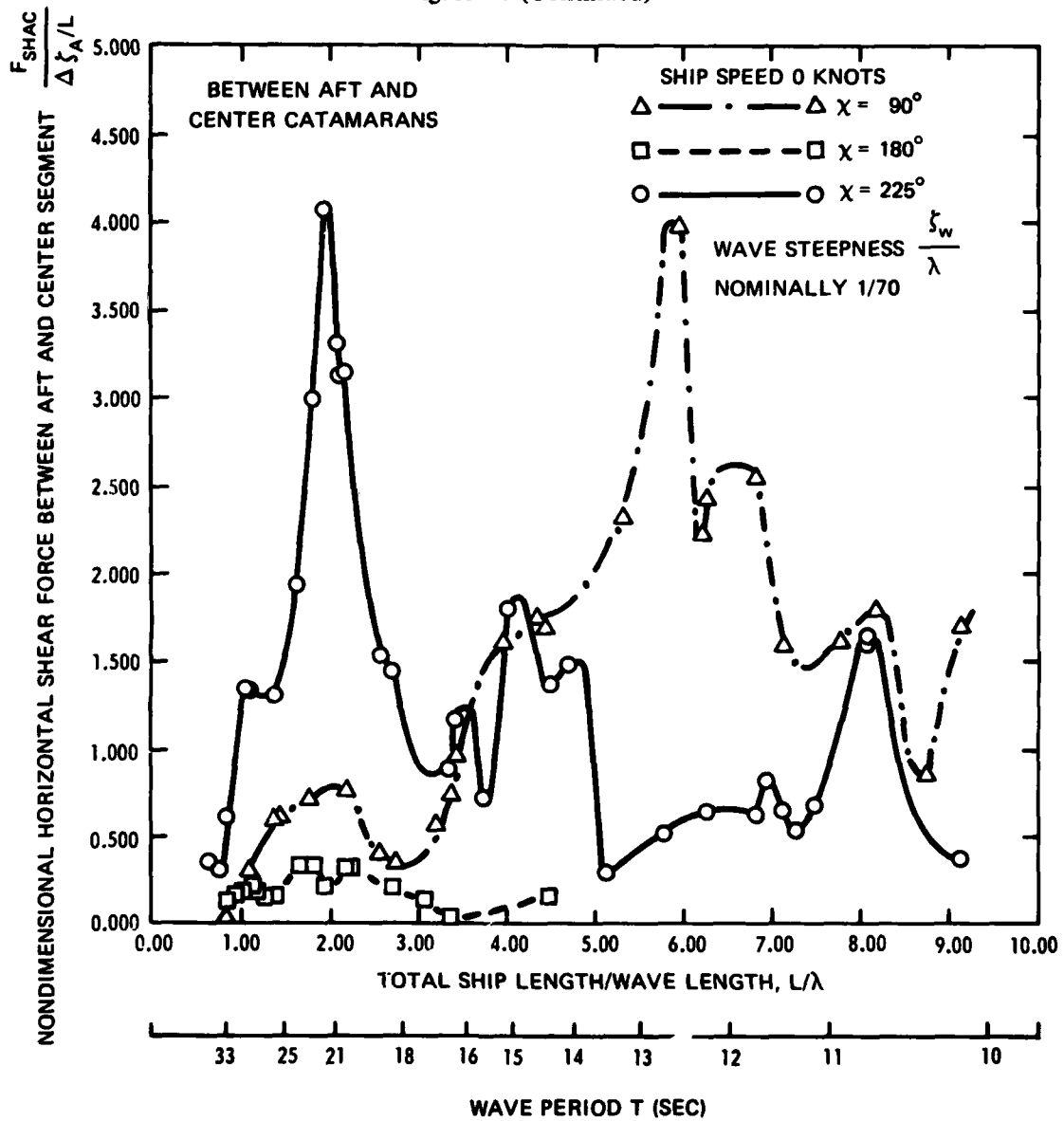


Figure 49 – Nondimensional Transfer Function of the Longitudinal Force between the Modules versus Total ISUS Length/Wave Length

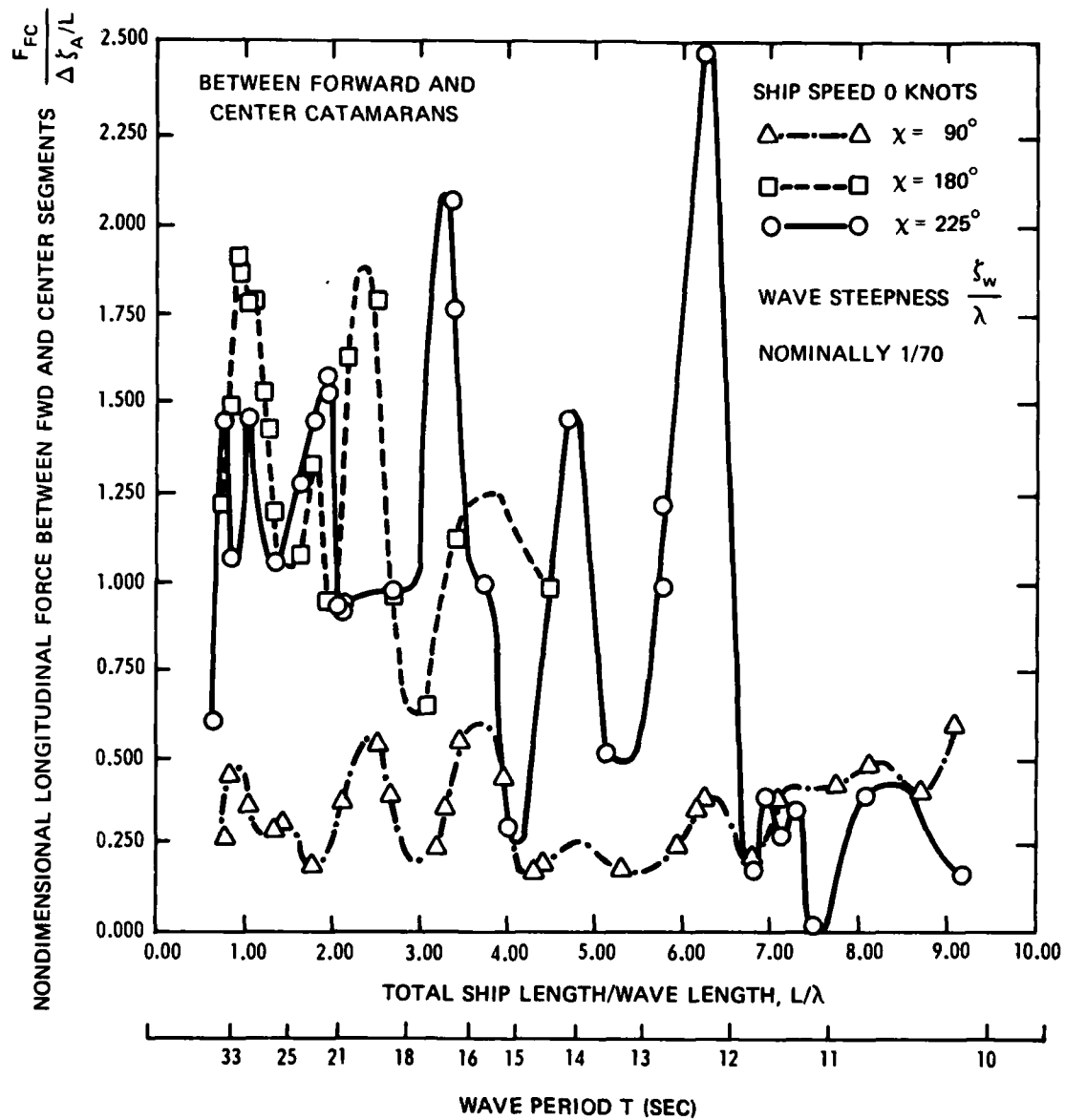


Figure 49 (Continued)

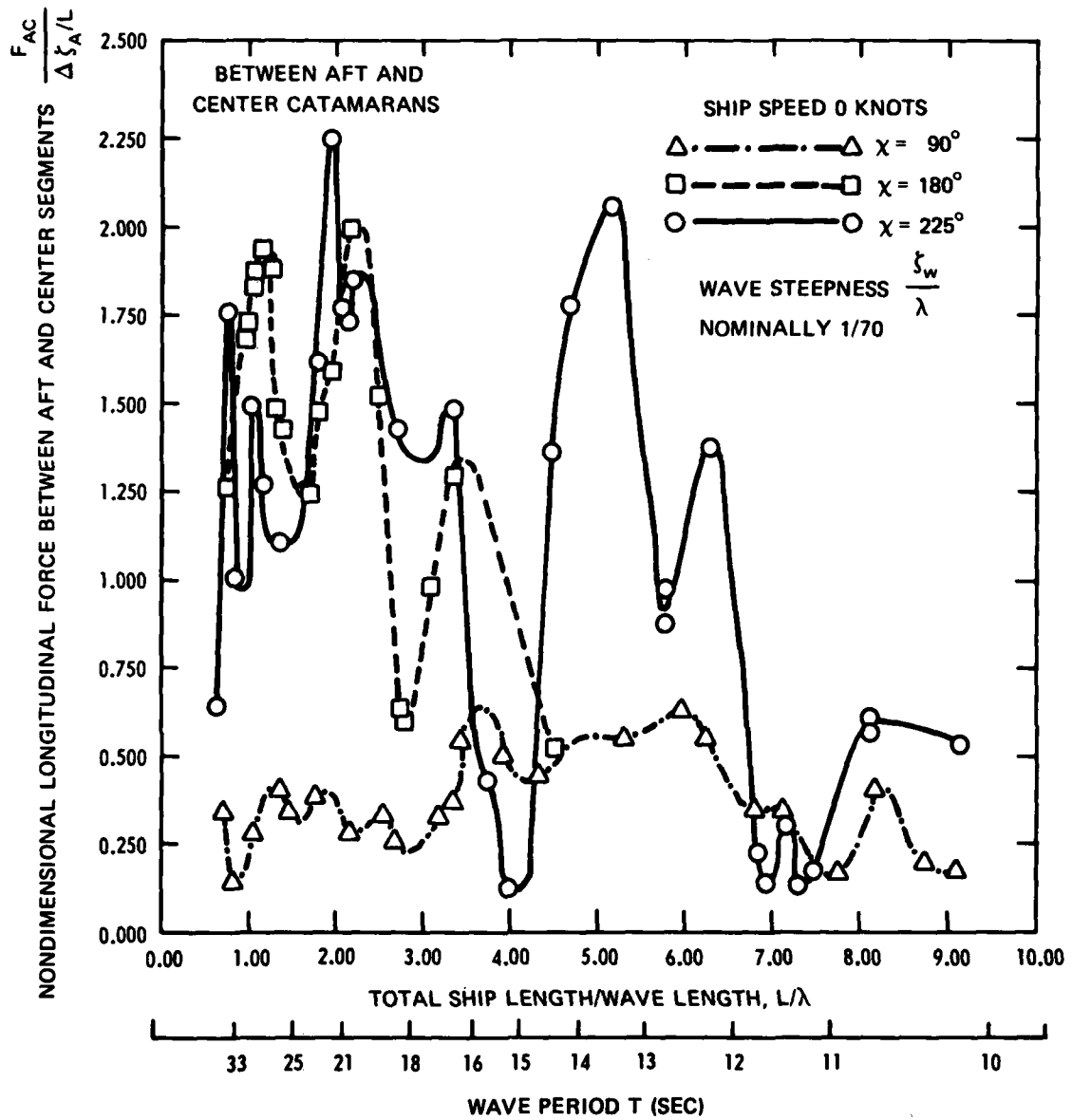


Figure 50 – Nondimensional Transfer Function of the Longitudinal Axial Moment between the Modules versus Total ISUS Length/Wave Length

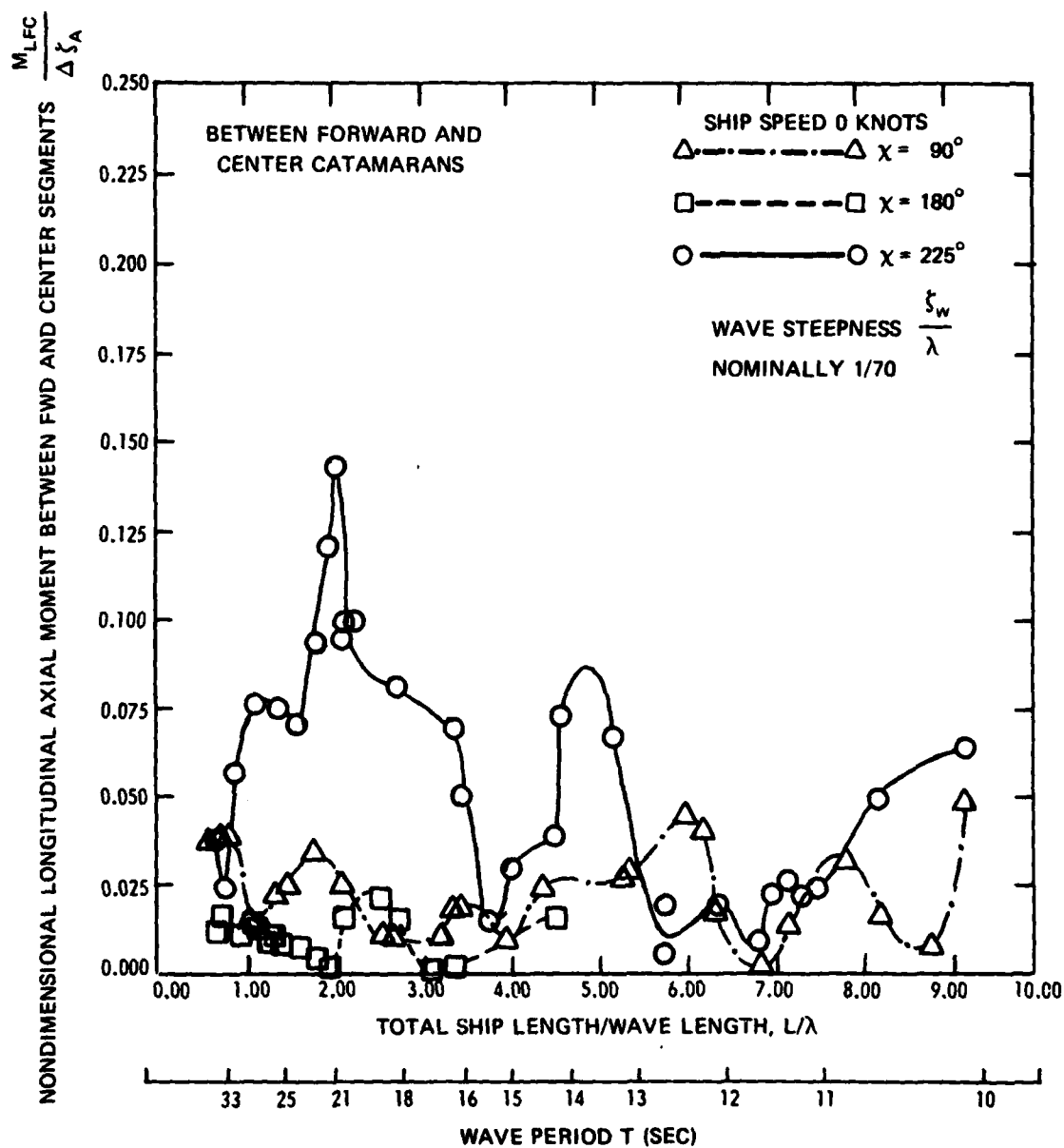


Figure 50 (Continued)

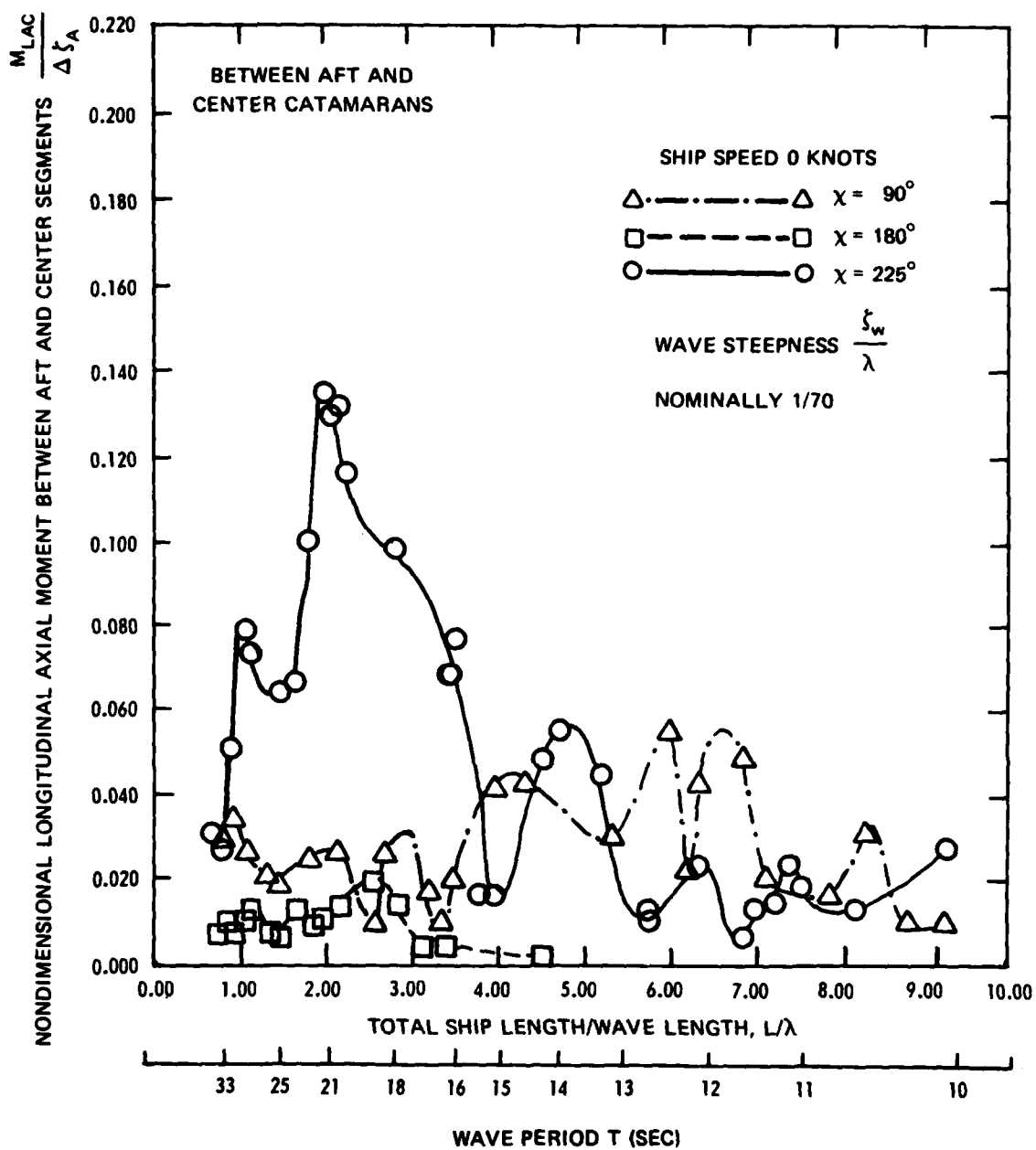


Figure 51 — Nondimensional Transfer Function of the Vertical Axial Moment between the Modules versus Total ISUS Length/Wave Length

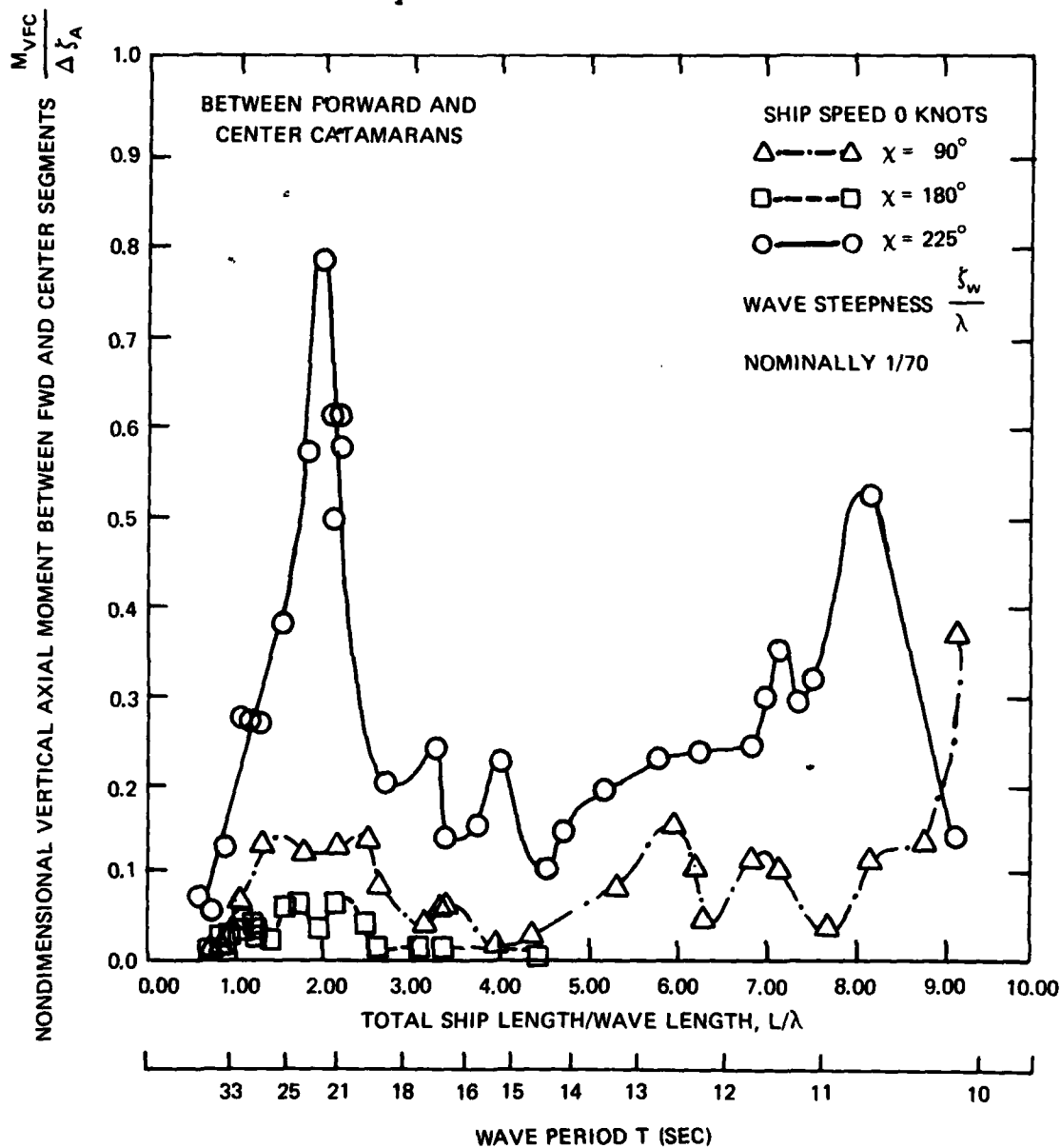
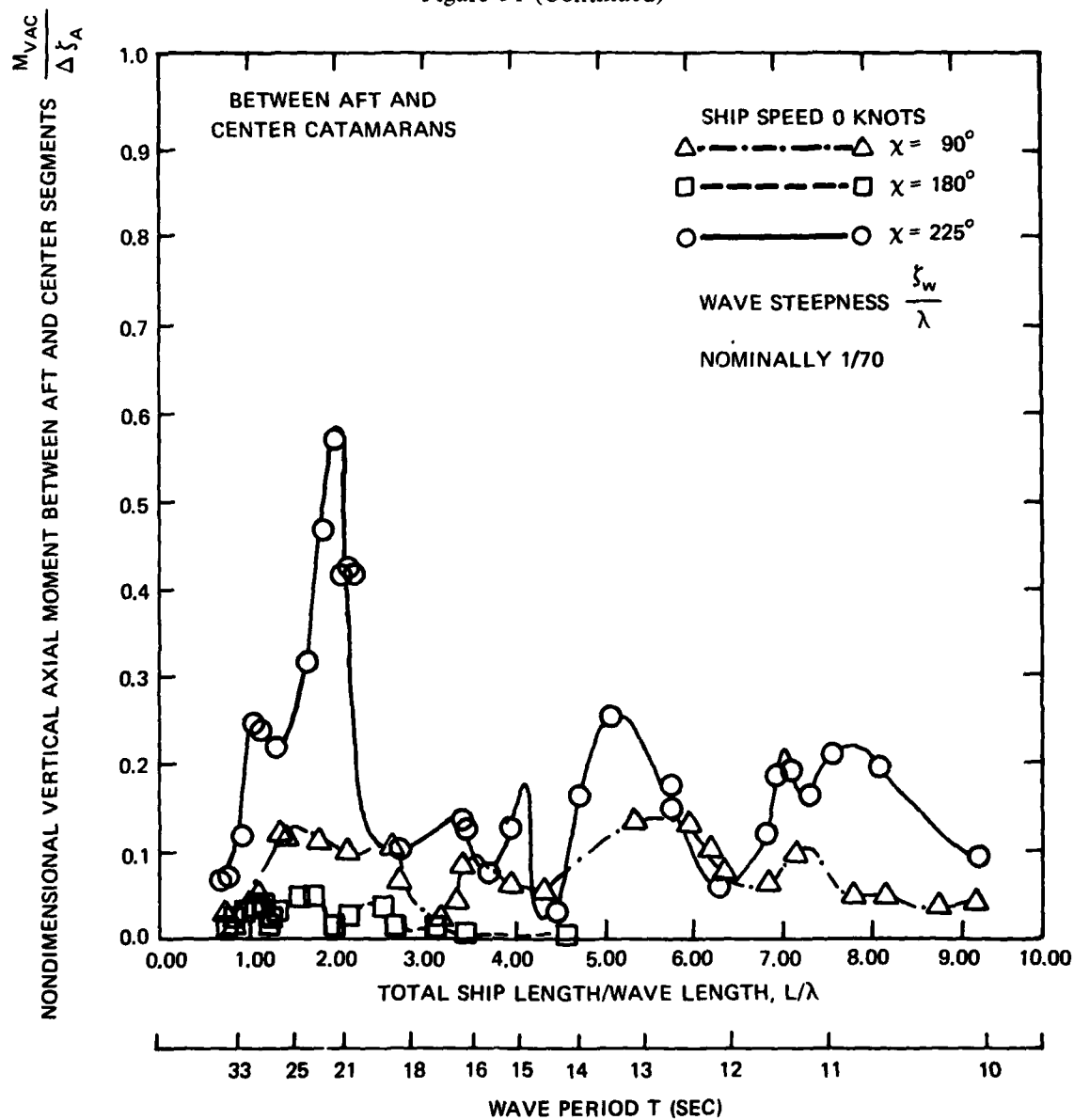


Figure 51 (Continued)



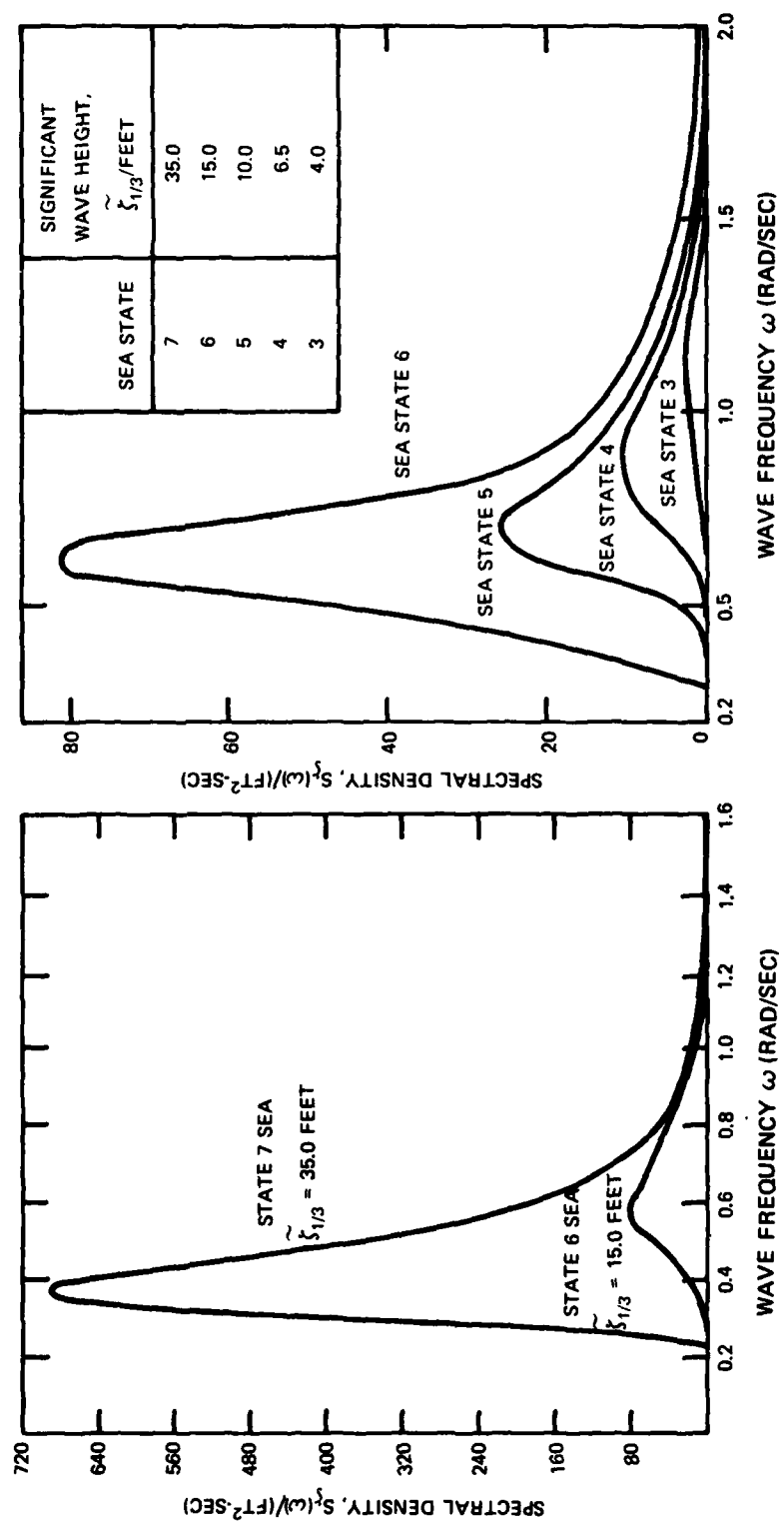


Figure 52 — Pierson-Moskowitz Wave Spectra for Various Sea States

TABLE 2 – CHARACTERISTICS OF 100,000-SHP
PROPELLERS OPTIMIZED AT 80 RPM

Characteristics	Symbol	Units	Ship Type	
			5000-Foot Supership	1600-Foot Catamaran
Propeller Type			Built-up	Built-up
Ship Speed	V	knots	12.0	18.0
Number of Shafts	n_s		2	2
Power/Shaft	P_s	hp	100,000	100,000
Shaft Speed	N	rpm	80.0	80.0
Propeller Diameter	D	ft	38.30	37.20
Pitch Ratio at 0.7 Radius	$P_{0.7}/D$		0.661	0.793
Blade Number	Z		5	5
Expanded-Area Ratio	A_E/A_0		0.596	0.575
Propeller Efficiency	η_0		0.434	0.565
Weight Built-up Prop.:				
Manganese-Bronze	W_p	lb	459,300	419,200
Ni-Al-Bronze	W_p	lb	395,600	362,900
Torque per Shaft	Q	lb-ft	6.6×10^6	6.6×10^6
Thrust per Shaft	T	lb	1.5×10^6	1.3×10^6
Thrust Loading Coeff.	C_{Th}		4.9	2.0
Cavitation Number at 0.7 Radius	$\sigma_{x,0.7}$		0.469	0.483
Wake Fraction	w		0.20	0.20
Thrust Deduction	t		0.15	0.15
Hull Efficiency	η_H		1.06	1.06

TABLE 3 – CHARACTERISTICS OF 30-FOOT DIAMETER
PROPELLERS FOR 100,000 SHP

Characteristics	Symbol	Units	Ship Type	
			5000-Foot Supership	1600-Foot Catamaran
Propeller Type			Fixed-bladed or CP	Fixed-bladed or CP
Ship Speed	V	knots	12.0	18.0
Number of Shafts	n_s		2	2
Power/Shaft	P_s	shp	100,000	100,000
Shaft Speed	N	rpm	104.5	102.4
Propeller Diameter	D	ft	30.0	30.0
Pitch Ratio at 0.7 Radius	$P_{0.7}/D$		0.784	0.886
Blade Number	Z		5	5
Expanded Area Ratio	A_E/A_0		0.851	0.792
Propeller Efficiency	η_0		0.374	0.506
Weight Ni-Al-Bronze:				
Fixed-Bladed Prop.	W_p	lb	215,100	205,400
CP Propeller	W_p	lb	277,300	267,700
Torque per Shaft	Q	lb-ft	5.0×10^6	5.1×10^6
Thrust per Shaft	T	lb	1.3×10^6	1.1×10^6
Thrust Loading Coeff.	C_{Th}		6.9	2.8
Cavitation Number at 0.7 Radius	$\sigma_{x,0.7}$		0.448	0.455
Wake Fraction	w		0.20	0.20
Thrust Deduction	t		0.15	0.15
Hull Efficiency	η_H		1.06	1.06

TABLE 4 – POWER PLANT FOR 1600-FOOT CATAMARAN SHIP MODULE
(170,000 hp, based on 18-knot speed and 37-foot diameter, built-up propeller)

System	Weight, tons		Volume, ft ³		Cost, \$		Fuel Consumption lb/hp-hr	Remarks
	Engine	Total	Engine	Total	Engine	Total		
Diesel	6900	9500	397,000	3,970,000	5,000,000	15,000,000	0.40	Total volume includes combining gearing.
Gas Turbine	30.0	1200	8,700	510,000	9,600,000	*	0.41	Total volume includes combining gearing; fuel for turbine is more expensive than diesel or steam.
Oil-Fired Steam	2500	4740	55,000	550,000	4,000,000	10,000,000	0.40	Total volume includes reduction gearing.
Values in table based on individual engines and engine specific values. * Cost data not available.								

TABLE 5 – POWER PLANT FOR 1800-FOOT CATAMARAN SHIP MODULE
(205,000 hp, based on 18-knot speed and 37-foot diameter, built-up propeller)

System	Weight, tons		Volume, ft ³		Cost, \$		Fuel Consumption lb/hp-hr	Remarks
	Engine	Total	Engine	Total	Engine	Total		
Diesel	8600	12,000	617,000	6,170,000	5,800,000	17,400,000	0.40	Total volume includes combining gearing.
Gas Turbine	38.0	1,500	10,900	640,000	12,000,000	*	0.41	Total volume includes combining gearing; fuel for turbine is more expensive than diesel or steam.
Oil-Fired Steam	3000	5,700	66,400	664,000	4,500,000	11,000,000	0.40	Total volume includes reduction gearing.
Values in table based on individual engines and engine specific values. * Cost data not available.								

TABLE 6 -- STEAM PLANT COMPONENT WEIGHTS

(All weights in long tons)

Components	HP Rating			
	Fore and Aft Modules		Midmodule	
	15 Knots	18 Knots	15 Knots	18 Knots
Main turbine, reduction gears, main condenser air pumps, sea-water circulation and lube oil systems	850	1260	1070	1510
Main boiler, forced draft fans, automatic controls, stacks, uptakes	1480	2190	1870	2640
Feed heaters, feed and condensate pumps, evaporator, low-pressure steam generator	384	566	484	684
Propulsion system piping including circulating water, feed, condensate, steam, exhaust, drain, oil, instrument, generator steam, feed	490	725	618	874
Total, tons	3204	4741	4042	5708
Note: Integrated ship: weight at 18-knot hp rating = 15,190 tons; machinery fraction at 18-knot hp rating = 0.0084 percent; weight at 15-knot hp rating = 10,450 tons; machinery fraction at 15-knot hp rating = 0.0058 percent.				

TABLE 7 -- FUEL WEIGHTS OF
MERCHANT SHIPS

	Ship A	Ship B	Ship C
Displacement, tons	25,510	34,640	49,660
Deadweight, tons	19,183	26,759	38,911
Fuel Weight, tons	1,969	2,679	3,836

TABLE 8 -- FUEL WEIGHTS FOR SUPERSHIP
AND COMPONENTS

Ship	Fuel, tons	Range, nautical miles	
		At 18 Knots	At 15 Knots
Fore and Aft Modules	38,500 (each)	22,828	28,122
Midmodule	61,500	30,240	35,628
Integrated Supership	138,500	(1)	(2)
<p>(1) Based on Figure 3; at reduced speed of 10 knots, 45,624 nautical miles.</p> <p>(2) Based on Figure 3; at reduced speed of 7.5 knots, 60,583 nautical miles.</p>			

TABLE 9 STEAM PLANT COMPONENT BLOCK VOLUMES
(All volumes in cubic feet)

Components	Fore and Aft Modules		Midmodule	
	At 15 Knots	At 18 Knots	At 15 Knots	At 18 Knots
Main turbine, reduction gears, main condenser, air pumps, seawater circulation, and lube oil systems	150,000	335,000	210,000	425,000
Main boiler, forced draft fans, automatic controls, stacks, uptakes	210,000	390,000	250,000	480,000
Feed heaters, feed and condensate pumps, evaporator, low-pressure steam generator	Volumes included within turbine and boiler blocks			
Propulsion system piping including circulating water, feed, condensate, steam, exhaust, drain, lube oil, instrument, low-pressure generator steam, feed	Volumes included within turbine and boiler blocks			
Total Volume	360,000	725,000	460,000	905,000

TABLE 10 - PROPELLER SHAFT STRESS CHARACTERISTICS

Characteristic	
Steady Shear Stress	$S_s = \frac{(5.1) (Q)}{D^3} = \frac{(5.1) (99,500,000)}{(57)^3}$ $= 2740 \text{ psi}$
Steady Compressive Stress	$S_c = \frac{(1.273) (T)}{D^2} = \frac{(1.273) (1,270,000)}{(57)^2}$ $= 498 \text{ psi}$
Resultant Steady Stress	$S_{sr} = \sqrt{(S_c)^2 + (2 S_s)^2}$ $= \sqrt{(498)^2 + (2 \times 2740)^2}$ $= 5500 \text{ psi}$
Alternating Shear Stress	$S_{AS} = (.05) (S_s)$ $= (.05) (2740) = 137 \text{ psi}$
Bending Stress	$S_b = \frac{(10.2) (M_t)}{D^3} = \frac{(10.2) (105,000,000)}{(57)^3}$ $= 5780 \text{ psi}$
Resultant Alternating Stress	$S_{ar} = \sqrt{(K_b \times S_b)^2 + (2 K_t \times S_{as})^2}$ $= \sqrt{(1 \times 5780)^2 + (2 \times 1.9 \times 137)^2}$ $= 5805 \text{ psi}$
Factor of Safety	$FS = \frac{1}{\frac{S_{sr}}{YP} + \frac{S_{ar}}{FL}}$ $= \frac{1}{\frac{5500}{45000} + \frac{5805}{40000}}$ $= 3.72$
<p>Q = torque, D = shaft diameter, T = thrust, M_t = total moment on shaft, K_b and K_t = stress concentration factors, YP = yield point, FL = fatigue limit.</p>	

TABLE 11 COMPARISON OF STOPPING TIME AND DISTANCE FOR 5000-FOOT ISUS, 1600-FOOT MODULE, AND 250,000-TON TANKER

(From Figures 33 and 34; approach speed = 12 knots)

Characteristics	Symbol	Units	Ship Type							
			5000-ft Supership				1600-ft Catamaran Module			
Displacement	Δ	tons	1,800,000				500,000			
Horsepower/Shaft		hp	100,000				100,000			
Propulsion Arrangement			80-RPM Engine	30-Foot Prop.	30-Foot CP Prop.	100,000	80-RPM Engine	30-Foot Prop.	30-Foot CP Prop.	Fixed-Bladed Prop.
Astern Power/Shaft	P_s	hp	40,000	40,000	100,000	40,000	40,000	40,000	100,000	10,000
Propeller Diameter	D	ft	37.0	30.0	30.0	30.0	37.0	30.0	30.0	28.0
Initial Speed Considered	V_0	knots	12.0	12.0	12.0	12.0	12.0	12.0	12.0	12.0
Time to Reverse Engine	t_r	min	1.5	1.5	0.5	1.5	1.5	1.5	0.5	1.0
Stopping Distance	S	ft	15,500	17,000	10,400	17,000	5,000	6,200	3,400	12,500
Stopping Time	t	min	28.0	31.5	19.6	31.5	10.5	11.5	6.0	22.5

TABLE 12 CHARACTERISTICS OF MODEL AND FULL-SCALE SUPERSHIP
(Scale Ratio: 120; F.W. designates freshwater and S.W. seawater)

Particular	Model	Units	Ship	Units
Length (LBP, Overall)	39.50	ft	4,740.00	ft
Length (LBP, Forward Model)	11.50	ft	1,380.00	ft
Length (LBP, Center Model)	15.00	ft	1,800.00	ft
Length (LBP, After Model)	11.50	ft	1,380.00	ft
Draft (H)	0.57	ft	68.64	ft
Displacement (Overall)	2157.00	lb, F.W.	1,707,235.00	long tons, S.W.
Displacement (Forward Model)	576.17	lb, F.W.	456,030.00	long tons, S.W.
Displacement (Center Model)	993.16	lb, F.W.	786,072.00	long tons, S.W.
Displacement (After Model)	587.67	lb, F.W.	465,133.00	long tons, S.W.
Beam (Forward Model)	4.50	ft	540.00	ft
Beam (Center Model)	4.84	ft	581.88	ft
Beam (After Model)	4.50	ft	540.00	ft
Longitudinal Radius of Gyration (Forward Model)	0.33 LBP _M	—	0.33 LBP _S	—
Longitudinal Radius of Gyration (Center Model)	0.31 LBP _M	—	0.31 LBP _S	—
Longitudinal Radius of Gyration (After Model)	0.32 LBP _M	—	0.32 LBP _S	—

TABLE 13 MEASURED AND PREDICTED SIGNIFICANT DOUBLE AMPLITUDES OF MOTIONS

Measurement	Units	Measured (State 7)			Predicted (Port Bow Sea)					
		Beam Sea	Head Sea	Port Bow Sea	State 7	State 6	State 5	State 4	State 3	
ζ	ft	22.88	38.00	35.00	35.00	15.00	10.00	6.50	4.00	
θ_F	deg	0.33	1.67	1.46	1.69	0.63	0.18	0.02	0.00*	
θ_C	deg	0.37	2.08	1.82	2.23	0.46	0.14	0.01	0.00	
θ_A	deg	0.62	3.16	3.10	3.66	0.52	0.16	0.01	0.00	
Z_F	ft	17.30	61.67	55.26	67.72	8.50	2.80	0.28	0.00	
Z_C	ft	14.01	9.08	12.39	16.46	3.05	0.93	0.15	0.00	
Z_A	ft	13.57	15.20	20.55	22.16	3.49	1.15	0.21	0.00	
θ_{FC}	deg	0.07	0.44	0.39	0.55	0.95	0.25	0.02	0.00	
θ_{AC}	deg	0.87	5.15	4.73	5.65	0.95	0.29	0.02	0.00	
ϕ	deg	6.27	0.59	2.07	2.99	0.59	0.11	0.01	0.00	

* No significant motion when rounded to two significant figures.

TABLE 14 -- MEASURED AND PREDICTED SIGNIFICANT DOUBLE AMPLITUDES OF FORCES AND MOMENTS

Measurement	Units	Measured (State 7)			Predicted (Port Bow Sea)						
		Beam Sea	Head Sea	Port Bow	State 7	State 6	State 5	State 4	State 3		
ξ	ft	22.80	38.00	35.00	35.00	15.00	10.00	6.50	4.00		
F_{SVFC}	lb	1.33×10^7	6.55×10^7	5.79×10^7	7.22×10^7	1.65×10^7	2.98×10^6	3.18×10^5	5.34×10^3		
F_{SVAC}		1.93×10^7	4.37×10^7	7.25×10^7	9.15×10^7	1.90×10^7	3.72×10^6	4.59×10^5	5.03×10^3		
F_{SHFC}		3.06×10^7	0.94×10^7	4.03×10^7	4.98×10^7	1.05×10^7	3.89×10^6	7.24×10^5	11.00×10^3		
F_{SHAC}		3.44×10^7	0.77×10^7	3.95×10^7	4.70×10^7	0.94×10^7	3.65×10^6	6.76×10^5	8.30×10^3		
F_{FC}		0.67×10^7	3.26×10^7	3.21×10^7	3.37×10^7	0.85×10^7	2.52×10^6	2.23×10^5	2.43×10^3		
F_{AC}	lb	0.75×10^7	3.21×10^7	3.51×10^7	3.81×10^7	0.85×10^7	2.35×10^6	3.52×10^5	6.37×10^3		
M_{LFC}	ft-lb	4.03×10^9	2.17×10^9	8.55×10^9	8.67×10^9	1.65×10^9	6.17×10^8	8.61×10^7	5.27×10^6		
M_{LAC}		3.13×10^9	1.58×10^9	7.68×10^9	9.42×10^9	1.16×10^9	4.03×10^8	8.91×10^7	2.06×10^6		
M_{VFC}		14.45×10^9	9.07×10^9	39.62×10^9	41.99×10^9	10.80×10^9	35.49×10^8	96.94×10^7	49.78×10^6		
M_{VAC}	ft-lb	12.23×10^9	6.48×10^9	28.52×10^9	28.50×10^9	4.55×10^9	14.04×10^8	80.99×10^7	33.37×10^6		

APPENDIX A

FORMULAS AND EQUATIONS

EQUATIONS OF CALCULATED MOTIONS, FORCES, AND MOMENTS

The equations for the computed time histories of the motions in terms of the measured time histories are:

$$\theta_F = \theta_C + \theta_{FC}$$

$$\theta_A = \theta_C - \theta_{AC}$$

$$Z_F = Z_C - \ell_2 \sin \left(\frac{\pi \theta_C}{180} \right) - \ell_1 \sin \left[\frac{\pi}{180} (\theta_C + \theta_{FC}) \right]$$

$$Z_A = Z_C + \ell_3 \sin \left(\frac{\pi \theta_C}{180} \right) + \ell_4 \sin \left[\frac{\pi}{180} (\theta_C - \theta_{AC}) \right]$$

where ℓ_2 = distance from the LCG of the center segment to the forward connecting rod between segments

ℓ_1 = distance from the LCG of the forward segment to the forward connecting rod between segments

ℓ_3 = distance from the LCG of the center segment to the after connecting rod between segments

ℓ_4 = distance from the LCG of the after segment to the after connecting rod between segments

The equations for the computed time histories of the forces and moments in terms of the measured time histories are:

$$F_{SVFC} = F_{z_1} + F_{z_2}$$

$$F_{SVAC} = F_{z_3} + F_{z_4}$$

$$F_{SHFC} = F_{y_1} + F_{y_2}$$

$$F_{SHAC} = F_{y_3} + F_{y_4}$$

$$F_{FC} = F_{x_1} + F_{x_2}$$

$$\begin{aligned}
 F_{AC} &= F_{x_3} + F_{x_4} \\
 M_{LFC} &= d/2 (F_{z_2} - F_{z_1}) \\
 M_{LAC} &= d/2 (F_{z_4} - F_{z_3}) \\
 M_{VFC} &= d/2 (F_{x_1} - F_{x_2}) \\
 M_{VAC} &= d/2 (F_{x_3} - F_{x_4})
 \end{aligned}$$

where d is the transverse distance between hull centerlines (37.0 in. model scale).

EQUATIONS FOR THE CALCULATIONS OF THE FOURIER COEFFICIENTS

The Fourier coefficient $C(\omega)$ is given by

$$C(\omega) = \left\{ \left[A(\omega) \right]^2 + \left[B(\omega) \right]^2 \right\}^{1/2}$$

where $A(\omega) = \frac{2}{T} \int_0^T X(t) \cos \omega t \, dt$ and $B(\omega) = \frac{2}{T} \int_0^T X(t) \sin \omega t \, dt$. Here $X(t)$

is the original time history.

FORMULAS FOR THE NONDIMENSIONALIZATION OF THE CHANNELS

Angular displacements (θ):	$\frac{\theta_A}{360 \xi_A / \lambda}$	$\frac{\text{deg}}{(\text{deg/rad}) (\text{ft/ft})}$
Linear displacements (Z):	$\frac{Z_A}{\xi_A}$	$\frac{\text{ft}}{\text{ft}}$
Forces (F):	$\frac{F_A}{\Delta \xi_A / L}$	$\frac{\text{lbs}}{\text{lbs}(\text{ft/ft})}$
Moments (M):	$\frac{M_A}{\Delta \xi_A}$	$\frac{\text{ft} \cdot \text{lbs}}{\text{lbs}(\text{ft})}$

CALCULATION OF SIGNIFICANT DOUBLE AMPLITUDES

The significant double amplitudes are computed by:

$$\text{Sig} = 2.83 \cdot \sqrt{A}$$

where A is the area under the particular spectral curve.

CALCULATION OF PIERSON-MOSKOWITZ (AMPLITUDE) SPECTRA

The equation for the Pierson-Moskowitz (amplitude) wave spectrum used in the predictions is:

$$S_{\zeta}(\omega) = \frac{16.768}{\omega^5} \exp \left[\frac{-79.281 \times 10^4}{\omega^4 U^4} \right] \text{ ft}^2 \cdot \text{sec}$$

where ω is the wave frequency in radians per second and U is the wind speed in feet per second. U can be calculated by:

$$U = 12.400 \sqrt{\tilde{\zeta}_{1/3}}$$

where $\tilde{\zeta}_{1/3}$ is the significant double amplitude wave height in feet.

APPENDIX B **LOGS OF MOTION PICTURES**

Part I — Normal Operating Conditions

Type of Waves	χ/deg	T/sec	λ/feet	L/λ	$1/\lambda \zeta_w$	ζ_w/feet	
Regular	180	18.58	1769	2.68	1/133	13.78	
		18.58	1769	2.68	1/82	22.12	
	90	14.52	1080	4.42	1/101	10.62	
		13.20	893	5.31	1/77	11.66	
		19.05	1859	2.55	1/81	22.86	
		17.03	1486	3.19	1/49	30.26	
	225	12.46	795	5.96	1/126	6.32	
		10.68	585	8.10	1/131	4.48	
		10.68	585	8.10	1/94	6.24	
		15.23	1188	3.99	1/53	22.30	
	Regular	180	13.41	922	5.14	1/74	12.50
			11.26	650	7.29	1/55	11.94
Irregular	90	Low State 7 sea $\tilde{\zeta}_{1/3} = 22.2$ feet					
Irregular	180	High State 7 sea $\tilde{\zeta}_{1/3} = 36.8$ feet					
Part II — Severe Storm Conditions							
Regular	180	20.75	2205	2.15	1/70	33.02	
		22.74	2648	1.79	1/56	48.72	
		21.90	2456	1.93	1/32	76.02	
		27.43	3854	1.23	1/51	76.14	
		31.72	5152	0.92	1/49	104.92	
Regular	225	21.24	2312	2.05	1/50	46.84	

REFERENCES

1. Lin, A.C.M., "A Feasibility Study of a Stable Mobile Ocean Platform as a Naval Base," NSRDC Report 3743 (Feb 1973).
2. Vossers, G. et al., "Vertical and Lateral Bending Moment Measurements on Series 60 Models," International Shipbuilding Progress, Vol. 8, No. 83 (Jul 1961).
3. Eda, H., "Studies of Barge Trains in a Coastal Seaway," Davidson Laboratory Technical Note 806 (Jun 1969).
4. Dinsenbacher, A.L., "A Method for Estimating Loads on Catamaran Cross-Structure," Marine Technology, Vol. 7, No. 4 (Oct 1970).
5. Thomas, G.O., "An Extended Static Balance Approach to Longitudinal Strength," Trans. SNAME, Vol. 76 (1968).
6. Boylston, J.W. and W.A. Wood, "The Design of a Hinged Tanker," Marine Technology, Vol. 4, No. 3 (Jul 1967).
7. Van Lammeren, W.P.A. et al., "The Wageningen B-Screw Series," Trans. SNAME, Vol. 77 (1969).
8. Todd, F.H., "Resistance and Propulsion," Chapter 7 in "Principles of Naval Architecture," SNAME, New York (1967).
9. "Rules for Building and Classing Steel Vessels," American Bureau of Shipping, New York (1970).
10. Brehme, H., "Propellers for Single-Screw Ships with Large Engine Powers," (in German) Jahrbuch der Schiffbautechnischen Gesellschaft, Vol. 62 (1968).
11. Brockett, T., "Minimum Pressure Envelopes for Modified NACA-66 Sections with NACA = 0.8 Camber and BUSHIPS Type I and II Sections," David Taylor Model Basin Report 1780 (Feb 1967).
12. Meyne, K., "Hydraulic Method of Fitting Marine Propellers," International Shipbuilding Progress, Vol. 17, No. 193 (Sep 1970).
13. Wadman, B.W., "Diesel and Gas Turbine Catalog," Diesel and Gas Turbine Progress, Vol. 34 (1969).
14. "Sawyer's Gas Turbine Catalog," Gas Turbine Publications, Vol. 7 (1969).
15. "Marine Steam Power Plant State of the Art Seminar," Babcock & Wilcox and General Electric (1970).

16. "Economic Comparison of Low Speed and Medium Speed Diesel and General Electric MST-13, MST-14 Non-Reheat and MST-14 Reheat Steam Power Plants for European Built and Operated Tankers," George G. Sharp Company, New York (Sep 1969).
17. Arnot, D., "Design and Construction of Steel Merchant Ships," SNAME, New York (1955).
18. Clarke, D. and F. Wellman, "The Stopping of Large Tankers and the Feasibility of Using Auxiliary Braking Devices," Trans. Roy. Inst. Nav. Arch., Paper 4 (Apr 1970).
19. Schmitz, G., "Horizontal Forces and Moments Due to the Motion of Catamaran-Ships and Consideration of Their Dynamic Stability and Control," (in German) Schiffbauforschung, Vol. 9 (Feb 1970).
20. Stuntz, G.R. and R.J. Taylor, "Some Aspects of Bow-Thruster Design," Trans. SNAME, Vol. (1964).
21. Spens, P.G. and P.A. Lalangos, "Measurements of the Mean Lateral Force and Yawing Moment on a Series 60 Model in Oblique Regular Waves," Davidson Laboratory Report R-880 (Jun 1962).
22. "Oceanographic Atlas of the North Atlantic Ocean, Section IV—Sea and Swell," U.S. Naval Oceanographic Office Publication 700 (1963).
23. "Oceanographic Atlas of the South Atlantic Ocean, Section IV—Sea and Swell," U.S. Naval Oceanographic Office Publication 799B (1948).
24. "Oceanographic Atlas of the Northwestern and Southwestern Pacific Ocean, Section IV—Sea and Swell," U.S. Naval Oceanographic Office Publication 799CE (1969).
25. "Oceanographic Atlas of the Indian Ocean, Section IV—Sea and Swell," U.S. Naval Oceanographic Office Publication 799G (1965).
26. "Oceanographic Atlas of the Northeastern Pacific Ocean, Section IV—Sea and Swell," U.S. Naval Oceanographic Office Publication 799D (1969).
27. "Movies of Supership Model Tests in Waves: Part I—Normal Operating Conditions, Part II—Severe Storm Conditions," NSRDC Movie M-2301 (Jul 1971).

INITIAL DISTRIBUTION

Copies		Copies	
1	ARPA	12	NAVSEA
1	ARMY CHIEF OF RES & DEV		1 SEA 03
2	AAMCA/AAMRDL		2 SEA 03M
1	ARMY ENGR R&D LAB		4 SEA 032 (SHIPS 03Z)
14	OP		2 SEA 035 (SHIPS 034)
	2 00K		1 SEA 03411
	1 96L		1 SEA 035C/Sorkin (SHIPS 0342)
	1 097		1 SEA 09G32 (SHIPS 2052)
	1 971	3	NAVAIR
	1 098		1 AIR 03
	1 982		1 AIR 03P
	1 987		1 AIR 04
	1 987T6	1	NELC LIB
	1 03H	1	NAVUSEACEN 1311 LIB
	1 32	1	NAVWPNSCEN 753 LIB
	1 04B	1	CIVENGRLAB L31 LIB
	1 040	1	NAVCOASTSYSLAB
	1 405	1	NOL 730 LIB
2	CHONR	6	NAVSEC
	1 102-0S		1 SEC 6100
	1 485		1 SEC 6100 B1
2	MC-AX/A. SLAFKOSKY		1 SEC 6110
7	NAVMAT		1 SEC 6114
	1 MAT 00CA		1 SEC 6140
	1 MAT 03		1 SEC 6144
	1 MAT 03L/J. LAWSON	1	MILITARY SEALIFT COMMAND
	1 MAT 03R	1	AF ACS STUDIES & ANALYSIS
	1 MAT 033	1	AF CHIEF SYSTEMS & LOGISTICS
	1 MAT 04	1	MAC
	1 MAT 09T	1	AFOSR/NAM
1	USNA LIB	1	ASRCNC-1
1	NAVPGSCOL LIB	2	DDC
1	NAVWARCOL	2	MARAD
2	CMC SMLS PROJECT OFF/ COL MUNN		1 SHIP CONSTRUCTION
			1 R&D
		1	DEPT OF STATE/CAPT DEWENTER

